

Catalyst immobilization via electrostatic interactions : polystyrene-based supports

Citation for published version (APA):

Kunna, K. (2009). *Catalyst immobilization via electrostatic interactions : polystyrene-based supports*. [Phd Thesis 1 (Research TU/e / Graduation TU/e), Chemical Engineering and Chemistry]. Technische Universiteit Eindhoven. <https://doi.org/10.6100/IR640072>

DOI:

[10.6100/IR640072](https://doi.org/10.6100/IR640072)

Document status and date:

Published: 01/01/2009

Document Version:

Publisher's PDF, also known as Version of Record (includes final page, issue and volume numbers)

Please check the document version of this publication:

- A submitted manuscript is the version of the article upon submission and before peer-review. There can be important differences between the submitted version and the official published version of record. People interested in the research are advised to contact the author for the final version of the publication, or visit the DOI to the publisher's website.
- The final author version and the galley proof are versions of the publication after peer review.
- The final published version features the final layout of the paper including the volume, issue and page numbers.

[Link to publication](#)

General rights

Copyright and moral rights for the publications made accessible in the public portal are retained by the authors and/or other copyright owners and it is a condition of accessing publications that users recognise and abide by the legal requirements associated with these rights.

- Users may download and print one copy of any publication from the public portal for the purpose of private study or research.
- You may not further distribute the material or use it for any profit-making activity or commercial gain
- You may freely distribute the URL identifying the publication in the public portal.

If the publication is distributed under the terms of Article 25fa of the Dutch Copyright Act, indicated by the "Taverne" license above, please follow below link for the End User Agreement:

www.tue.nl/taverne

Take down policy

If you believe that this document breaches copyright please contact us at:

openaccess@tue.nl

providing details and we will investigate your claim.

Catalyst Immobilization via Electrostatic Interactions: Polystyrene-based Supports

Catalyst Immobilization via Electrostatic Interactions: Polystyrene-based Supports

Proefschrift

ter verkrijging van de graad van doctor aan de
Technische Universiteit Eindhoven, op gezag van de
Rector Magnificus, prof.dr.ir. C.J. van Duijn, voor een
Commissie aangewezen door het College voor
Promoties in het openbaar te verdedigen
op maandag 19 januari 2009 om 16.00 uur

door

Katharina Kunna

geboren te Rostock, Duitsland

Dit proefschrift is goedgekeurd door de promotor:

prof.dr. D. Vogt

Copromotor:
dr. C. Müller

Catalyst Immobilization via Electrostatic Interactions: Polystyrene-based supports
by Katharina Kunna Eindhoven: Eindhoven University of Technology, 2008

A catalogue record is available from the Eindhoven University of Technology Library

ISBN: 978-90-386-1509-7

Omslag: Oranje Vormgevers Eindhoven

Druk: Universiteitdrukkerij, Technische Universiteit Eindhoven

Copyright © 2008 K. Kunna

Dit proefschrift is goedgekeurd door de manuscript commissie:

prof.dr. D. Vogt (Technische Universiteit Eindhoven)

dr. C. Müller (Technische Universiteit Eindhoven)

prof.dr. A. B. de Haan (Technische Universiteit Eindhoven)

prof.dr. S. Mecking (Universität Konstanz)

prof.dr. B. J. M. Klein Gebbink (Universiteit Utrecht)

In der Mitte von Schwierigkeiten liegen die Möglichkeiten
(Albert Einstein)

In der Ruhe liegt die Kraft
(unbekannt)

**Für meinen geliebten Vater,
als Dank für seine Liebe, Geduld und Vertrauen in mich**

Chapter 1:	1
Electrostatic Immobilization of Transition Metal Complexes	
Chapter 2:	31
Synthesis and Characterization of Latexes as Phase Transfer Agents	
Chapter 3:	59
Latexes as Phase Transfer Agents and Supports for Electrostatic Immobilization: Biphasic Hydroformylation of Higher Alkenes	
Chapter 4:	95
Immobilization of Cationic Hydrogenation Complexes <i>via</i> Electrostatic Interactions	
Chapter 5:	127
Application of Latex-incorporated Nixantphos in the Biphasic Hydroformylation of Higher Alkenes: <i>Initial Results and Outlook</i>	
Summary	141
Samenvatting	145
List of Publications	148
Curriculum vitae	149
Dankwoord	151

Electrostatic Immobilization of Transition Metal Complexes

Recovery of homogeneous catalysts from the reaction mixture represents a crucial feature for industrial applications. A possible solution is the immobilization of catalysts *via* non-covalent interactions.

The immobilization *via* electrostatic interactions is a very attractive strategy as it circumvents time consuming, often difficult ligand modifications, as well as the unpredictable effects on activity and selectivity. Successful applications of electrostatically immobilized catalysts in homogeneous catalysis will be discussed.

1.1. Introduction

During the last decades the number of applications of soluble transition metal complexes as selective homogeneous catalysts has increased significantly. In comparison to heterogeneous catalysts, homogeneous catalysts can be applied under milder conditions and the selectivity for the required product is generally higher. Thus, a number of important large-scale processes, such as the production of adiponitrile, butanal (Ruhchemie Rhône Poulenc process), α -olefins (SHOP process), acetic acid, and acetic anhydride are based on homogeneous catalysis.^[1,2] However, the separation and recovery of the catalyst from the reaction mixture represents a crucial feature for industrial applications. Consequently, there is considerable interest in the development of immobilized homogeneous catalysts.

Several strategies for the immobilization of homogeneous catalysts have been developed and investigated. Among those are, for instance, applications in fluorous phase,^[3,4] supported aqueous phase,^[5] ionic liquids^[6-11] and in super critical fluids.^[12-14] Other common approaches to facilitate catalyst–product separation is the attachment of homogeneous catalysts to dendritic,^[15-21] polymeric, organic, inorganic, or hybrid organic/inorganic supports.^[22-27]

However, in most of the examples reported so far, the catalyst has been linked covalently to the support. An interesting alternative strategy is the non-covalent anchoring of the catalyst. Nevertheless, the immobilization of catalysts by means of non-covalent binding has found relatively little attention so far.

This chapter exclusively focuses on the application of electrostatically immobilized catalysts. Examples and highlights of their performance are presented.

1.2. Covalent *versus* non-covalent bond

Catalyst immobilization can either be achieved by a covalent bond or *via* non-covalent interactions.

Covalent bonding includes many kinds of interactions such as σ -bonding, π -bonding, and 3c-2e bonds.

The three main types of non-covalent interactions are hydrogen bonds, ionic and electrostatic interactions, and Van der Waals interactions. One of the most famous examples of non-covalent bonding is the interaction between two DNA strands in the DNA double helix.

In general, a non-covalent bond is weaker than a covalent bond (Figure 1.1). However, combinations of non-covalent interactions can result in rather strong binding.

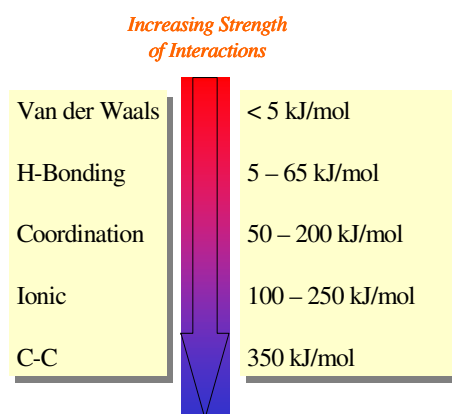


Figure 1.1 Increasing strength of covalent bond and non-covalent interactions^[28]

Even though covalent bonds are stronger than the non-covalent bonds, the covalent attachment of catalysts (Figure 1.2, I) has also disadvantages. Most often, these catalysts are less effective than their homogeneous analogues. Consequently, a higher loading is often employed in order to obtain reasonable conversions. Moreover, in most cases synthetic modifications are necessary to achieve covalent immobilization. For these reasons, the non-covalent immobilization of transition metal complexes is highly desirable. This can even circumvent the need of time consuming and often difficult ligand modification as well as the implied unpredictable effects on activity and selectivity.

Electrostatically supported complexes have been prepared through adsorption (Figure 1.2, II), and supported liquid phase (Figure 1.2, III). The immobilization by adsorption is achieved by simple physisorption of a ligand, a non-charged or a charged metal complex on the support through van der Waals interactions. In supported liquid phase the catalyst remains in a different phase than the product/substrate. Although high activities and enantioselectivities can be observed using these methods, catalyst recycling still needs to be addressed. A possible solution for this problem is the immobilization of the complexes *via* ionic interactions (Figure 1.2, IV).

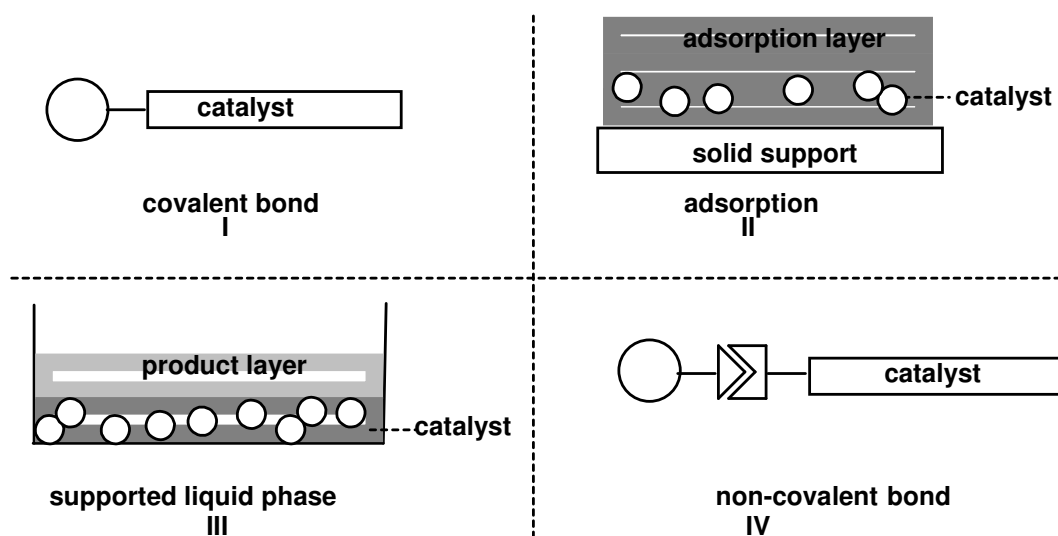


Figure 1.2 Different immobilization methods for transition metal complexes^[29]

A number of excellent articles of covalently and non-covalently immobilized catalysts have been published.^[5,15,27,30-34] Therefore, this chapter mainly focuses on non-covalent anchoring of homogeneous catalysts *via* ionic interactions. Furthermore, the immobilization *via* ionic interactions is strongly related to our concepts. Examples and highlights of their performance are presented.

1.3. Non-covalent anchorage of homogeneous catalysts *via* ionic interactions

1.3.1 Clays

The first example for the electrostatic immobilization of a chiral homogeneous catalyst on mineral clays was reported by Mazzei *et al.*^[35] in 1980.

Smectite clay minerals are swelling lattice silicates. They are distinguished by their large surface area and a high cation exchange capacity.^[36] These minerals have mica-type structures in which two dimensional silicate sheets are separated by monolayers of alkali- or alkaline earth metal cations. The silicate sheets are characterized by corner SiO_4 tetrahedra, which share 3 of its vertex oxygen atoms with other tetrahedra forming a hexagonal array in two-dimensions. The interlayer regions occupied by the alkali- or alkaline earth metal cations can be swelled up to 1000 Å by the adsorption of polar

solvents, such as water or alcohols, which allows the ion exchange of the interlayer cations with a large transition metal complex ion (Figure 1.3).

Mazzei and coworkers exchanged the interlayer cations with the $[\text{Rh}(\text{cod})(\text{P}^{\wedge}\text{P})]^+$ cations in the interlayer between the silicate layers *via* ion exchange in methanol. Mineral clays including hectorite ($\text{Na}_{0.4}\text{Mg}_{2.7}\text{Li}_{0.3}\text{Si}_4\text{O}_{10}(\text{OH})_2$), bentonite ($(\text{Na},\text{Ca})_{0.33}(\text{Al},\text{Mg})_2(\text{Si}_4\text{O}_{10})(\text{OH})_2 \cdot n\text{H}_2\text{O}$), halloysite ($\text{Al}_2\text{Si}_2\text{O}_5(\text{OH})_4$) and nontronite ($(\text{CaO}_{0.5},\text{Na})_{0.3}\text{Fe}^{3+}_2(\text{Si},\text{Al})_4\text{O}_{10}(\text{OH})_2 \cdot n\text{H}_2\text{O}$) were used. The Rh-loading was between 1.3 and 1.5 w%. It was observed that the heterogeneous catalysts were far more stable in the presence of H_2 than the homogeneous analogues.

In the asymmetric hydrogenation of prochiral substituted acrylic acids using the immobilized catalysts the optical yield of the hydrogenated product was similar to that of the homogeneous analogue (72-75%), depending on the used clays. In the hydrogenation of α -acetamidocinnamic acid (ACA) a significant decrease of enantioselectivity was observed comparing hectorite (49%), bentonite (9%) and nontronite (0%).

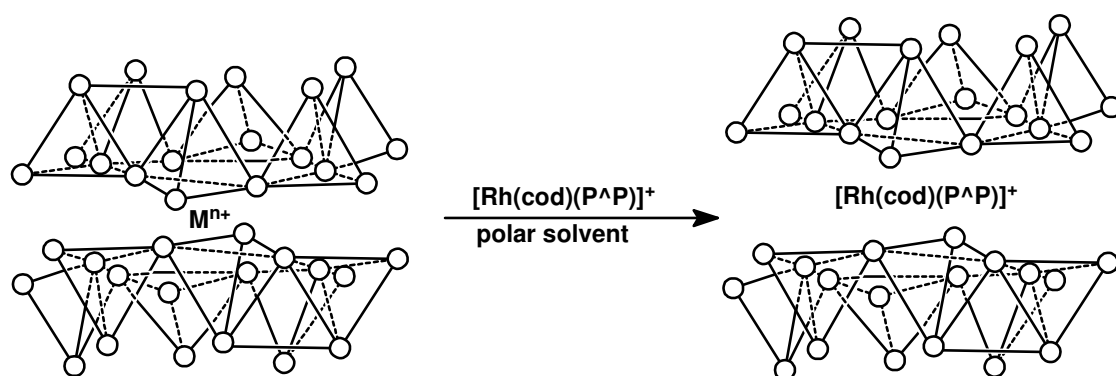


Figure 1.3 Depiction of swelling and immobilization of complexes using mineral clays as support

Shimazu *et al.*^[37] reported on the immobilization of $[\text{Rh}((S)\text{-BINAP})(\text{cod})]^+$ and $[\text{Rh}((S)\text{-}(R)\text{BPPFA})(\text{cod})]^+$ between the silicate sheets of the sodium hectorite clays in a $\text{CH}_3\text{CN}/\text{H}_2\text{O}$ mixture. Their investigations focused mainly on the catalytic behavior of the supported catalyst in the hydrogenation of α,β -unsaturated carbonyl compounds. Interestingly, the enantioselectivity is dependent on the interlayer spacing of the hectorite, which is dependent on the used solvents. It was postulated that by using 1-PrOH instead of MeOH as a solvent the interlayer space is less swollen. Thus, the limited interlayer space may enforce interactions between the active site of the catalyst (α -ester group) and substrate (face-phenyl group). In case of using the

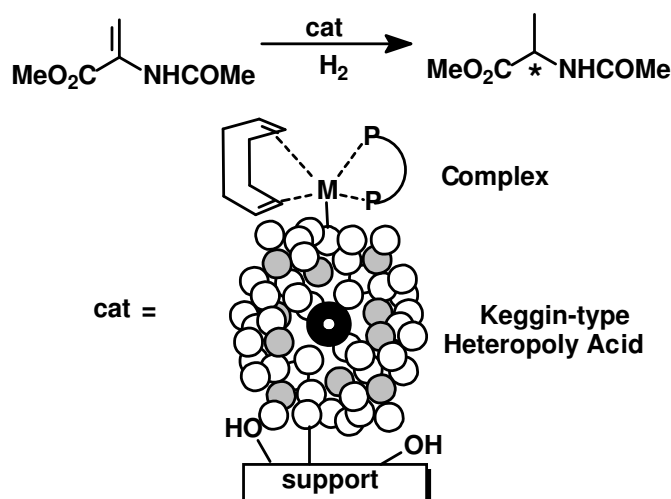
$[\text{Rh}((S)\text{-BINAP})(\text{cod})]^+$ and $[\text{Rh}((S)\text{-}(R)\text{-BPPFA})(\text{cod})]^+$ complexes this effect enhances the enantioselectivity of up to 66% (BINAP) and 84% (BPPFA) for the itaconate (ITA) precursors in comparison to the homogeneous analogues of 55% (BINAP) and 56% (BPPFA).

In contrast to the reported work of Shimazu *et al.*, Sento *et al.*^[38] demonstrated that the heterogeneous catalyst $[\text{Rh}(\text{DIOP})(\text{cod})]^+$ /hectorite showed lower enantioselectivity than the homogeneous catalyst in the hydrogenation of ITA precursors. For instance, in the hydrogenation of dibutylitaconate using $[\text{Rh}(\text{DIOP})(\text{cod})]^+$ /hectorite the enantioselectivity decreased to 1.4% with respect to the enantioselectivity of 29% using the homogeneous analogue. Here, the previously described effect of the reduced interlayer space takes also place, but results in a lowering of the enantioselectivity.

1.3.2 Heteropolyacids

Augustine *et al.*^[39] have pioneered the investigation of heteropolyacids as immobilization agents for ionic transition metal complexes. He reported the use of phosphotungstic acid (PTA) ($\text{H}_3\text{PW}_{12}\text{O}_{40}$) as agent to anchor a catalyst on a support such as carbon, Al_2O_3 , and montmorillonite ($(\text{Na,Ca})_{0.33}(\text{Al,Mg})_2(\text{Si}_4\text{O}_{10})(\text{OH})_2 \cdot n\text{H}_2\text{O}$). The catalyst carriers were synthesized by stirring an acid containing ethanolic solution of the support material. It was proposed that the hydroxyl groups of the acid interact with the support. The catalyst is anchored to the heteropolyacid through the oxygen atoms on its surface, which is shown in Scheme 1.1.

The heterogeneous catalysts $[\text{Rh}(\text{cod})(\text{P}^{\wedge}\text{P})]/\text{PTA}/\text{support}$ ($\text{P}^{\wedge}\text{P}$ = Dipamp, Prophos, Me-Duphos, Bophos, Skewphos) were used in the asymmetric hydrogenation of methyl-2-acetoamidoacrylate (Scheme 1.1). Interestingly, the enantioselectivity in the catalysis was enhanced relative to the enantioselectivity using the homogeneous analogues (76%). For instance, the enantioselectivity increased to 93% using the heterogeneous catalyst $[\text{Rh}(\text{cod})(\text{DiPamp})]/\text{PTA}/\text{Al}_2\text{O}_3$. The catalytic complexes could be reused up to 15 times with constant activity and selectivity. Furthermore, no Rh-loss was detected.



Scheme 1.1 Heterogeneous catalyst proposed by Augustine *et al.* for hydrogenation of methyl-2 acetoamidoacrylate

Furthermore, Augustine *et al.*^[40,41] reported that the benefits of using heteropoly acids are dependent on the type of acid. Keggin structures are the most common structural form for heteropoly acids. The general formula of these acids is $[\text{XM}_{12}\text{O}_{40}]^n$, where X is the heteroatom (most common are P^{5+} , Si^{4+} , or B^{3+}), M is the addenda atom (most common are molybdenum and tungsten).^[42] Phosphotungstic acid (PTA), silicotungstic acid ($\text{H}_4\text{Si}(\text{W}_3\text{O}_{10})_4 \cdot n\text{H}_2\text{O}$) (STA), phosphomolybdic acid ($\text{H}_3[\text{P}(\text{Mo}_3\text{O}_{10})_4]$) (PMA) and silicomolybdic acid ($\text{H}_4\text{SiMo}_{12}\text{O}_{40}$) (SMA) were used in this investigation. The enantioselectivity and the activity in the hydrogenation of dimethylitaconate (DMI) increased using strong acids, such as PTA ($[\text{Rh}(\text{cod})(\text{Me-DuPhos})]/\text{PTA}/\text{Al}_2\text{O}_3$ TOF=1050 h^{-1} ; $ee=97\%$) in comparison to weaker acids, such as SMA ($[\text{Rh}(\text{cod})(\text{Me-DuPhos})]/\text{SMA}/\text{Al}_2\text{O}_3$ TOF= 145 h^{-1} ; $ee=88\%$). The relative acidities of these Keggin acids is reported to be PTA > PMA > STA > SMA.^[43] Augustine *et al.* drew the conclusion that the most crucial parameter is the interaction of the acid with the metal. They further concluded that the heteropolyacid can be attached covalently or electrostatically to the transition metal complex. Thus, the interactions and the catalytic behavior in the catalytic process are different.

Brandts and coworkers^[44] used the concept developed by Augustine *et al.* to electrostatically anchor the Rh precursors $[\text{Rh}(\text{cod})_2]\text{BF}_4$ and $[\text{Rh}(\text{cod})\text{Cl}]_2$ on $\gamma\text{-Al}_2\text{O}_3$ using PTA. The resulting immobilized Rh precursors were treated with the chiral ligand (*R,R*)-Me-DuPhos to form the immobilized catalyst $\gamma\text{-Al}_2\text{O}_3/\text{PTA}/[\text{Rh}(\text{cod})((\text{R,R})\text{-Me-DuPhos})]\text{BF}_4$ and $\gamma\text{-Al}_2\text{O}_3/\text{PTA}/[\text{Rh}(\text{cod})((\text{R,R})\text{-Me-DuPhos})\text{Cl}]$, (Figure 1.4). Brandts

research was mainly focused on the influence of the anion of the immobilized metal complex in catalysis. The asymmetric hydrogenation of dimethyl itaconate indicated that the γ -Al₂O₃/PTA/[Rh(cod)((*R,R*)-Me-DuPhos)]BF₄ complex is twice as active as γ -Al₂O₃/PTA/[Rh(cod)((*R,R*)-Me-DuPhos)Cl]. For the BF₄ complex turnover frequencies of up to 19,000 h⁻¹ and enantioselectivities of 96% *ee* were achieved. The complexes were successfully reused several times and the Rh leaching could be minimized.

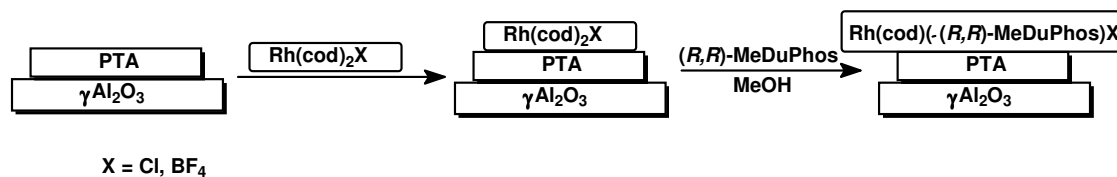


Figure 1.4 Immobilization of catalysts *via* heteropolyacids proposed by Brandts *et al.*

Recently, Zsigmond *et al.*^[45] reported the direct immobilization of the catalysts [Rh(nbd)((*2S,4S*)-bdpp-3,5-*X*-4-*Y*)]PF₆ (*X* = H, Me, *Y* = H; *X* = Me, *Y* = OMe) on PTA (loading of ~ 0.7 wt%) and the anchorage of the Rh precursor [Rh(nbd)Cl]₂ (~0.1 wt%) on the PTA with later *in situ* coordination of the chiral ligand.

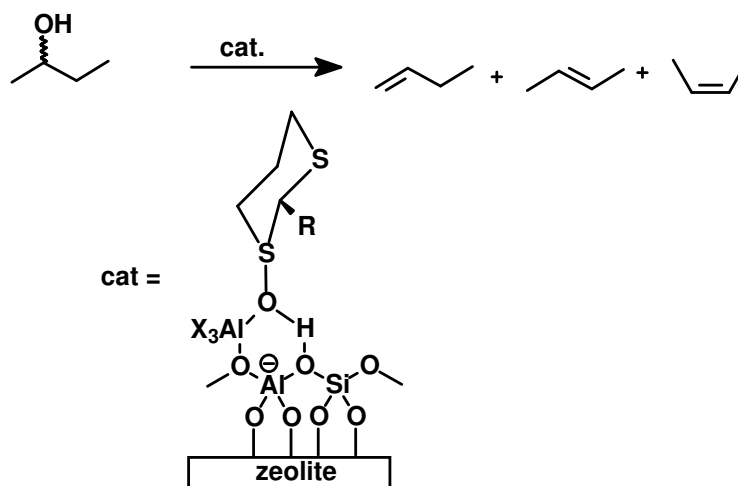
Interestingly, the heterogeneous catalysts were much more active in the asymmetric hydrogenation of methyl (*Z*)- α -acetamidocinnamate (MAC) and ACA (TOF up to 2000 h⁻¹ and *ee* up to 98.5%) compared to the homogeneous catalysts (TOF up to 180 h⁻¹; and *ee* up to 93%). It was proposed that this effect is due to the site isolation in the immobilized catalyst. The enantiomeric excess was above 90% in all experiments and the heterogeneous catalysts were reused for 3 times.

1.3.3 Zeolites

A very elegant method of electrostatic immobilization of cationic catalyst complexes is the use of mesoporous silica, such as zeolites as support. Zeolites have an "open" structure that can accommodate a wide variety of cations, such as Na⁺, K⁺, Ca²⁺, Mg²⁺ and others.

In 1996, Hutchings *et al.*^[46,47] reported on the electrostatic immobilization of catalysts on the acidic form of zeolite Y with chiral dithiane 1-oxides as chiral ligands (Scheme 1.2). This heterogeneous catalyst was used in the enantioselective dehydration of

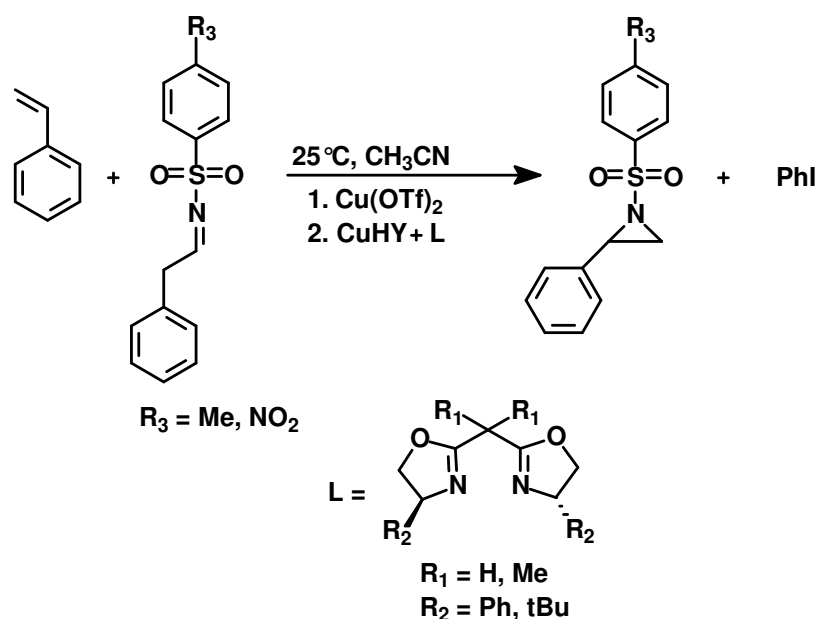
racemic butan-2-ol to butene. The kinetic resolution proceeds with a stereoselectivity factor s (k_s/k_r) of 39.5 leaving enantiomerically enriched (R)-butan-2-ol using the (R)-1,3-dithiane 1-oxide modified zeolite. It has been proposed that the enantioselective rate enhancement is due to the activation of the Brønsted acid group of the zeolite through interactions with the dithiane 1-oxide.



Scheme 1.2 Proposed active site of zeolite modified with dithiane oxide for the dehydration of 2-butanol

In expanded investigations, Hutchings *et al.*^[48] described the immobilization of copper-(II)-bis(oxazoline) complexes on zeolite Y and Al-MCM-41. A loading of 3-5 wt% catalysts was obtained.

The aziridination of alkenes using immobilized copper-(II)-bis(oxazoline) complexes (Scheme 1.3) gave an enantiomeric excess of 95% and good yields. Although, the catalyst was found to be rather stable, some catalyst loss was detected during the reaction. Interestingly, applying the heterogeneous catalyst, much higher enantioselectivities of up to 77% were achieved in comparison to the non-immobilized analogues (28%). The authors suggested^[49] that the Cu²⁺ is chelated by the bis(oxazoline) in the zeolite pores as a square planar complex, which places additional constraints on the approach of the substrate. Consequently, the enantioselectivity increased.



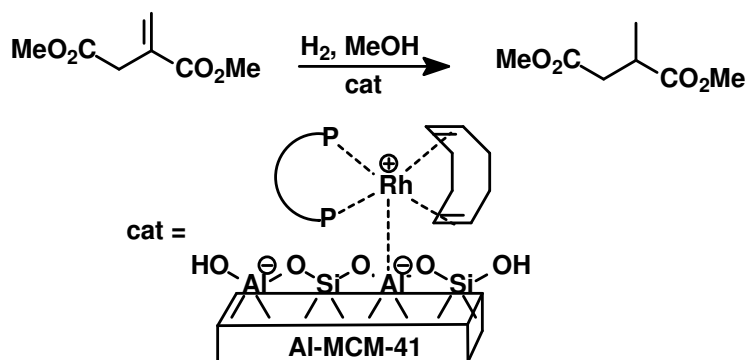
Scheme 1.3 Reaction scheme for the aziridination of styrene catalyzed by copper-bis(oxazoline)

Hutchings *et al.* applied immobilized copper-(II)-bis(oxazoline) complexes in the carbonyl-ene and imino-ene reactions^[50] and reported on the use of a chiral Mn(III)-salen complex immobilized on Al-MCM-41 in the enantioselective epoxidation of (*Z*)-stilbene.^[51] In addition, O'Leary *et al.* reported on the electrostatic immobilization of copper-(II)-bis(oxazoline) complexes on silica and their application in Diels-Alder reactions.^[52,53]

Hutchings *et al.*^[54] extended their methodology to support [Rh(cod)(Josiphos)]BF₄ and [Rh(cod){(*R,R*)-MeDuPhos}]BF₄ onto Al-MCM-41. The direct immobilization was obtained by stirring the Rh(I) complex with the acidic form of the support.

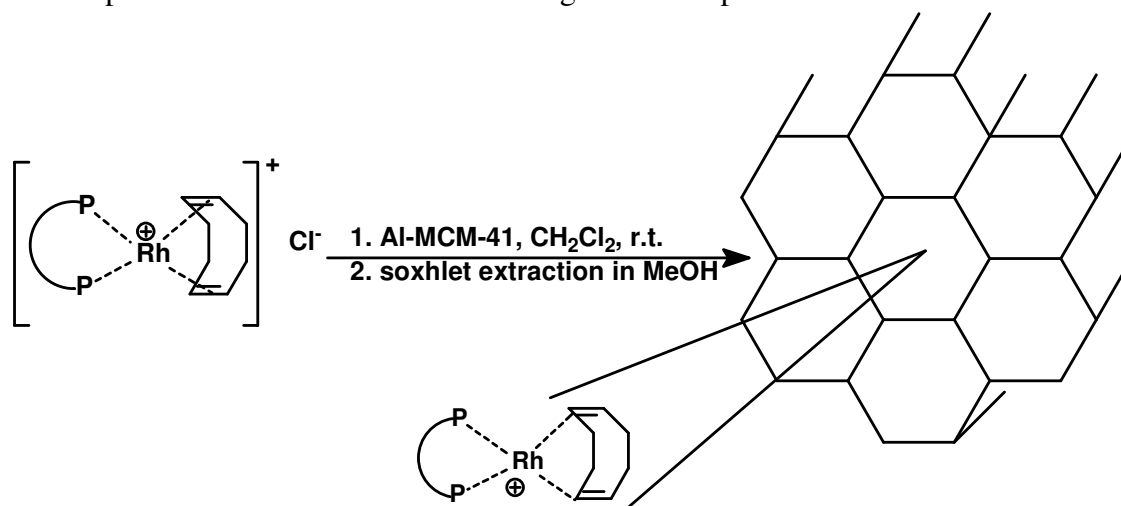
The resulted heterogeneous catalyst [Rh(cod){(*R,R*)-MeDuPhos}]/Al-MCM-41 was used in the asymmetric hydrogenation of DMI and methyl-2-acetamidoacrylate. The immobilized catalyst provides enantioselectivities (up to 99%) comparable to the homogeneous analogues even after 8 recycle runs. However, the activity decreased slightly on reuse. Also the hydrogenation of DMI using [Rh(cod)(Josiphos)]/Al-MCM-41 gave the same successful results as obtained using [Rh(cod){(*R,R*)-MeDuPhos}]/Al-MCM-41 (Scheme 1.4). By application of Al-SBA-15 as catalyst support, the catalyst was inactive and a significant amount of Rh leached out during catalysis. Hutchings *et al.* proposed that this effect is caused by the different structures of these zeolites. Al-SBA-15 is characterized by a one dimensional (1D) and Al-MCM-41 by a three dimensional (3D) structure, which allows more efficient diffusion of the substrate to the catalytic sites. Furthermore, the smaller pore size of the Al-MCM-41 results in a

decrease of free space for the substrate, which results in an enhancement of the enantioselectivity.



Scheme 1.4 Al-MCM-41 immobilized transition metal complexes for hydrogenation of DMI

Also Wagner *et al.*^[55] used Al-MCM-41 to immobilize Rh-diphosphine complexes. Initially, it was assumed that the cationic complex is impregnated on the support. (Scheme 1.5) For instance, electrostatic interaction of the cationic complexes occurs with the anionic framework of the support and also direct bridging of the rhodium to the surface oxygen of the mesoporous walls has been achieved. Several Rh-diphosphine complexes bearing chiral ligands, such as *S,S*-Me-Duphos, *R,R*-DIOP, *S,S*-Chriaphos and Norphos were immobilized. The loading of the complexes was around 0.5 wt%.



Scheme 1.5 Al-MCM-41 impregnated with transition metal complexes for hydrogenation of DMI

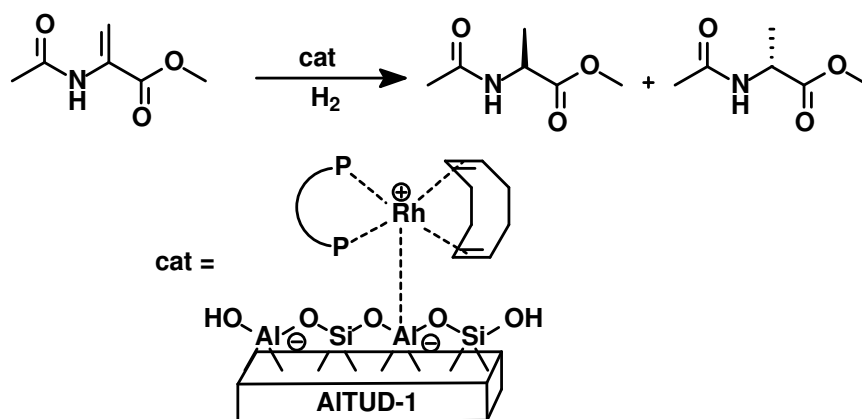
The heterogeneous catalysts were applied in the hydrogenation of DMI and it was observed that the Me-Duphos complex was the most efficient catalyst compared to the previous investigated ones. The turnover frequency was 166 h^{-1} and the enantiomeric

excess 92%. Furthermore, all catalysts were reused several times without significant Rh-leaching detected.

In further investigations^[56,57] $[\text{Rh}(\text{cod})(S,S\text{-Me-Duphos})]^+$ was immobilized on Al-MCM-48 and Al-SBA-15. Interestingly, different results were obtained for the hydrogenation of DMI. Using the $[\text{Rh}(\text{cod})(S,S\text{-Me-Duphos})]/\text{Al-MCM-48}$ in the catalysis, the turnover frequency (234 h^{-1}) and also the enantiomeric excess (98%) increased. Applying the catalyst immobilized on Al-SBA-15, an enantiomeric excess of up to 94% and a turnover frequency (TOF) of 44 h^{-1} was observed. It was suggested that these differences were due to the different structures of the zeolites. This effect was already described by Hutchings *et al.*^[54]

Simons *et al.*^[58,59] also reported on the electrostatic immobilization of $[\text{Rh}(\text{cod})(\text{MonoPhos})]\text{BF}_4$, $[\text{Rh}(\text{cod})\{(R,R)\text{-MeDuPhos}\}]\text{BF}_4$ and $[\text{Rh}(\text{cod})\{(S,S)\text{-DiPAMP}\}]\text{BF}_4$ complexes using the mesoporous aluminosilicate, Al-TUD-41. Al-TUD-41 has a high surface area, up to ca. $1000 \text{ m}^2\text{g}^{-1}$ and a three dimensional pore structure. The 3D pores should allow better access to the catalyst compared to 1D pore systems, such as MCM-41. The heterogeneous catalyst was synthesized by a simple ion exchange procedure.

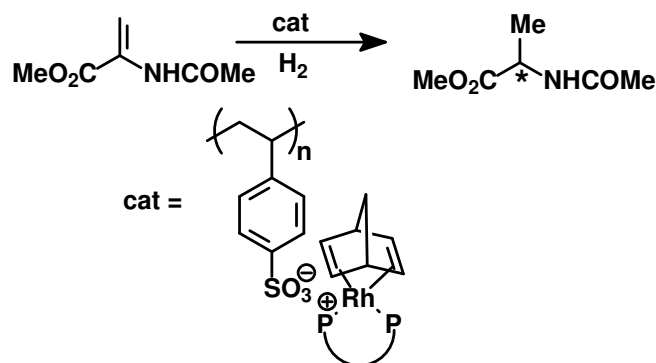
$[\text{Rh}(\text{cod})(\text{MonoPhos})]/\text{Al-TUD-41}$ is as active as the homogeneous catalyst in the asymmetric hydrogenation of methyl-2-acetamidoacrylate (Scheme 1.6) Enantioselectivities of up to 97% were obtained by varying the solvent. Application of the heterogeneous catalyst $[\text{Rh}(\text{cod})\{(R,R)\text{-MeDuPhos}\}]/\text{Al-TUD-41}$ in hydrogenation led to high enantioselectivity of up to 98% and a small increase in activity ($\text{TOF} > 1000 \text{ h}^{-1}$) compared to the homogeneous system.



Scheme 1.6 Rh-catalyst immobilized on AL-TUD-41 proposed by Simons *et al.* for hydrogenation of methyl-2 acetamidoacrylate

1.3.4 Ion exchange resins

Barbaro *et al.*^[60,61] electrostatically immobilized the $[\text{Rh}(\text{nbd})(+)\text{DIOP}]\text{PF}_6$ and $[\text{Rh}(\text{nbd})(-)\text{TMBTP}]\text{PF}_6$ on the lithium exchanged resin, Dowex 50WX2-100, which is a sulfonate gel-type resin. The non-covalently bound catalyst was prepared by stirring the resin with a methanol solution of the appropriate Rh(I) complex. The Rh-loading on the resin was found to be approximately 1 wt%.



Scheme 1.7 Rh-catalyst electrostatically immobilized on sulfonated ion exchange resin proposed by Barbaro *et al.* for hydrogenation of methyl-2 acetoamidoacrylate

By using the heterogeneous catalysts in the hydrogenation of methyl α -acetamidoacrylate (Scheme 1.7), similar activities and enantioselectivities were obtained relative to the homogeneous ones ((+)-DIOP yield 99.9%; *ee* 55%) ((-)-TMBTP yield 99.9%; *ee* 99.9%). The catalyst could be used for several cycles, although, the activity and selectivity decreased slightly. Only a small amount of metal loss (< 2%) was detected, which was mainly attributed to oxidation.

Oehme *et al.*^[62] electrostatically anchored the Rh-complex $[\text{Rh}(\text{cod})(\text{bppm})]\text{BF}_4$. In contrast to the other methods, the authors immobilized the catalyst within the hydrophobic surface layer produced by surfactants. These surfactants were covalently or electrostatically bound to several supports (Figure 1.5, I and II), such as silica, alumina, or a sulfonated ion exchange resin. The average loading was around 0.2 wt%. The heterogeneous catalyst was used in the asymmetric hydrogenation of MAC in water. Interestingly, the enantioselectivity was increased from 70% up to ~ 95% using the surfactants. The catalyst could be reused up to 10 times without significant loss of activity and only 0.12- 0.30 w% of Rh-leaching was detected.

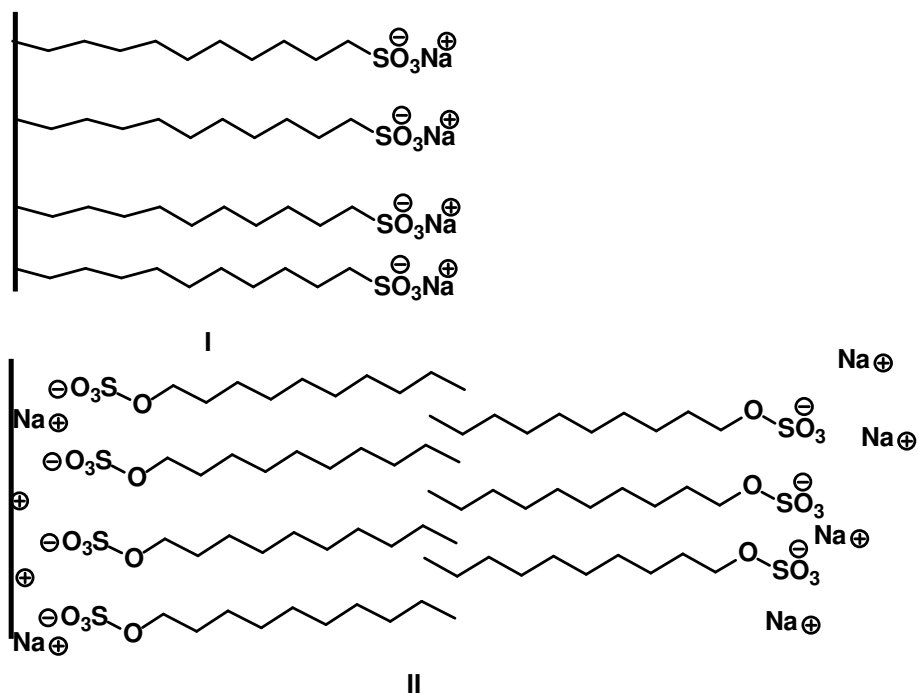
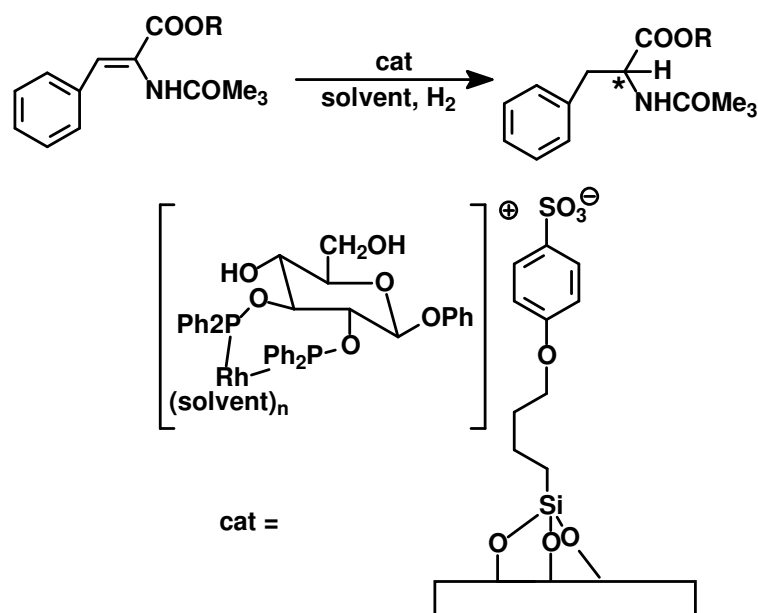


Figure 1.5 Possible interactions between surfactant and solid surface in water, suggested by Oehme *et al.*

Selke *et al.*^[63-66] reported on the immobilization of $[\text{Rh}(\text{cod})(\text{Ph}-\beta\text{-glup})]\text{BF}_4$ on a sulfonated polystyrene resin, crosslinked with 2% DVB. In this case the resin was converted into the acid form followed by the ion exchange with the catalyst.



Scheme 1.8 Rh-hydrogenation complex electrostatically immobilized on sulfonated polystyrene-resin

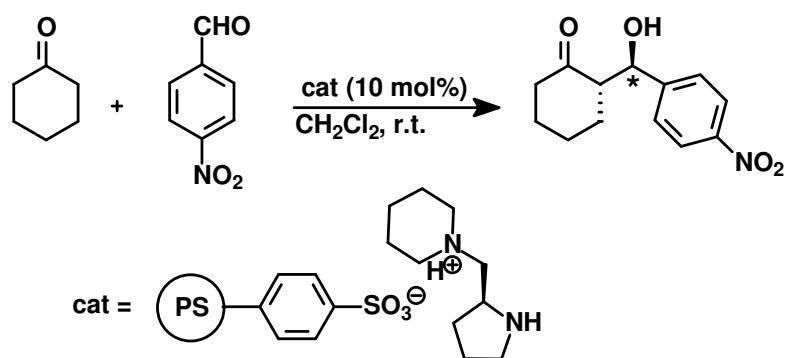
Although, the activity in hydrogenation of α -acylamidoacrylic acid ester using the heterogeneous catalyst decreased in comparison to the homogeneous analogues, the enantioselectivity increased up to 94% (Scheme 1.8).

This phenomenon is due to the acid hydrolysis of the ligand by the acid form of the resin. The catalyst could be reused for several times without significant Rh or ligand loss. Similar procedures were employed by Brunner *et al.*^[67] and Tóth *et al.*^[68,69]

Luo *et al.*^[70] investigated the use of polystyrene-based sulfonic acids as supports for chiral amine catalyst, used in asymmetric aldol reactions and Michael addition. Polystyrene was treated with chlorosulfonic acid in order to functionalize the polymer. Afterwards the polymer was simply treated with a solution of 1.2 equivalents of catalyst in CH_2Cl_2 . The loading of the catalyst was in line with the expected data and suggested that the active sites in the polystyrene-based sulfonic acids were available for the catalyst.

The heterogeneous catalysts were tested in the asymmetric direct aldol reaction and the asymmetric Michael addition. In the direct aldol reaction, it was observed that the catalyst loading influenced the activity and enantioselectivity. It was found that the optimal catalyst loading on the support was 1.09 mmol/g and CH_2Cl_2 the most suitable solvent.

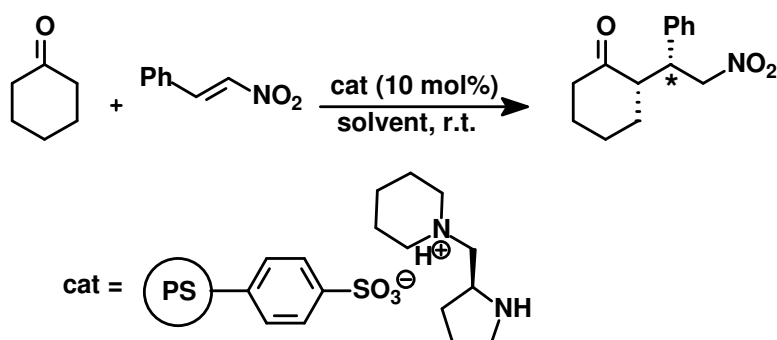
The best results in the reaction of cyclohexanone with benzylaldehyde were obtained using the chiral diamine (1*S*,2*S*)-(+)-*N,N*-Dimethyl diaminocyclohexane supported on a polystyrene-based sulfonic acid (loading 1 mmol/g) (Scheme 1.9). A conversion of 97% and an enantiomeric excess of up to 99% was achieved. Although, after the fourth and fifth cycle the activity decreased. It was proposed that this is caused by the deactivation of the catalyst. The catalyst could be reactivated by washing the reaction mixture with HCl/dioxane and recharging with the chiral diamine catalyst.



Scheme 1.9 Amine catalyst immobilized through acid-base interaction for Aldol addition

In the Michael addition reaction the best catalytic activity has been observed using the heterogeneously bound catalyst, depicted in Scheme 1.10. A diastereomeric excess of up to 96:4 and an enantiomeric excess of up to 90% respectively was observed.

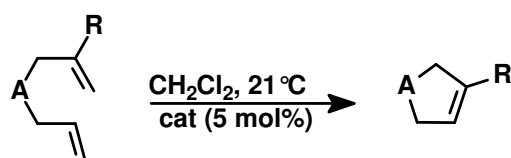
In the Michael addition of nitrostyrene to cyclohexanone, the catalyst could be reused while maintaining the same activity. After the 6th recycle run, the polymer support had to be reactivated and recharged with fresh catalyst. In both reactions the heterogeneous catalyst showed comparable or even better activity in comparison to the homogeneous ones.



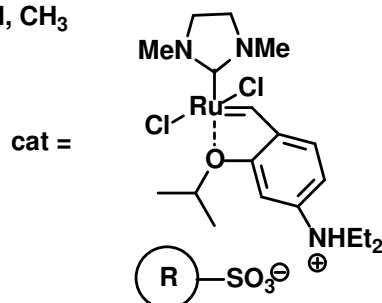
Scheme 1.10 Amine catalyst immobilized through acid-base interaction for Michael addition

Michrowsak *et al.*^[71] applied immobilized catalysts, anchored *via* ion exchange resins in the cross metathesis reaction. The olefin metathesis catalyst 1 (Scheme 1.11), bearing the electron-donating diethylamino group, was immobilized on several supports. The supports were an ion exchange resin, Dowex 50X2, an acidic ion exchange resin, consisting of very small particles (0.2-2 μm) and an indirect immobilization on glass-polymer composite Raschig rings.

The catalyst anchored to the Raschig rings, was the most active catalyst in the olefin metathesis of *N,N*-diallyl-4-methylbenzenesulfonamide to *N*-(*p*-Toluenesulfonyl)-3-pyrroline (conversion of 99.9%). However, the catalyst could be only reused for up to 6 runs with a gradual loss of activity.



A = NTs, C(CO₂Et)₂
 R = H, CH₃



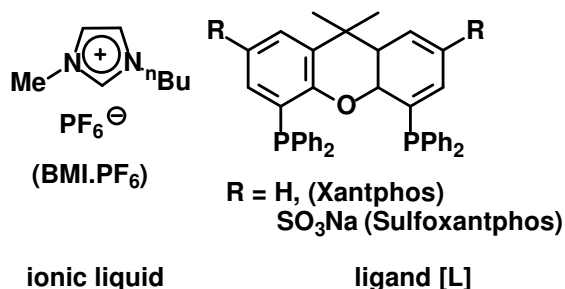
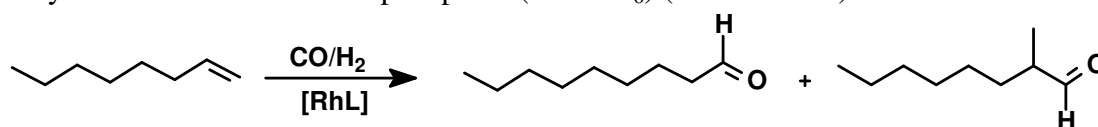
R = acidic ion exchange resin
 Dowex 50Wx2
 acidic ion exchange resin + Raschig rings

Scheme 1.11 Ion exchange resins as support for electron donating diethyl amino group-substituted catalysts for olefin metathesis

1.3.5 Ionic liquids

An important alternative for the immobilization of transition metal complexes is the biphasic organometallic catalysis using ionic liquids.

Dupont *et al.*^[72] and van Leeuwen *et al.*^[73,74] reported on the biphasic hydroformylation of higher alkenes such as 1-octene, 1-decene, and 1-dodecene using Rh(acac)(CO)₂/xantphos and Rh(acac)(CO)₂/sulfoxantphos immobilized in 1-*n*-butyl-3-methylimidazolium hexafluorophosphate (BMI.PF₆) (Scheme 1.12).



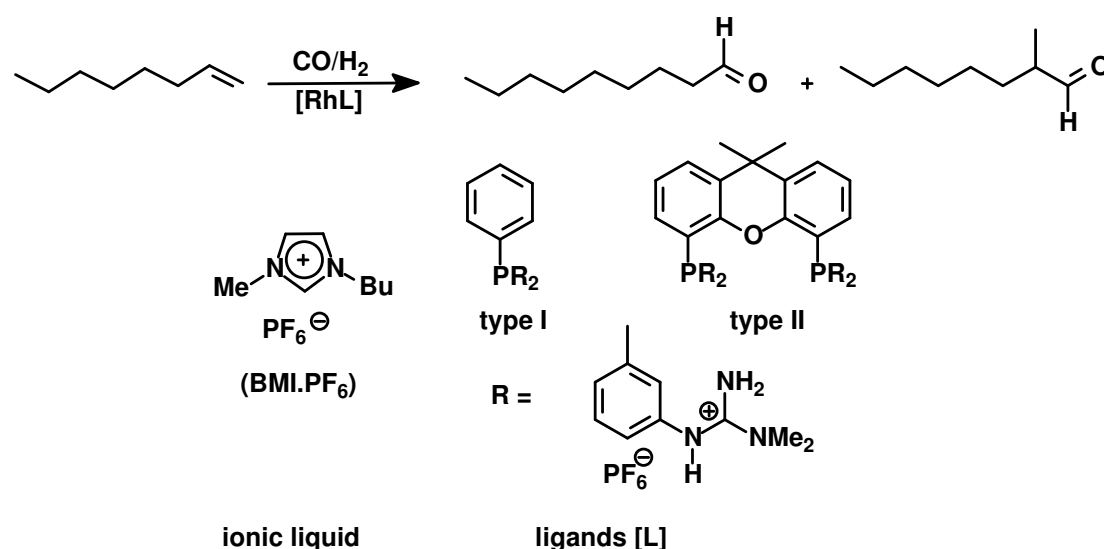
Scheme 1.12 Immobilized xanthene ligands in ionic liquid BMI.PF₆ for biphasic hydroformylation of 1-octene

The transition metal complex was immobilized by stirring a solution of catalyst in MeOH with the ionic liquid (BMI.PF₆). After this addition the volatiles were removed, which afforded an ionic liquid catalyst solution.

By using Rh(acac)(CO)₂/xantphos in BMI.PF₆, a TOF of up to 245 h⁻¹ and 99% conversion of 1-octene were reached. However, catalyst recycling proved to be difficult, since most of the catalysts had leached into the organic phase after the 1st recycle run.

The activity of Rh(acac)(CO)₂/sulfoxantphos in BMI.PF₆ was rather low compared to Rh(acac)(CO)₂/xantphos in BMI.PF₆ in the biphasic catalysis. Only a TOF of up to 41 h⁻¹ was obtained. However, it was possible to recycle the catalyst 5 times without significant Rh-loss. This effect is most probably caused by the fact that the sulfonated groups of xantphos interact with the ionic liquids by ion exchange, which is impossible in case of Rh(acac)(CO)₂/xantphos in BMI.PF₆.

Another example for the successful application of ionic liquids as immobilization medium was reported by Wasserscheid *et al.*^[75] In this particular case, the biphasic hydroformylation of 1-octene using cationic phosphine ligands containing phenylguanidinium moieties (type I) and guanidinium-modified xanthene (type II) immobilized in the ionic liquid (BMI.PF₆) were examined in detail (Scheme 1.13).

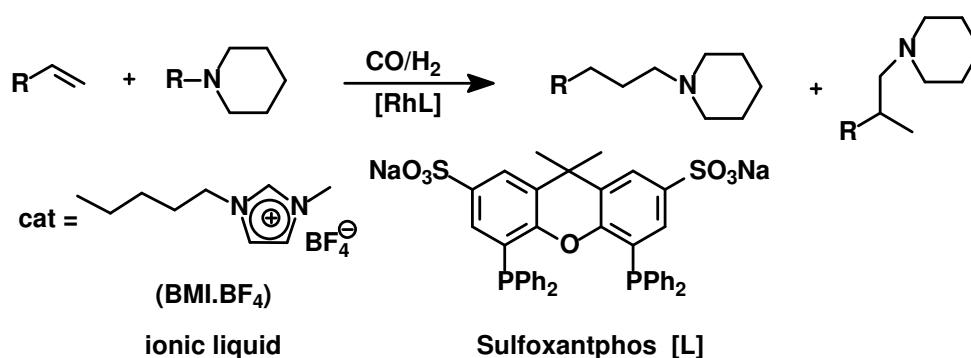


Scheme 1.13 Biphasic hydroformylation of 1-octene using cationic phosphine ligands containing phenylguanidinium moieties (type I) and guanidinium-modified xanthene (type II) immobilized in the ionic liquid [BMI.PF₆]

A TOF of up to 330 h^{-1} was reached after 3 runs using the ligand type I (Scheme 1.13) and only 0.7% of Rh-loss was detected. The activity is much higher in comparison to PPh_3 (100 h^{-1}) and NaTPPTS (80 h^{-1}) immobilized in BMI.PF_6 .

By using type II immobilized in the ionic liquid (BMI.PF_6) a TOF of up to 58 h^{-1} was reached after the 7th run in the biphasic hydroformylation. The Rh-leaching into the organic layer was found to be very low ($< 0.07\%$) and in all cycles good selectivity for the linear aldehyde (up to 21) was achieved.

Hamers *et al.*^[10] reported on the immobilization of $\text{Rh}(\text{acac})(\text{CO})_2/\text{sulfoxantphos}$ in the ionic liquid (BMI.BF_4). The catalytic system has been applied in the hydroaminomethylation of alkenes with piperidine (Scheme 1.14).



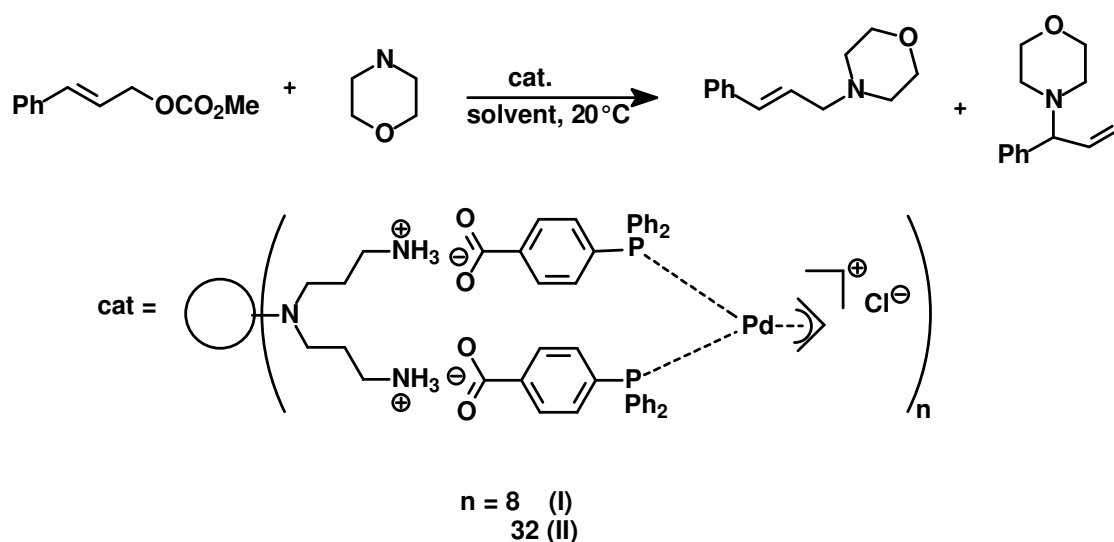
Scheme 1.14 Immobilized Sulfoxantphos in (BMI.BF_4) for hydroaminomethylation of n-alkenes with piperidine

The influence of different parameters such as temperature, reaction time, and substrate/Rh ratio was examined in the hydroaminomethylation using $\text{Rh}(\text{acac})(\text{CO})_2/\text{sulfoxantphos}$ in (BMI.BF_4). It was found that the optimal reaction conditions are $110 \text{ }^\circ\text{C}$, a reaction time of 4-6 h and a substrate/ Rh ratio < 1000 .

Furthermore, the catalytic system was recycled 3 times and a Rh-leaching of only 0.09% was detected. Moreover, it was observed that the catalyst was easily recycled by simple phase separation and high chemo- (up to 99%) and regioselectivities (linear/branched ratio of 52) were achieved.

1.3.6 Dendrimers

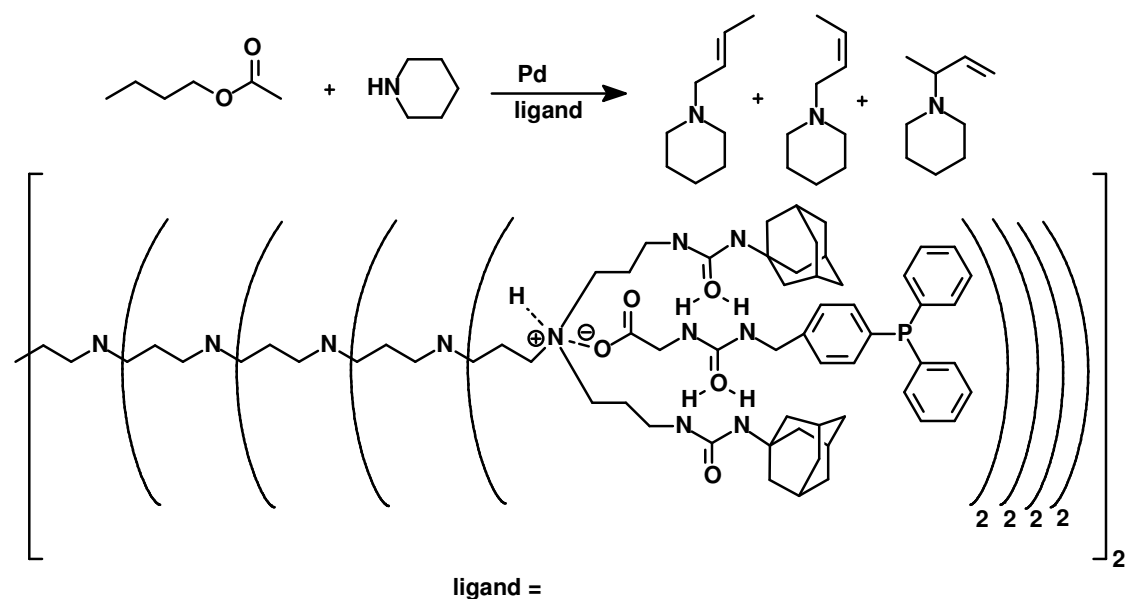
Another possibility to immobilize catalysts is demonstrated by Ooe *et al.*^[76] Palladium phosphine complexes could be electrostatically attached to the unmodified poly(propyleneimine) dendrimers. The immobilization was carried out in two steps. In the first step, 4-(diphenylphosphino) carboxylic acid was non-covalently anchored to the dendrimer's periphery *via* an acid-base reaction. This was followed by the addition of $[\text{PdCl}(\pi\text{-C}_3\text{H}_5)]_2$ to the reaction mixture which resulted in the dendrimer-supported Pd(II) complexes (Scheme 1.15, I, II). The supported catalyst was used in the allylic amination and displayed similar activities and selectivities as in the related homogeneous reactions. Moreover, a similar activity compared to the unsupported analogues was observed using a different Pd/P ratio. The highest activity was achieved using a ratio of 1:2.



Scheme 1.15 Dendrimer-supported Pd-complex for allylic amination

De Groot *et al.*^[77] reported on the synthesis of a non-covalently functionalized dendrimer with 32 phosphine ligands. These dendrimers were synthesized by the reaction of propylene imine dendrimers equipped with urea adamantyl groups and phosphorous ligands functionalized with urea acetic acid groups (Scheme 1.16).

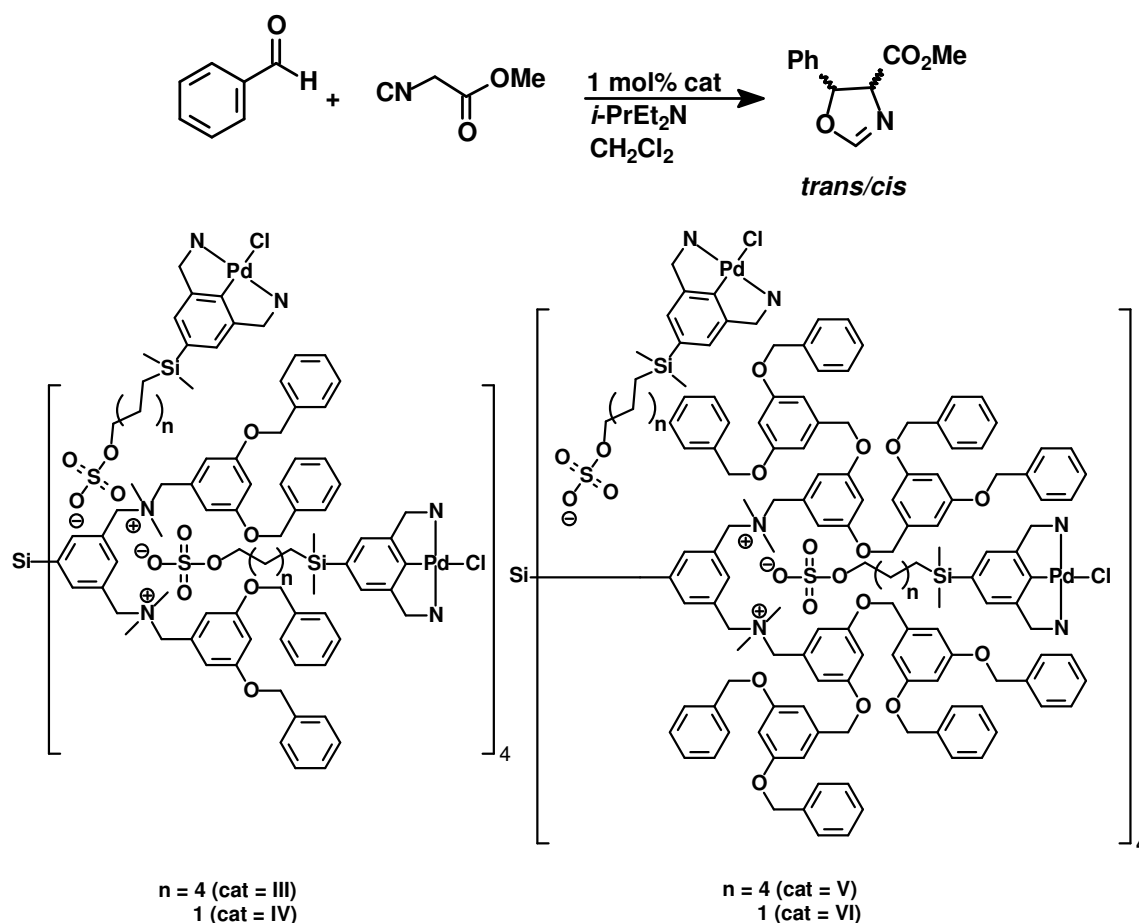
The resulting complex was applied in the palladium-catalyzed allylic amination reaction of crotyl acetate and piperidine under continuous conditions. A conversion of up to 80% was reached after 1.5 h. Remarkably, the supramolecular host-guest Pd complex could be retained in up to 99.4% by membrane filtration.



Scheme 1.16 Phosphine ligands assembled to the periphery of an urea adamantyl functionalized poly(propylene imine) dendrimer for allylic amination of crotylacetate and piperidine

Furthermore, van de Coevering *et al.* reported on the electrostatic immobilization of catalysts on dendrimers.^[78] The investigations focus on the synthesis of catalytic metallodendritic assemblies (Scheme 1.17) and the incorporation of a catalytic moiety with a positively charged Pd-center. The arylpalladium complexes were anchored to the first, second and third generation of octacationic core-shell dendrimers *via* ion exchange in CH₂Cl₂ (Scheme 1.17). The ratio between the octacationic dendritic supports and the Pd(II)-complexes as analyzed by ¹H NMR spectroscopy, resulting in a ratio of 1:8.

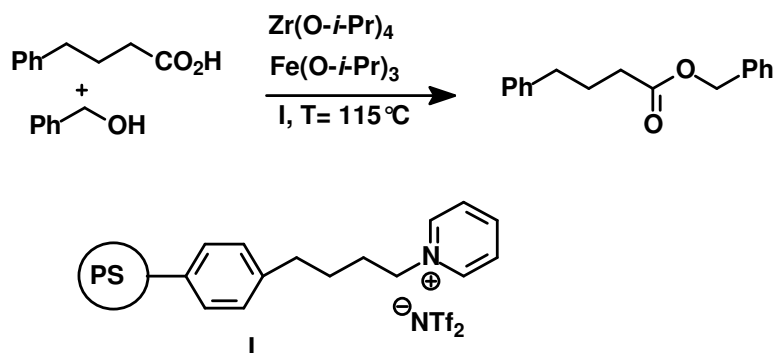
The metallodendritic assemblies were applied in the aldol condensation reaction between benzaldehyde and methyl isocyanoacetate to *cis/trans* oxazoline products. During the first hour the turnover frequencies (TOF of up to 17 h⁻¹) were slightly higher compared to the unsupported Pd(II)-complex (TOF= 12 h⁻¹). However the conversions of the aldol reaction after 24 h are lower (83-69%) in comparison to the unsupported Pd(II)-complex (95%). The stereoselectivity in terms of *cis* and *trans* oxazoline products remained almost the same comparing the supported and unsupported Pd(II)-complexes.



Scheme 1.17 Metallodendritic assemblies (first and second generation) for the aldol condensation reaction of benzaldehyde and methyl isocyanoacetate

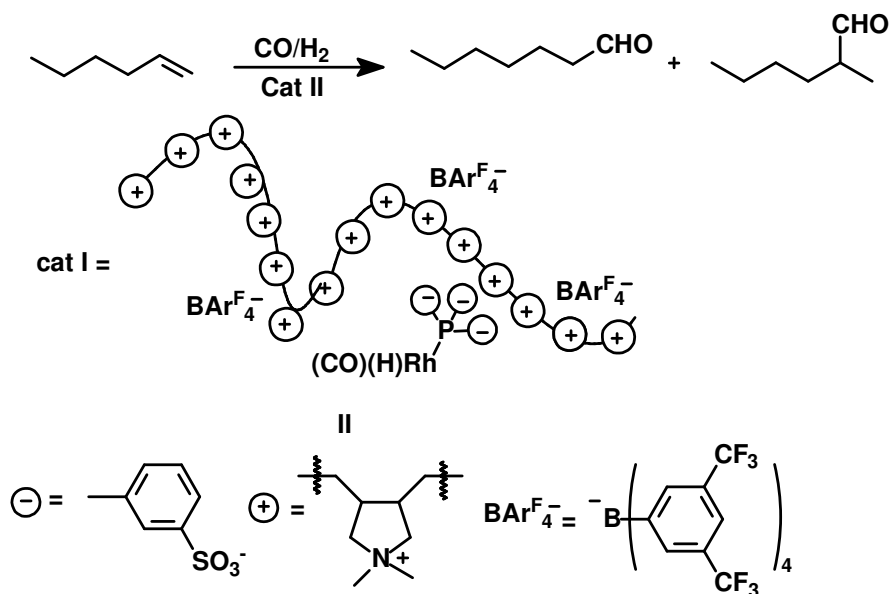
1.3.7 Other supports

Another immobilization method was established by Nakamura *et al.*^[79] They reported on the immobilization of a catalyst of the type I (Scheme 1.18) on *N*-(polystyrylbutyl)pyridiniumtriflyimides. These heterogeneous catalysts were applied in the esterification of a mixture of carboxylic acids and alcohols. The catalysts were reused for 10 recycle runs without any loss of activity. Interestingly, the Zr(IV)-Fe(III) catalysts were acting as a homogeneous catalyst in the presence of the carboxylic acids. After the consumption of the substrates the catalyst was re-immobilized on the support and could be reused.



Scheme 1.18 N-(polystyrylbutyl)pyridinium triflylimide supported Zr(IV)-Fe(III) catalysts for esterification

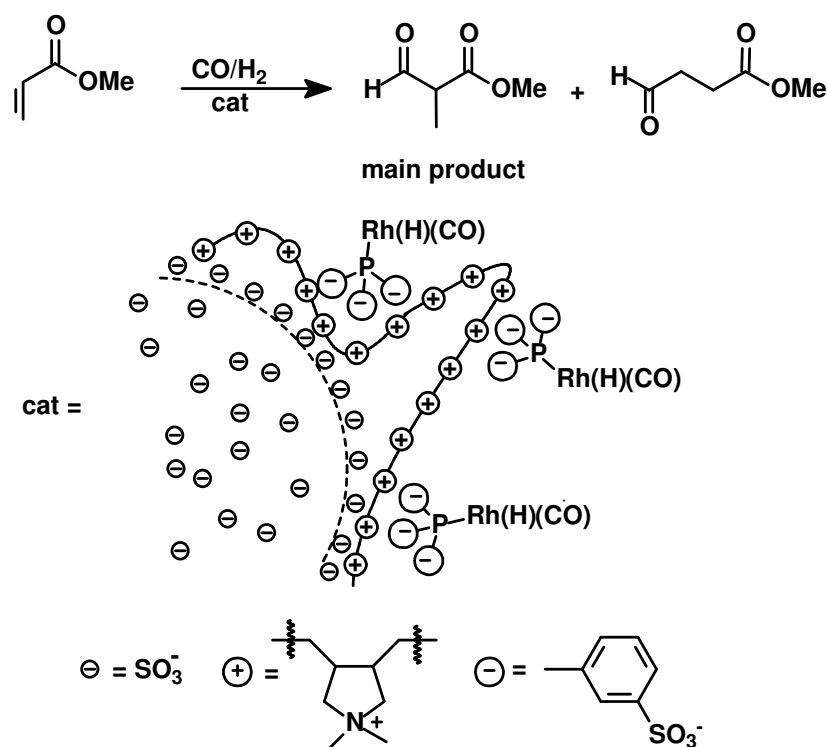
Schwab and Mecking^[80] electrostatically anchored the $[\text{HRh}(\text{CO})(\text{NaTPPTS})_3]$ complex to a soluble polyelectrolyte of the type II (Scheme 1.19). The support was synthesized by reacting poly(diallyldimethyl-ammonium chloride) with $\text{NaBAr}_4^{\text{F}}$. The catalyst was immobilized *via* ion-exchange of the multiple BAr_4^{F} anions with the catalyst. The resulting immobilized catalyst was applied in the hydroformylation of 1-hexene and comparable activities ($\text{TOF} = 160 \text{ h}^{-1}$) to the homogeneous systems could be obtained. The catalyst could be easily recovered from the reaction mixture by simple ultrafiltration, using a poly(ether sulfone) membrane supplied by Sartorius. A retention of 99.8% was observed and in the recycle runs virtually the same catalytic activity was obtained. A Rh-loss of 2-7% was observed. It was proposed that the Rh-leaching is most likely caused by the partial oxidation of the phosphine ligand.



Scheme 1.19 Polyelectrolyte as support for water-soluble Rh-hydroformylation catalyst

Furthermore Mecking and Thomann^[81] have reported on the investigation of latexes as immobilization agents for ionic transition metal complexes. The polystyrene-based latex particles, with particle sizes of 100-400 nm diameter were synthesized by copolymerization of styrene and potassium *p*-styrenesulfonate. The anionic particles were coated with an excess of the cationic polyelectrolyte poly(diallyldimethylammonium chloride) and the complex [(H)Rh(CO)(TPPTS)₃] containing tri-sulfonated ligands was bound to the polyelectrolyte-coated latex. The adsorption was analyzed by AAS resulting in 50% loading with respect to the capacity of the latex.

The resulting catalyst-coated latex was applied in the hydroformylation of methyl acrylate (Scheme 1.20). Turnover frequencies of 30 h⁻¹ were observed using the immobilized catalyst, which is rather similar to the homogeneous catalytic system. The main product obtained is the methyl 2-formylpropionate, which is in line with the literature results for non-immobilized systems. However, in recycling experiments a significant decrease of activity and a Rh-loss of ≤ 20% was observed. It was proposed that the Rh-leaching is most likely caused by leaching of the phosphine ligand and the formation of carbonyl complexes during the catalysis.



Scheme 1.20 Schematic representation of catalyst-coated latex for hydroformylation of methyl acrylate

Sablong *et al.*^[82] also reported on latexes as electrostatic supports for cationic Rh(I) complexes. The catalyst carriers, based on polymerizable *p*-styryltriphenylborate anions were easily obtained by emulsion polymerization. The resulting latex particles electrostatically interacted with transition metal complexes carrying a cationic charge on the metal itself. The redispersible polystyrene-based latex was stirred with a solution of the achiral catalyst in MeOH. The resulting immobilized catalyst [Rh(cod)(dppp)]BPh₃polymer (Figure 1.6) was used in the hydrogenation of ACA and could be reused for 6 recycle runs with constant activity and low metal leaching.

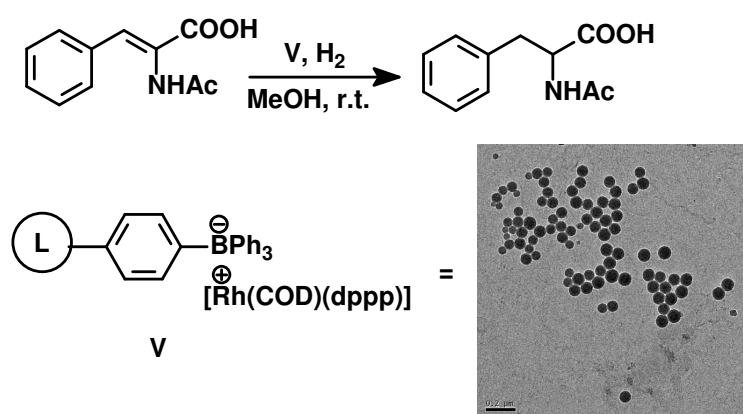


Figure 1.6 Borate-functionalized polystyrene-based latexes as support for cationic Rh-complexes, which can catalyze the hydrogenation of ACA

1.4. Aim and Scope of this Thesis

The aim of this thesis is to systematically explore different concepts for the electrostatic immobilization of catalysts and their application in the aqueous phase hydroformylation of higher alkenes, as well as in the asymmetric hydrogenation.

The influence of different support compositions and the influence of different solvents were examined in order to rationalize the results obtained in catalysis.

Chapter 2 is dedicated to the synthesis and characterization of polystyrene-based latexes as phase transfer agents. A series of latexes of different compositions were

synthesized and characterized. Thus, various styrylsalts, surfactants, Divinylbenzene (DVB) fraction, and monomers were prepared. The influence of the nature of the latex particles on the particle size, shape, and stability was examined *via* Dynamic Light Scattering (DLS), Transmission Electron Microscopy (TEM) and the zeta potential. Furthermore, from results of partitioning experiments promising perspectives for the use of these latexes in catalytic reactions could be drawn.

In **Chapter 3** the application of polystyrene-based latex particles as a phase transfer agent in the aqueous phase hydroformylation of higher alkenes is described. Within these studies the mass transfer limitations and the influence of latex compositions are discussed in detail. In terms of turnover frequency, the use of polystyrene-based latexes in the biphasic hydroformylations (TOF= 2000 h⁻¹) compares well with homogeneous systems (TOF= 3000 h⁻¹).

Chapter 4 focuses on the electrostatic immobilization of Rh(I) complexes on *p*-styryltriphenylborate-functionalized polymers. The immobilized complexes were applied in the hydrogenation of MAC, DMI and imines. Within these studies the solvent effect and the influence of the counterion in the hydrogenation reaction are discussed in detail.

Chapter 5 presents the possible future applications of latexes in catalysis. The Chapter discusses some preliminary results of new potential strategies to minimize the mass transfer limitation in the aqueous phase hydroformylation of higher alkenes. Therefore, the synthesis, characterization and application of latex-incorporated Nixantphos in the aqueous phase hydroformylation were examined.

1.5. References

- [1] B. Cornils, W. A. Herrmann, *Applied Homogeneous Catalysis with Organometallic Compounds*, 2nd Ed. Wiley-VCH, **2002**.
- [2] D. Vogt, in *Aqueous Phase Organometallic Catalysis- Concepts and Applications* (Eds.: B. Cornils, W.A. Herrmann) 2nd, Wiley-VCH **2004**, 541-547.
- [3] I. T. Horváth, J. Rábai, *Science* **1994**, 266, 72-75.
- [4] E. de Wolf, G. van Koten, B-J. Deelman, *Chem. Soc. Rev.* **1999**, 28, 37-41.
- [5] J. Horn, F. Michalek, C. C. Tzschucke, W. Bannwarth, *Top. Curr. Chem.* **2004**, 242, 43-75.
- [6] T. Welton, *Chem. Rev.* **1999**, 99, 2071-2083.
- [7] P. Wasserscheid, W. Keim, *Angew. Chem., Int. Ed.* **2000**, 39, 3772-3789.
- [8] P. Wasserscheid, T. Welton, *Ionic Liquids in Synthesis*, Wiley-VCH, Weinheim, Germany, **2003**.
- [9] W. Keim, D. Vogt, H. Waffenschmidt, P. Wasserscheid, *J. Catal.* **1999**, 186, 481-484.
- [10] B. Hamers, P. S. Bäuerlein, C. Müller, D. Vogt, *Adv. Synth. Catal.*, **2008**, 350, 332-342.
- [11] W. Miao, T. H. Chan, *Acc. Chem. Res.* **2006**, 39, 897-908.
- [12] S. Bektesevic, T. Tack, M.R. Mason, M.A. Abraham, *Ind. Eng. Chem. Res.* **2005**, 44, 4973-4981.
- [13] W. Leitner, *Acc. Chem. Res.* **2002**, 35, 746-756.
- [14] P. Stephenson, B. Kondor, P. License, K. Scovell, S. K. Ross, M. Poliakoff, *Adv. Synth. Catal.* **2006**, 348, 1605-1610.
- [15] R. van de Coevering, R. J. M. Klein Gebbink, G. van Koten, *Prog. Polym. Sci.* **2005**, 30, 474-490.
- [16] R. van Heerbeek, P.C. J. Kamer, P. W. N. M. van Leeuwen, J. N. H. Reek, *Chem. Rev.* **2002**, 102, 3717-3756.
- [17] R. Kreiter, A. W. Kleij, R. J. M. Klein Gebbink, G. van Koten, in *Dendrimer IV: Metal Metal Coordination Self-Assembly, Catalysis* (Eds.: F. Vögtle, C. A. Schalley,) Springer Verlag Berlin **2001**.
- [18] G. E. Oosterom, J. N. H. Reek, P. C. J. Kamer, P. W. N. M. van Leeuwen, *Angew. Chem. Int. Ed.* **2001**, 40, 1828-1849.
- [19] C. Müller, D. Vogt, in *Multiphase Homogeneous Catalysis* (Eds.: B. Cornils, W. A. Herrmann, I.T. Horváth, W. Leitner, S. Mecking, H. Olivier-Bourigou, D. Vogt) Chapter 7.4.1, Wiley-VCH **2005**, 776-793.
- [20] N. J. Ronde, D. Vogt, in *Recovery and Recycling of Homogeneous Catalysts* (Eds.: D. Cole-Hamilton, R.P. Tooze), Chapter 4, Springer Verlag **2005**.
- [21] C. Müller, M. G. Nijkamp, D. Vogt, *Eur. J. Inorg. Chem.* **2005**, 4011-4021.
- [22] P. Mc Morn, G. J. Hutchings, *Chem. Soc. Rev.* **2004**, 33, 108-122.

- [23] I. F. J. Vankelecom, P. A. Jacobs, in *Chiral catalyst Immobilization and Recycling* (Eds.: D. E. Vos, I. F. J. Vankelecom, P. A. Jacobs) Wiley-VCH, Weinheim, **2000**, 19-42.
- [24] C. E. Song, S. G. Lee, *Chem. Rev.* **2002**, *102*, 3495-3524.
- [25] C. Li, *Catal. Rev.* **2004**, *46*, 419-492.
- [26] R. Augustine, S. Tanielyan, S. Anderson, H. Yang, *Chem. Commun.* **1999**, 1257-1258.
- [27] D. E. Bergbreiter, *Chem. Rev.* **2002**, *102*, 3345-3384.
- [28] A.J. Goshe, I.M. Steele, C. Ceccarelli, A.L. Rheingold, B. Bosnich, *Proc. Natl. Acad. Sci.* **2002**, *99*, 4823-4829.
- [29] S. Luo, J. Li, L. Zhang, H. Xu, J. Cheng, *Chem Eur. J.* **2008**, *14*, 1273-1281.
- [30] R. Chen, R. P. J. Bronger, P. C. J. Kramer, P. W. N. N. Leeuwen, J. N. H. Reek, *J. Am. Chem. Soc.* **2004**, *126*, 14554-14566.
- [31] A. Corma, H. Garcia, *Top. Catal.* **2008**, *48*, 8-31.
- [32] B. Dooos, I. F. J. Vankelecom, P. A. Jacobs, *Adv. Synth. Catal.* **2006**, *348*, 1413-1446.
- [33] A. F. Masters, A. J. Ward, T. Maschmeyer, in *Phosphorus Ligands in Asymmetric Catalysis* (Eds.: A. Börner) 1st, Wiley-VCH **2008**, *3*, 1074-1100.
- [34] C. Müller, D. Vogt, in *Green Chemistry* (Eds. R. Crabtree), Wiley-VCH, in press.
- [35] M. Mazzei, W. Marconi, M. Riocci, *J. Mol. Cat.* **1980**, *9*, 381-387.
- [36] R. E. Grim, *Clay Mineralogy*, 2nd Edn. MacGraw-Hill, New York, **1968**.
- [37] S. Shimazu, K. Ro, T. Sento, N. Ichikuni, T. Uematsu, *J. Mol. Cat. A.: Chem.* **1996**, *107*, 297-303.
- [38] T. Sento, S. Shimazu, N. Ichikuni, T. Uematsu, *J. Mol. Cat. A.: Chem.* **1999**, *137*, 263-267.
- [39] R. Augustine, S. Tanielyan, S. Anderson, H. Yang, *Chem. Commun.* **1999**, 1257-1258.
- [40] R. L. Augustine, S. K. Tanielyan, N. Mathata, Y. Gao, A. Zsigmond, H. Yang, *Appl. Catal. A: General* **2003**, *256*, 69-76.
- [41] R. L. Augustine, P. Goel, N. Mahata, C. Reyes, S. K. Tanielyan, *J. Mol. Cat. A.: Chem.* **2004**, *216*, 189-197.
- [42] C.E. Housecroft; A.G. Sharpe. *Inorganic Chemistry*, 2nd Ed., Pearson Education Limited, **2005**, 660-662.
- [43] Y. Izumi, K. Urabi, M. Onaka, in *Zeolithe, Clay and Heteropoly Acid in Organic Reactions*, VCH, New York, **1992**.
- [44] J. A. M. Brandts, P. H. Berben, *Org. Proc. Res. Dev.* **2003**, *7*, 393-398.
- [45] A. Zsigmond, S. Undrala, F. Notheisz, A. Szöllösy, J. Bakos, *Appl. Catal. A: Gen.* **2006**, *303*, 29-34.
- [46] S. Feast, D. Bethell, P.C.B. Pate, F. King, C.H. Rochester, M. R. H. Siddiqui, D. J. Willock, G.J. Hutchings, *J. Chem. Soc., Chem. Commun.* **1995**, *23*, 2409-2411.

- [47] S. Feast, M. R. H. Siddiqui, R. P. K. Wells, D. J. Willock, F. King, C. H. Rochester, D. Bethell, P. C. B. Page, G. J. Hutchings, *J. Catal.* **1997**, *167*, 533-542.
- [48] S. Taylor, J. Gullick, P. McMorn, D. Bethell, P. C. B. Page, F. E. Hancock, F. King, G. J. Hutchings, *J. Chem. Soc., Perkin Trans. 2* **2001**, 1714-1723.
- [49] Y. Traa, D. M. Murphy, R. D. Farley, G. J. Hutchings, *Phys. Chem. Chem. Phys.* **2001**, *3*, 1073-1080.
- [50] F. E. Hancock, G. J. Hutchings, N. A. Caplan, Patent WO 03/018191, **2003**.
- [51] P. Piaggio, P. McMorn, D. Murphy, D. Bethell, P. C. B. Page, F. E. Hancock, C. Sly, O. J. Kerton, G. J. Hutchings, *J. Chem. Soc., Perkin Trans. 2* **2000**, 2008-2015.
- [52] P. O'Leary, N. P. Krosveld, K. P. De Jong, G. van Koten, R. J. M. Klein Gebbink, *Tetrahedron Lett.* **2004**, *45*, 3177-3180.
- [53] C. McDonagh, P. O'Conghaile, R. J. M. Klein Gebbink, P. O'Leary, *Tetrahedron Lett.* **2007**, *48*, 4387-4390.
- [54] W. P. Hems, P. McMorn, S. Riddel, S. Watson, F. E. Hancock, G. J. Hutchings, *Org. Biomol. Chem.* **2005**, *3*, 1547-1550.
- [55] H. H. Wagner, H. Hausmann, W. F. Hölderich, *J. Catal.* **2001**, *203*, 150-156.
- [56] A. Crosman, W. F. Hölderich, in *Enantioselective Hydrogenation Over Immobilised Transition Metal Complex Catalysts*, (EDs.: E van Steen, L. H. Callalan, M. Claeys) 14th International Zeolite conference, Cape Town, South Africa, The Catalysis Society of South Africa, Cape town, **2004**, 976-977.
- [57] A. Crosman, W. F. Hölderich, *J. Catal.* **2005**, *232*, 43-50.
- [58] C. Simons, U. Hanefeld, I. W. C. E. Arends, A. J. Minnaard, T. Maschmeyer, R. A. Sheldon, *Chem. Commun.* **2004**, 2830-2831.
- [59] C. Simons, U. Hanefeld, I. W. C. E. Arends, R. A. Sheldon, T. Maschmeyer, *Chem. Eur. J.* **2004**, *10*, 5829-5835.
- [60] P. Barbaro, *Chem. Eur. J.* **2006**, *12*, 5666-5675.
- [61] P. Barbaro, C. Bianchini, G. Giambastiani, W. Oberhauser, L. Morassi Bonzi, F. Rossi, V. Dal Santo, *Dalton Trans.* **2004**, 1783-1783.
- [62] H. N. Flach, I. Grassert, G. Oehme, M. Capka, *Colloid Polym. Sci* **1996**, *274*, 261-268.
- [63] R. Selke, *J. Mol. Catal.* **1986**, *37*, 227-234.
- [64] R. Selke, *J. Organomet. Chem.* **1989**, *370*, 241-248.
- [65] R. Selke, M. Capka, *J. Mol. Catal.* **1990**, *63*, 319-334.
- [66] R. Selke, K. Häupke, W. Krause, *J. Mol. Chem.* **1989**, *56*, 315-328.
- [67] H. Brunner, E. Bielsteiner, J. Wiehl, *J. Organomet. Chem.* **1990**, *284*, 223-241.
- [68] I. Tóth, B. E. Hanson, M. E. Davis, *J. Organomet. Chem.* **1990**, *396*, 363-373.
- [69] I. Tóth, B. E. Hanson, M. E. Davis, *J. Organomet. Chem.* **1990**, *397*, 109-117.

- [70] S. Luo, J. Li, L. Zhang, H. Xu, J. Cheng, *Chem Eur. J.* **2008**, *14*, 1273-1281.
- [71] A. Michrowsak, K. Menneke, U. Kuntz, A. Kirschning, K. Grela, *J. Am. Chem. Soc.* **2006**, *128*, 13261-13267.
- [72] J. Dupont, S. M. Silva, R. F. de Souza, *Catal. Lett.* **2001**, *77*, 131-133.
- [73] S. M. Silva, R. P. J. Bronger, Z. Freixa, J. Dupont, P. W. N. M. van Leeuwen, *New J. Chem.* **2003**, *27*, 1294-1296.
- [74] R. P. J. Bronger, S. M. Silva, P. C. J. Kamer, P. W. N. M. van Leeuwen, *Dalton Trans.* **2004**, 1590-1596.
- [75] P. Wasserscheid, H. Waffenschmidt, P. Machnitzki, K. W. Kottsieper, O. Stelzer, *Chem. Commun.* **2001**, 451-452.
- [76] M. Ooe, M. Murata, A. Takahama, T. Mizugaki, K. Ebitani, K. Kaneda, *Chem. Lett.* **2003**, *32*, 692-693.
- [77] D. de Groot, B. F. M. de Waal, J. N. H. Reek, A. P. H. J. Schenning, P. C. J. Kamer, E. W. Meijer, P. W. N. M. van Leeuwen, *J. Am. Chem. Soc.* **2001**, *123*, 8453-8458.
- [78] R. van de Coevering, A. P. Alferys, J. D. Meeldijk, E. Martinez-Viviente, P. S. Pregosin, R. J. M. Klein Gebbink, G. van Koten, *J. Am. Chem. Soc.* **2006**, *128*, 12700-12713.
- [79] Y. Nakamura, T. Maki, X. Wang, K. Ishihara, H. Yamamoto, *Adv. Synth. Catal.* **2006**, *348*, 1505-1510.
- [80] E. Schwab, M. Mecking, *Organometallics* **2001**, *20*, 5504-5506.
- [81] S. Mecking, R. Thomann, *Adv. Mater.* **2000**, *12*, 953-956.
- [82] R. Sablong, J. I. van der Vlugt, R. Thomann, S. Mecking, D. Vogt, *Adv. Synth. Catal.* **2005**, *347*, 633-636.

Synthesis and Characterization of Latexes as Phase Transfer Agents

A series of polystyrene-based latexes, consisting of various styrylsalts, surfactants, divinylbenzene as cross-linker, and monomers were synthesized by means of batch emulsion polymerization. The influence of different compositions on the particle size, shape and stability was examined by DLS, TEM, and zeta potential measurements. Furthermore, the prepared latexes were applied as phase transfer agents and quantified by partitioning experiments. Important conclusions could be drawn from the results and the potential of these latexes as phase transfer agents in catalytic applications.

2.1 Introduction

2.1.1 Motivation for the use of latexes

In homogeneous catalysis the recovery and reuse of expensive catalysts from the reaction mixtures is a crucial feature.

In order to provide generic solutions to this problem, a number of concepts have been developed and investigated, such as the immobilization of homogeneous catalysts on solid supports,^[1] supramolecular architectures, or the application of catalysts in *sc*CO₂.^[2-7] Another option is aqueous/organic biphasic catalysis. In this particular concept the catalysis takes place in the aqueous phase where the catalyst is situated. The substrate (Figure 2.1, **S**), is transferred into the aqueous phase and the products (Figure 2.1, **P**), which are nearly insoluble in water are separated into the organic phase (Figure 2.1, **I**).

Unfortunately this method is only suitable for substrates, which are partially water soluble. Otherwise the substrate cannot reach the catalyst and no reaction takes place.

In order to use also water-insoluble substrates the addition of a phase-transfer agent is a possible strategy. Examples for such agents are surfactants, cyclodextrins, and latexes. These additives (Figure 2.1, **II**) should transfer the lipophilic substrate, represented as **S** in Figure 2.1, into the aqueous phase where the catalysis is performed. Afterwards the lipophilic product, represented as **P** in Figure 2.1, is transferred back into the organic phase.

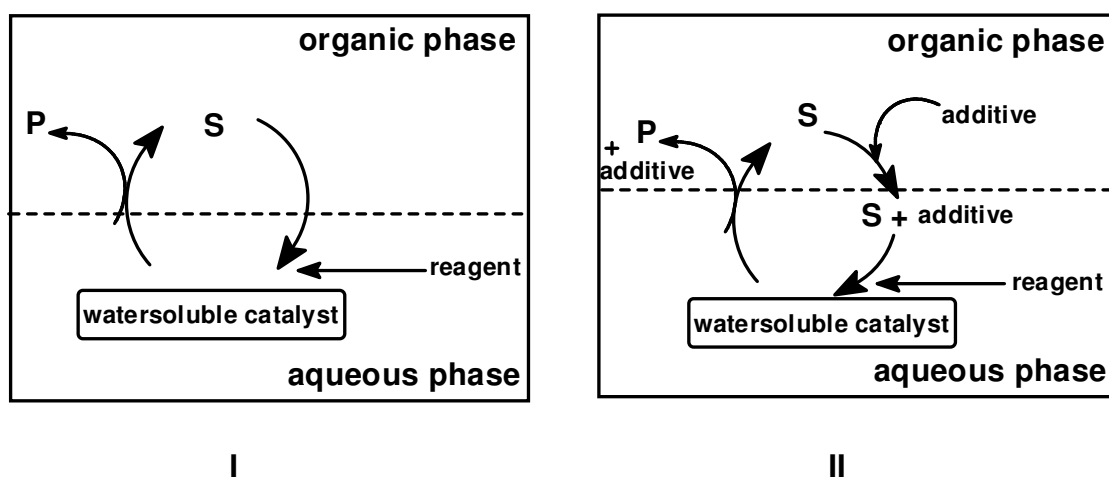


Figure 2.1 Schematic representation of an aqueous/biphasic catalysis (I) without any additives; (II) with a phase transfer agent

The application of cyclodextrins^[8-13] and microemulsions^[14-20] as phase transfer agents is well documented. However, to the best of our knowledge, latexes^[21,22] have hardly ever been considered as phase transfer agents for organic synthesis. On the other hand, latexes and microemulsions show quite some resemblance. Both consist of a lipophilic core and a hydrophilic shell. The only difference is the composition of the lipophilic core. In contrast to the core of microemulsions, which consists of an oil, such as alkenes or styrene etc., the core of latexes consists of organic polymers, such as polystyrene. Based on the latex composition, latexes are so called “macromolecular micelles”. The use of latexes is unique and innovative in contrast to the use of cyclodextrins and microemulsions, because:

- Cyclodextrins are too expensive for large scale application.
- Microemulsions are dynamic objects, which can easily fall apart, resulting in a leaching of surfactant into the organic phase.

Therefore, latexes can be considered as excellent phase transfer agents.

2.1.2 *Properties of latex particles*

Latexes are thermodynamically stable dispersions of submicron-sized polymer particles in water. The size of the particles range from 4 to 100 nm and their shape depends on the latex composition, leading to structures such as spheres, rods or disks.^[23,24] An example of a polystyrene-based latex is depicted in Figure 2.2.

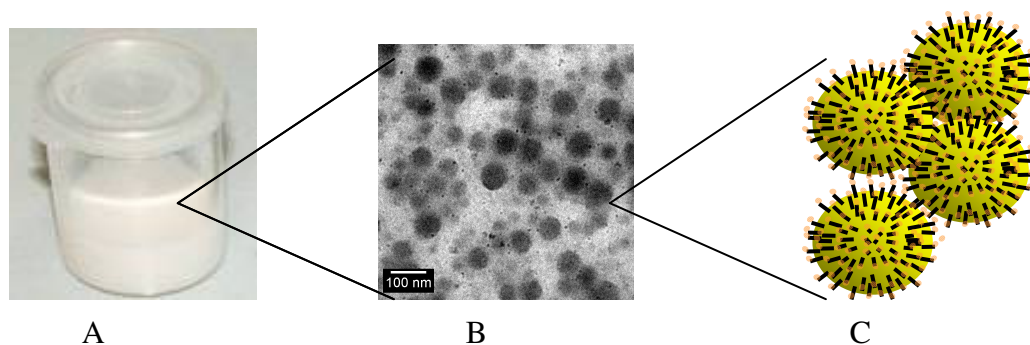


Figure 2.2 Picture of a polystyrene-based latex (A); TEM picture of the latex particles (B); schematic representation of the latex particles (C)

Nowadays, latexes are applied in industry in paints and coatings, textiles, non-wovens, packaging, construction (mainly in adhesives and binders), furniture, paper (e.g.,

coatings), medical equipment, personal protective equipment, carpet backing, adhesives, polish, belts, seals, etc. The market for latexes has expanded dramatically. The capability of microemulsions to solubilize a very broad spectrum of substances in one single formulation has found many technical applications, such as excellent surface cleaning agents.^[25]

Conventional latex particles consist of a lipophilic core of organic polymers and a hydrophilic shell of surfactants. The latex particles are stabilized by the hydrophilic surfactant, while the lipophilic core can absorb organic compounds.

Due to the amphiphilic properties (Figure 2.3) the benefits of utilizing latexes as media for organic reaction include the elimination of solubility problems of reactants. Moreover, the partitioning and concentration of reactants around the catalyst can lead to a rate enhancement in contrast to an one-phase system. In addition, the resulting large oil-water interface of the system can/might be used as support for catalysts.

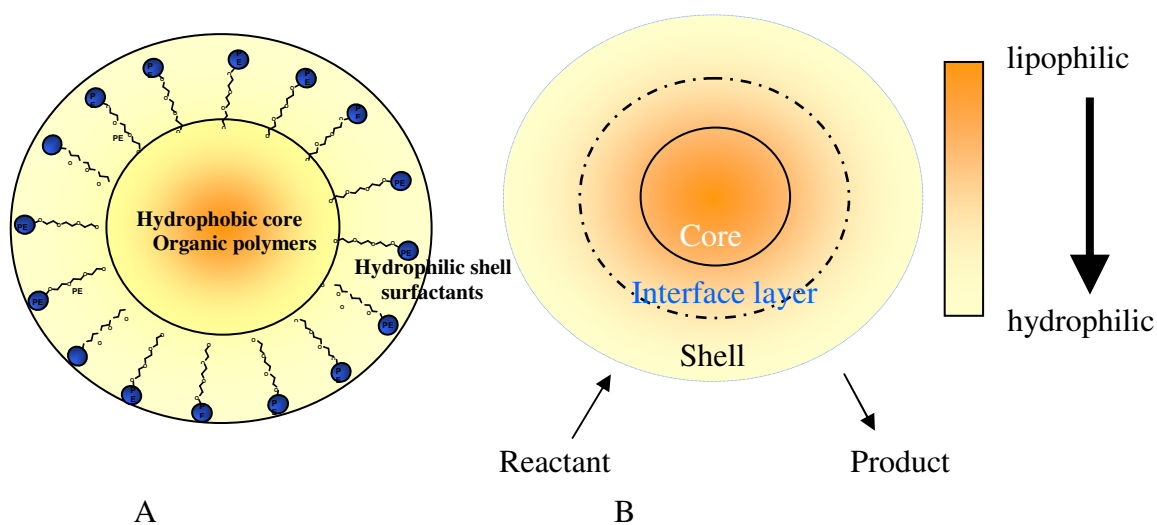


Figure 2.3 (A) Composition of a latex particle; (B) Schematic representation of the amphiphilic properties of latex particles

We expect that these properties (Figure 2.3) provide the possibility to use latexes as phase transfer agents and immobilization supports for example in the biphasic hydroformylation of higher alkenes using water soluble catalyst.

2.1.3 *Synthesis of Latexes*

Latexes are synthesized by emulsion polymerization. The emulsion polymerization is a free-radical initiated polymerization where a monomer or a mixture of monomers is dispersed in water by means of a surfactant. An emulsion polymerization can be performed using three different common processes: batch, semi-continuous (or semi batch) and continuous^[26] polymerization.

A reaction mixture for an emulsion polymerization contains monomer, water, initiator, surfactant, and sometimes a buffer and/or chain transfer agents.^[27]

The lipophilic droplets in an emulsion polymerization largely comprise of monomers with a limited solubility in water. The most common monomers are styrene, butadiene, vinyl acetate, acrylate and methylacrylates, acrylic acid, and vinyl chloride.

The most common water-soluble initiators used in the laboratory are potassium and ammonium salts of persulphate salts. Often water-soluble azo-compounds, especially those containing an ionic group, such as 2,2'-azobis(2-methylpropionamide) dihydrochloride (V-50) or 2,2'-Azobis[2-methyl-N-(2-hydroxyethyl)propionamide] (VA-086) are used. In cases where the polymerization has to be performed at lower temperatures (below 50°C), a redox system, such as Rongalite, can be used (Figure 2.4). Another way to create free radicals is for instance the use of γ -radiation.

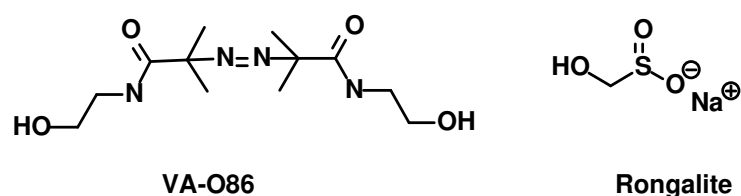


Figure 2.4 Emulsion polymerization initiators

The surfactant,^[28] a surface active agent, is also referred to as an emulsifier, soap or stabilizer. A surfactant consists of hydrophilic and hydrophobic segments and exhibits the tendency to self assemble on oil-water interfaces. Important purposes of these reagents within an emulsion polymerization are the emulsification of the monomer droplets, the generation of micelles and the stabilization of the growing particles leading to a stable emulsion. Surfactants can be classified according to the hydrophilic group, such as anionic, cationic, amphoteric or non-ionic. Another classification divides them as polymeric stabilizer or electrostatic stabilizer. Another surfactant class is the

reactive surfactant. In this particular case, the reactive surfactant is bound covalently rather than electrostatically to the particle. They can be a combination of a surfactant and an initiator (inisurf), a surfactant and a transfer agent (transurf), or a surfactant and a monomer referred to as a surfmer. The advantages of using reactive surfactants include the reduction of total surface active matter by increasing of particle stability, redisperse capability and latex particle surface functionalization.

Polyelectrolytes can be added as a buffer, preventing hydrolysis and maintaining the efficiency of the initiator.

The latexes prepared within this work were synthesized via batch emulsion polymerization, because it is the easiest procedure. All the ingredients, i.e. water, surfactant, monomer, and initiator, are charged into the autoclave before the start of the reaction.

In general a batch emulsion polymerization can be subdivided into three intervals,^[29,30] as depicted in Figure 2.5.

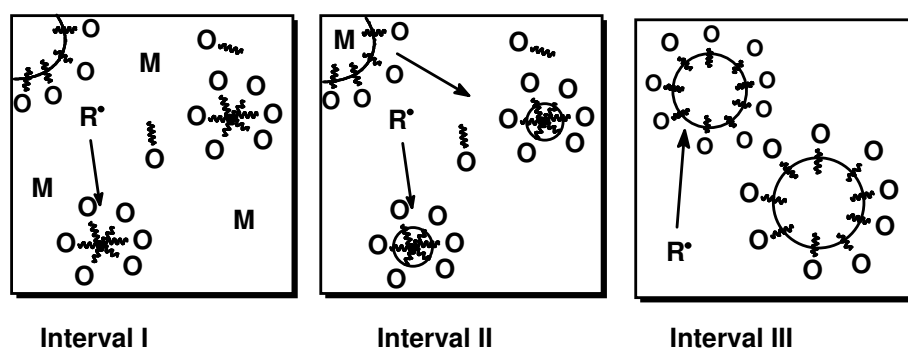


Figure 2.5 Schematic representation of the three intervals of an emulsion polymerization M: monomer; R^{*}: radical generated by the initiator, $\text{---}\text{O}$: surfactant molecule

The reaction mixture initially consists of monomer droplets stabilized by the surfactant, monomer-swollen surfactant micelles, and small amounts of monomer dissolved in a continuous aqueous phase.

The polymerization starts in Interval I, also referred to as the nucleation stage. Radicals generated from the dissociation of a water-soluble initiator react with the monomer present in the water phase. This reaction results in the formation of monomeric radicals, which undergo the different reactions related to conventional free-radical polymerization.

The particle nucleation is a complex process. The three mechanisms of particle formation are droplet, homogeneous, and micellar nucleation:

Droplet nucleation predominates in miniemulsion and microemulsion polymerizations^[27] and it occurs, when radicals, generated in the water phase, enter the monomer droplets and propagate to form particles.

If radicals do not enter the particle and the oligoradicals continue to grow in the water phase, they are rendered insoluble in the water phase at a critical chain length (z-mer). At this point they precipitate to form a primary particle. These particles adsorb surfactant molecules to increase their stability and adsorb monomer to propagate. This mechanism describes homogeneous nucleation.^[31-34]

The third mechanism of particle formation is micellar nucleation proposed by Harkins *et al.*^[35] The monomeric oligomeric radicals grow to a z-mer. Above this critical chain length, the radicals become surface active and enter the monomer-swollen micelles, thereby creating particles.

The three mentioned mechanisms of particle nucleation may occur simultaneously. However, their contribution is mostly dependent on the surfactant concentration and the monomer water solubility.

Most probably in our investigations the homogeneous nucleation and the micellar nucleation is taking place, due to fact that we used reactive surfactants. They need to become firstly surface active (z-mer), before a particle can be formed.

The end of Interval I (Figure 2.5) is marked by the disappearance of all micelles. The Interval II, which is shown in Figure 2.5, is characterized by a constant number of particles and the presence of monomer droplets. The monomer-swollen particles grow and the monomer concentration within the particles is kept constant by monomer that diffuses through the water phase from the monomer droplets. The Interval II is finished right after the disappearance of the monomer droplets. During Interval III (Figure 2.5) the monomer in the particles is polymerized. The end of Interval III is marked by the depletion of monomer in the particles and in the water phase.

The particles are growing over the whole period of emulsion polymerization and the intervals are comprehensive.^[36]

In this chapter, the synthesis and characterization of polystyrene-based latexes is presented.

Furthermore, the application of the produced latexes as phase transfer agents in partitioning experiments with higher alkenes is discussed in detail.

2.2 Synthesis of polystyrene-based latexes

All polystyrene-based latexes applied in the present work were synthesized following the procedure reported by R. Sablong *et al.*^[37] We considered polystyrene as organic polymer for the lipophilic core, because it is rather stable at higher temperatures and relative rigid in comparison to other polymers.

This procedure consists in the batch addition of the polymerization ingredients. The functionalized styrylsalt was dissolved in water and heated to 80°C, followed by the addition of styrene and divinylbenzene (responsible for the lipophilic core of the latex particles) and the initiator VAO86, see Figure 2.3. In contrast to the reported method where no reactive surfactant was added to the emulsion mixture, the addition of the reactive surfactant, which is responsible for the stability and the building of the hydrophilic shell of the particles, was necessary. This addition is due to the fact that the functionalized styrylsalt, we chose to apply could not act as surfactant. In order to remove impurities, the latexes were dialyzed. All latexes were further characterized by means of TEM and DLS.

Several latex compositions were investigated in order to examine the influence of latexes as a phase transfer agents in catalysis. Different styrylsalts, surfactants, divinylbenzene (DVB) fractions and monomers were used and the resulted latexes are depicted in Table 2.1.

The latex influence as phase transfer agent in catalysis will be presented and discussed in Chapter 3.

Different styrylsalts such as sodium *p*-styrenesulfonate and *p*-vinylbenzyltrimethylammonium tetraphenylborate were used in the emulsion

polymerization shown in Figure 2.6. The ionic groups present the possibility for electrostatic immobilization of water-soluble catalysts.

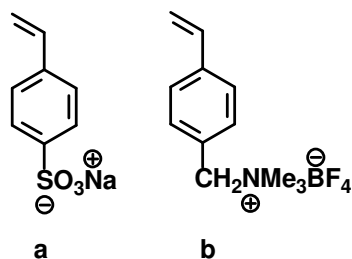


Figure 2.6 Schematic drawings of applied styrylsalts

In order to stabilize the latex particles and to examine the influence of the surfactant, three reactive surfactants (surfmers) were used; each containing a polyethyleneglycol (PEG) chain. PEG's of 3 different chain length were used, namely 360 g/mol (**1**), 1650 g/mol (**2**) and 3000 g/mol (**3**). The schematic structures are depicted in Figure 2.7.

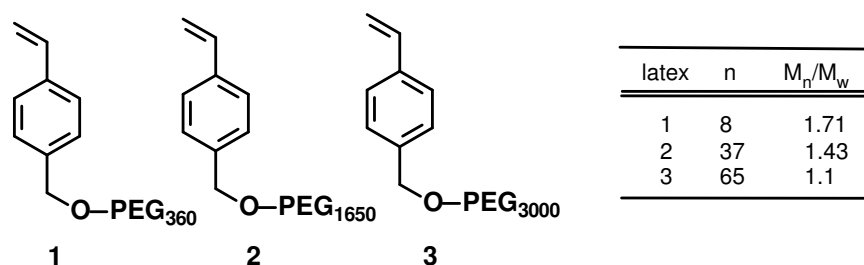


Figure 2.7 Schematic drawings of used surfactants

Furthermore, the amount of DVB as crosslinking agent was varied from 0- 5 mol%. We were interested in the influence of the crosslinking degree with respect to the behavior as a phase transfer agent.

Different mixtures of monomers were investigated as well. Styrene (S) was copolymerized with methyl methacrylate (MMA), *n*-butyl methacrylate (BMA) and lauryl methacrylate (laurylMA). The different comonomers are depicted in Figure 2.8. Thus, the rigidity of the latex particles was modified and also the behavior of the latex particles as phase transfer agent.

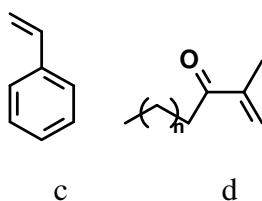


Figure 2.8 Monomers used in the emulsion polymerization (c) styrene, (d) methacrylates n: 0, 3, 13

Table 2.1 Composition of the applied latexes

Latex	Monomer	DVB [mol%]	Styrylsalt	Surfactant
1	S	2	-	PEG ₃₀₀₀
2	S	2	PS-SO ₃ Na	PEG ₃₀₀₀
3	S	2	PS-CH ₂ NMe ₃ BF ₄	PEG ₃₀₀₀
4	S	2	PS-SO ₃ Na	PEG ₁₆₅₀
5	S	2	PS-CH ₂ NMe ₃ BF ₄	PEG ₁₆₅₀
6	S	2	PS-SO ₃ Na	PEG ₃₆₀ ^a
7	S	2	PS-CH ₂ NMe ₃ BF ₄	PEG ₃₆₀
8	S	0	PS-CH ₂ NMe ₃ BF ₄	PEG ₁₆₅₀
9	S	1	PS-CH ₂ NMe ₃ BF ₄	PEG ₁₆₅₀
10	S	3	PS-CH ₂ NMe ₃ BF ₄	PEG ₁₆₅₀
11	S	4	PS-CH ₂ NMe ₃ BF ₄	PEG ₁₆₅₀
12	S	5	PS-CH ₂ NMe ₃ BF ₄	PEG ₁₆₅₀
13	S/MMA (1:1)	2	PS-CH ₂ NMe ₃ BF ₄	PEG ₁₆₅₀
14	S/BMA (1:1)	2	PS-CH ₂ NMe ₃ BF ₄	PEG ₁₆₅₀
15	S/BMA (1:9)	2	PS-CH ₂ NMe ₃ BF ₄	PEG ₁₆₅₀
16	S/laurylMA (1:1)	2	PS-CH ₂ NMe ₃ BF ₄	PEG ₁₆₅₀

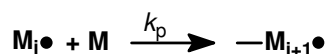
(a) 5 mol% of PEG₃₆₀

2.3 Characterization of the polystyrene-based latexes by means of DLS, TEM and zeta potential

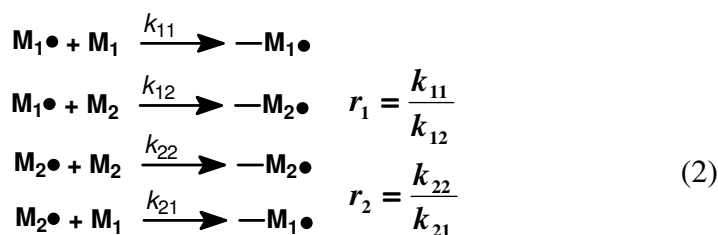
2.3.1 Characterization by means of DLS and TEM

In general the particle size of latex particles is dependent on the number of particles (N_p) during the emulsion polymerization. The number of particles is dependent on the rate of the particle nucleation (Figure 2.5 Interval I), which describes the formation of particles. Furthermore, this depends on the formation of the so-called z-mers, which are the surface active, amphiphilic oligoradicals. The z-mer can enter a micelle, a pre-existing particle, or a monomer droplet. It can propagate further or undergo aqueous-phase termination. The rate of z-mer formation depends on the propagation rate coefficient k_p of the monomer and of the reactive surfactants as well as on the concentration of surfactants (Equation 1). Using multiple monomers requires additional reactivity ratios, which have an impact on the propagation rate depicted in Equation 2.

In this case, the reactivity ratios represent the preference of the polymer chainend radical – $M_1 \bullet$ for addition of monomer 1 over monomer 2 (r_1) and of polymer chainend radical – $M_2 \bullet$ for addition of monomer 2 over monomer 1 (r_2).



$$R_p = k_p [M_i \bullet][M] \quad (1)$$



For instance, when the hydrophilicity of the monomer is high, more monomer is present in the water phase. This results in a higher propagation rate. Consequently, the formation of z-mers is fast, allowing for a higher nucleation rate. This leads to a higher number of particles and hence to smaller particles.

Dynamic light scattering (DLS)^[38] is one of the most popular methods for measuring the particle size because of the large size range (1 nm – 5 μ m) and approximate independence from optical properties.

The latexes were also characterized by means of transmission electron microscopy (TEM).^[39] TEM is an optical method to characterize the particle size distribution as well as the shape and to some extent the surface of the analyzed particles.^[40]

The particle sizes of the latexes determined are summarized in Table 2.2.

Table 2.2 Particle size measurements by DLS

Latex	Monomer	DVB [mol%]	Styrylsalt	Surfactant	DLS D ^a (nm)	TEM D ^a (nm)
1	S	2	-	PEG ₃₀₀₀	50	29
2	S	2	PS-SO ₃ Na	PEG ₃₀₀₀	117	78
3	S	2	PS-CH ₂ NMe ₃ BF ₄	PEG ₃₀₀₀	132	90
4	S	2	PS-SO ₃ Na	PEG ₁₆₅₀	86	60
5	S	2	PS-CH ₂ NMe ₃ BF ₄	PEG ₁₆₅₀	79	37
6	S	2	PS-SO ₃ Na	PEG ₃₆₀	56	38
7	S	2	PS-CH ₂ NMe ₃ BF ₄	PEG ₃₆₀	47	27
8	S	0	PS-CH ₂ NMe ₃ BF ₄	PEG ₁₆₅₀	99	69
9	S	1	PS-CH ₂ NMe ₃ BF ₄	PEG ₁₆₅₀	91	43
10	S	3	PS-CH ₂ NMe ₃ BF ₄	PEG ₁₆₅₀	61	33
11	S	4	PS-CH ₂ NMe ₃ BF ₄	PEG ₁₆₅₀	46	29
12	S	5	PS-CH ₂ NMe ₃ BF ₄	PEG ₁₆₅₀	35	25
13	S/MMA (1:1)	2	PS-CH ₂ NMe ₃ BF ₄	PEG ₁₆₅₀	76	n.d.
14	S/BMA (1:1)	2	PS-CH ₂ NMe ₃ BF ₄	PEG ₁₆₅₀	78	n.d.
15	S/BMA (1:9)	2	PS-CH ₂ NMe ₃ BF ₄	PEG ₁₆₅₀	53	n.d.
16	S/laurylMA (1:1)	2	PS-CH ₂ NMe ₃ BF ₄	PEG ₁₆₅₀	348	n.d.

(a) particle size average

Both methods have revealed that the latexes have a wide particle size distribution. An example is depicted in Figure 2.9. The particle size distributions measured by DLS and TEM were rather broad in all latexes. However, the average particle sizes are different, comparing the results obtained by DLS and TEM. For instance, the average particle size for latex 5 determined by means of DLS was 79 nm while the observed average particle size for latex 5 determined by TEM was only 37 nm. The difference can be due to the low tolerance of DLS for the background contamination, such as dust, and to the limited resolution. Furthermore, it has to be considered that the DLS samples were analyzed in a wet status. Therefore the hydrophilic surfactant units (PEGchains), which are situated on the particle shell, are spreading into the aqueous phase. The DLS measurements cannot distinguish between particles including or excluding surfactant units. Thus the diameter of the particle seems to be larger.

In contrast, the TEM measurements are performed in dry status. There the surfactant units are not spread and stabilized by solvation. Thus, the units are situated rather close to the particles and a smaller particle diameter is measured.

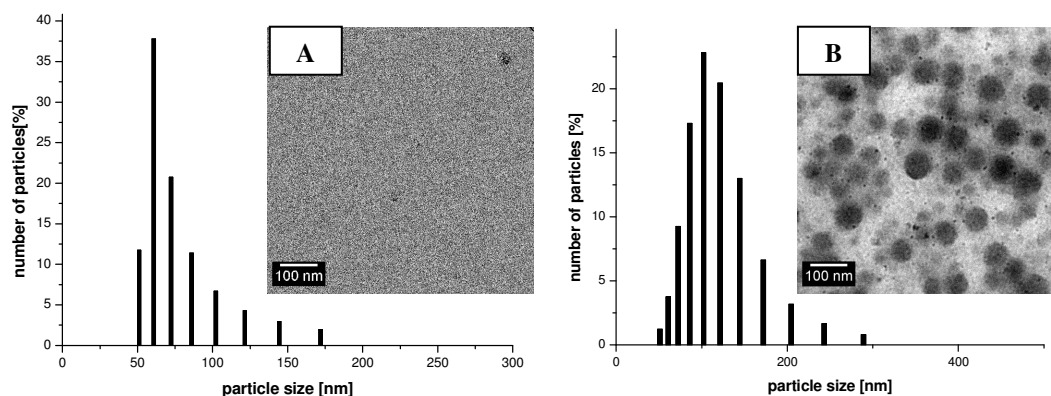


Figure 2.9 Particle size distribution measured by means of TEM (based on 100 particles) (A) latex 10, (B) latex 8

Therefore, TEM is a quite accurate technique in measuring the particles excluding surfactant units. A better insight in the shape and in the contamination of the latex solution is obtained compared to DLS. Both methods can be used also to determine the particle size distribution. The benefit of DLS is the possibility of analyzing all particles in solution, which is rather difficult for methods such as TEM. On the other hand, the DLS measurements can be easily influenced by dust or contamination of the sample solution.

Clear trends can be noticed when comparing the results. With both methods it has been observed that by decreasing the surfactant molecular weight (PEG chains), the corresponding particle size decreases (Entries 2,4,6 and 3,5,7). By using longer surfactants, being more hydrophilic, a larger number of lipophilic monomers need to co-polymerize with the surfactant in order to form an amphiphilic or surface active structure. Such a structure, containing an equivalent amount of lipophilic and hydrophilic units can start to build micelles (Interval I, Figure 2.5). Such particle nucleation results in a lower number of particles. Consequently, these particles are loaded with more monomer, which leads to larger particles.

Applying shorter polyethyleneglycol chains, the hydrophilicity is lower and thus a lower amount of monomer is needed before the surface activity is reached. This leads to a higher number of particles. Thus, the particles contain less monomer, leading to smaller particle sizes as shown in Figure 2.10.

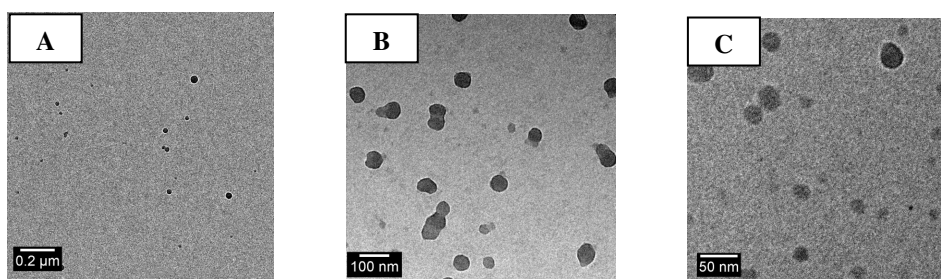


Figure 2.10 TEM pictures of latexes with different surfactant chain length, (A) Latex 3 PEG₃₀₀₀, (B) Latex 5 PEG₁₆₅₀, (C) Latex 7 PEG₃₆₀

Another trend observed by both methods is the decrease of particle size with increasing amount of crosslinking agent, as shown in Table 2.3 (Entries 5,8-10) and Figure 2.11. This observation is in line with results obtained by Sheu *et al.*,^[41,42] who used polystyrene seed latexes cross-linked with different amounts of DVB in a second styrene polymerization. The reason for this phenomenon is that for higher quantities of DVB the particles rapidly become densely cross-linked. Due to the cross-linking, the particles are restricted in their ability to swell.

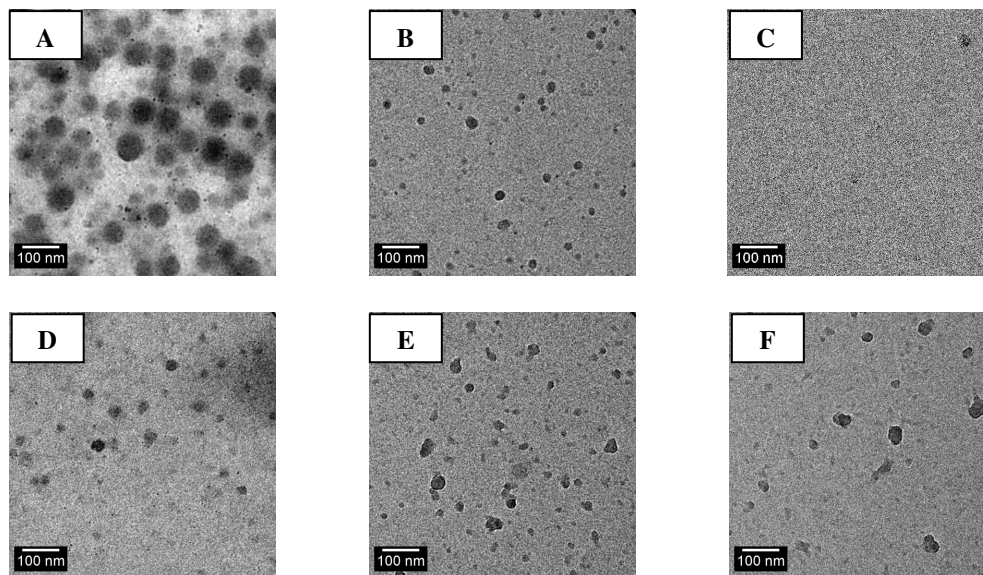


Figure 2.11 TEM pictures of latexes with different concentration of divinylbenzene, (A) latex 8 DVB 0%, (B) latex 9 DVB 1%, (C) latex 5 DVB 2%, (D) latex 10 DVB 3%, (E) latex 11 DVB 4%, (F) latex 12 DVB 5%

Moreover, the latex particles prepared from a styrene/MMA mixture (latex 13) are similar in size to the particles prepared from a styrene/BMA mixture (latex 14). This

indicates that the lipophilicity of the added methacrylate has no impact in the particle size. However, by increasing the BMA fraction with respect to styrene, the average particle size decreased from 78 nm to 53 nm. This trend implies that the amount of BMA has a significant influence. In comparison to styrene, BMA is more hydrophilic. When using BMA as monomer, the monomer concentration in the aqueous phase is higher compared to the styrene concentration in the aqueous phase. From this it can be concluded that the propagation rate coefficient k_p is higher and consequently the rate of z-mer formation is higher. Thus, the rate of the particle nucleation is increasing and the particle number is higher. Higher numbers of particle contain less monomer, which leads to a smaller average particle size.

The average particle size of styrene/LMA (latex 16) is 348 nm, indicating that coagulation of the particles has taken place. The same conclusion could be drawn from the TEM data, shown in Figure 2.12, D. This is due to the fact that LMA is completely insoluble in water. Thus, the z-mer propagation rate is almost zero and the particles are only swollen by styrene, resulting in very small particles. Small particles are leading to coagulation.

Another trend observed in the TEM pictures of latex 14, 15 is that the particles are not perfectly spherical. This is most probably caused by the lower glass transition temperature T_g ($T_g = 40\text{--}45^\circ\text{C}$) of PBMA compared to PS ($T_g = 100^\circ\text{C}$). Thus, it is likely that during the preparation of the TEM sample and the measurement, the latex particles begin to flow. This results in fused structures (Figure 2.12).

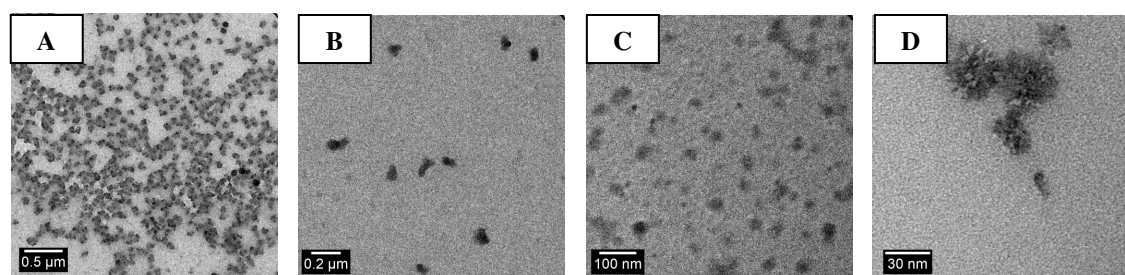


Figure 2.12 TEM pictures of latexes with a mixture of styrene and methacrylates, (A) latex 13 styrene/MMA, (B) latex 14 styrene/ BMA, (C) latex 5 styrene/BMA (1:9), (D) latex 16 styrene/LMA

2.3.2 Characterization via zeta potential^[43]

The zeta potential is the electric potential in the interfacial electrical double layer at the location of the slipping plane versus a point in the bulk fluid away from the interface (Figure 2.13). The zeta potential determines the net interparticle forces in electrostatically stabilized systems and their relative stability.^[44]

In order to get a better insight into the stability of latex particles, their zeta potential can be determined. Due to the fact that almost all prepared polystyrene-based latexes contain styrylsalts, this method is suitable to determinate the latex particle stability. In fact, the styrylsalts are situated in the hydrophilic shell and form the electrical double layer.

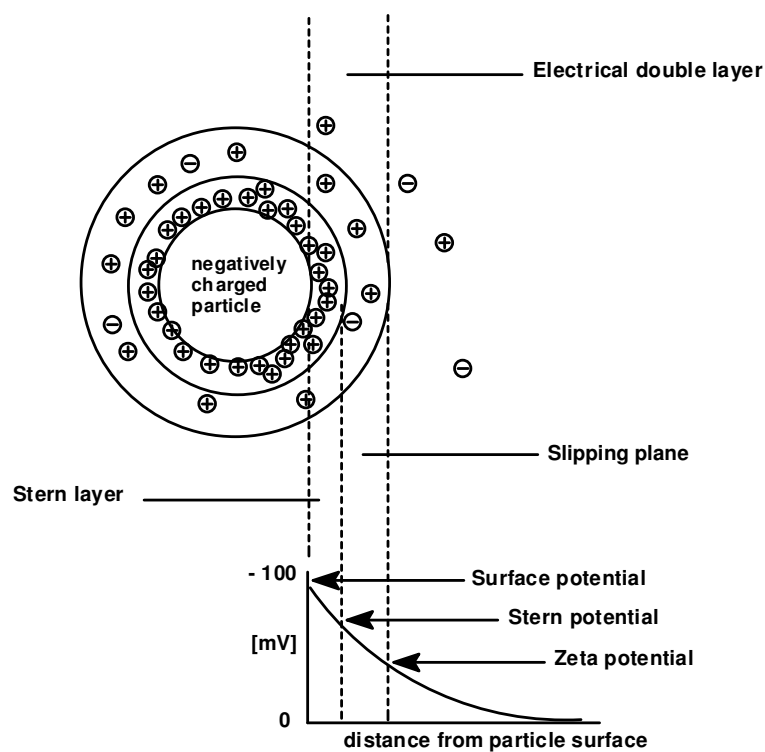


Figure 2.13 Schematic representation of the zeta potential

The particles are stable if the zeta potential value is far from zero. In contrast, the particles become unstable if their zeta potential value approaches zero. Consequently, they will most likely coagulate or flocculate.

The zeta potential measured for the prepared polystyrene latexes are given in Table 2.3.

Table 2.3 Results of zeta potential measurements

Latex	Monomer	DVB [mol%]	Ionic character	Surfactant ^c	Zeta potential [mV]
2	S	2	PS-SO ₃ Na	PEG ₃₀₀₀	-58
3	S	2	PS-CH ₂ NMe ₃ BF ₄	PEG ₃₀₀₀	59
4	S	2	PS-SO ₃ Na	PEG ₁₆₅₀	-59
5	S	2	PS-CH ₂ NMe ₃ BF ₄	PEG ₁₆₅₀	58
6	S	2	PS-SO ₃ Na	PEG ₃₆₀	- 63
7	S	5	PS-CH ₂ NMe ₃ BF ₄	PEG ₃₆₀ ^d	100
8	S	0	PS-CH ₂ NMe ₃ BF ₄	PEG ₁₆₅₀	60
9	S	1	PS-CH ₂ NMe ₃ BF ₄	PEG ₁₆₅₀	60
10	S	3	PS-CH ₂ NMe ₃ BF ₄	PEG ₁₆₅₀	59
11	S	4	PS-CH ₂ NMe ₃ BF ₄	PEG ₁₆₅₀	59
12	S	5	PS-CH ₂ NMe ₃ BF ₄	PEG ₁₆₅₀	58
13	S/MMA ^a	2	PS-CH ₂ NMe ₃ BF ₄	PEG ₁₆₅₀	58
14	S/BMA ^a	2	PS-CH ₂ NMe ₃ BF ₄	PEG ₁₆₅₀	58
15	S/BMA ^b	2	PS-CH ₂ NMe ₃ BF ₄	PEG ₁₆₅₀	49
16	S/LMA ^a	2	PS-CH ₂ NMe ₃ BF ₄	PEG ₁₆₅₀	47

(a) ratio 1:1; (b) ratio 1:9; (c) 2 mol%; (d) 5 mol%

All zeta potentials are quite similar around 59 mV for positively charged latexes and -59 mV for negatively charged latexes. Latex 7, however, has a rather high zeta potential. This is most likely due to the fact that the surfactant concentration is increased by a factor of 2.5 with respect to the other latexes.

Consequently, it seems that all prepared polystyrene-based latexes are stable, considering that the colloidal sol becomes unstable^[45] below a zeta potential of 25 mV, see zeta potential Table 2.4. The similarity of the zeta potentials is not surprising because the proportion of the styrylsalt in the emulsion polymerization was equal in almost all cases.

Table 2.4 Stability behavior of latex particles at different zeta potential

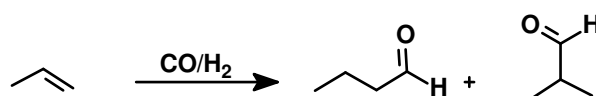
Zeta Potential [mV]	Stability behavior of latex particle
0 to ± 5 ,	Rapid coagulation or flocculation
± 10 to ± 30	Incipient instability
± 30 to ± 40	Moderate stability
± 40 to ± 60	Good stability
more than ± 61	Excellent stability

In conclusion, all characterization results suggest that the prepared latexes are rather stable. However, all analyses were performed at room temperature and not under catalytic conditions. Thus, in the following section the latexes were applied as phase transfer agents under conditions similar to those for catalytic hydroformylation. The outcome of these experiments gives further information about the stability of the latexes and their behavior as phase transfer agents under biphasic hydroformylation conditions.

2.4 Partitioning experiments for 1-octene and *n*-nonanal using polystyrene-based latexes

The concept and reasoning to apply latexes as phase transfer agents in aqueous biphasic catalysis for lipophilic substrates has already been discussed in Section 2.1.1. In this case, the latex particle should transfer the organic compounds into the aqueous phase, where the water-soluble catalyst is situated, see Figure 2.1, II.

A well known aqueous biphasic catalytic reaction is the biphasic hydroformylation of alkenes. This process has been commercialized in the Ruhrchemie/Rhône-Poulenc process^[46] for the hydroformylation of propene to *n*-butyraldehyde (Figure 2.14).

**Figure 2.14** Hydroformylation of propene to *n*-butyraldehyde

The biphasic hydroformylation mixture of alkenes consists of two layers, the organic phase and the aqueous phase. The catalysis is carried out in the water phase using a water-soluble catalyst. Alkenes up to C₅ are transferred into the aqueous phase, due to their partial water solubility. Alkenes > C₅ remain in the organic phase. They show negligible water-solubility, as depicted in Figure 2.15. Thus, without any additive, catalysis cannot occur.

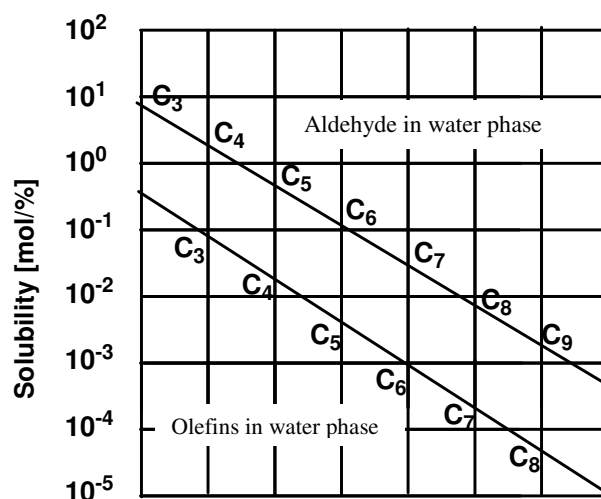


Figure 2.15 Solubility of alkenes and aldehydes in water at 25-30°C

In order to overcome this solubility problem, we tried to use latexes as phase transfer agents in the biphasic hydroformylation of higher alkenes (Figure 2.16). We chose 1-octene (**1**) as model substrate, which is transformed into nonanal (**2**) during the hydroformylation.

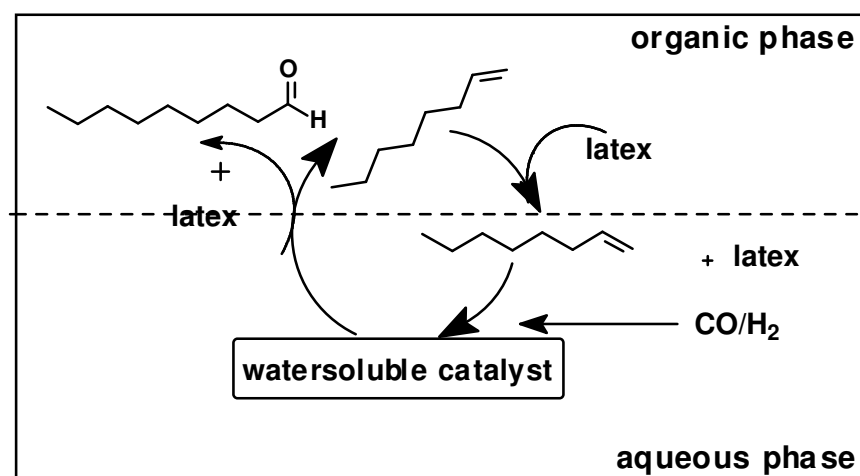


Figure 2.16 Schematic representation of the biphasic hydroformylation of 1-octene using latex as phase transfer agent

To verify the possibility to use polystyrene-based latexes as phase transfer agents or additives in the biphasic hydroformylation, the latex was preliminarily tested in partitioning experiments.

In those experiments the transfer of a lipophilic compound from the organic layer into the aqueous layer by means of an additive, such as latex, was examined.

Thereby, at given temperatures and stirring rates, it was possible to determine the ability of the additive to act as phase transfer agent as well as to measure its stability under different conditions.

The organic phase consists of the organic compounds 1-octene and *n*-nonanal, which are the envisaged substrate and the corresponding product of the hydroformylation reaction (Figure 2.17).

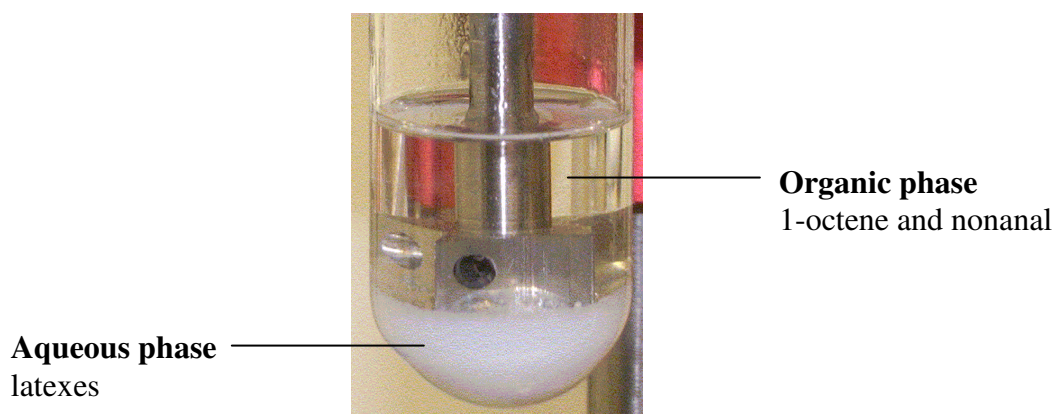


Figure 2.17 Picture of two-phase system for partitioning experiment

The latexes were diluted in water and the organic phase was added to the aqueous phase (Figure 2.17). The resulting biphasic system was heated to the required temperature and stirred for 12 hours. Subsequently, the organic phase was analyzed by means of gas chromatography. The residue amount of 1-octene and *n*-nonanal indicated how much of the lipophilic compounds were transferred into the aqueous phase.

It was observed that increased coagulation occurs at higher temperature and stirring rate. At stirring rates above 700 rpm coagulation was observed in all cases. The same holds for temperatures higher than 80°C. Thus, the temperature and stirring rate limits using polystyrene-based latexes as phase transfer agents in biphasic hydroformylation are 80°C and 700 rpm.

From the partitioning experiments at 80°C and 700 rpm (Table 2.5) clear trends can be noticed. The behavior of the latexes differs for different surfactants. Upon a decrease in

surfactant chain length (latex 2, latex 4 and latex 6), an increase in transfer for both organic components was observed. Not only does the transfer of 1-octene and nonanal increase, but also the 1-octene/nonanal ratio changes. Latexes with the surfactant PEG₃₀₀₀ show a transfer ratio of 1-octene/nonanal of 2.5. There is a clear preference for the transfer of 1-octene. The ratio decreases dramatically to 1.0 when latexes with surfactant PEG₁₆₅₀ and PEG₃₆₀ are used. In these cases there is no preference for the transfer of 1-octene over *n*-nonanal into the latex phase.

Table 2.5 Results of partitioning experiments^a

Latex	Monomer	DVB [mol%]	Ionic character	Surfactant	1-Octene ^c [%]	Nonanal ^c [%]
1	S	2	nonionic	PEG ₃₀₀₀	44	22
2	S	2	PS-SO ₃ Na	PEG ₃₀₀₀	44	23
3	S	2	PS-CH ₂ NMe ₃ BF ₄	PEG ₃₀₀₀	41	24
4	S	2	PS-SO ₃ Na	PEG ₁₆₅₀	35	29
5	S	2	PS-CH ₂ NMe ₃ BF ₄	PEG ₁₆₅₀	77	80
6	S	2	PS-SO ₃ Na	PEG ₃₆₀	84	90
7 ^b	S	2	PS-CH ₂ NMe ₃ BF ₄	PEG ₃₆₀	40	32
8	S	0	PS-CH ₂ NMe ₃ BF ₄	PEG ₁₆₅₀	70	59
9	S	1	PS-CH ₂ NMe ₃ BF ₄	PEG ₁₆₅₀	75	70
10	S	3	PS-CH ₂ NMe ₃ BF ₄	PEG ₁₆₅₀	72	77
11	S	4	PS-CH ₂ NMe ₃ BF ₄	PEG ₁₆₅₀	78	78
12	S	5	PS-CH ₂ NMe ₃ BF ₄	PEG ₁₆₅₀	77	76
13	S/MMA	2	PS-CH ₂ NMe ₃ BF ₄	PEG ₁₆₅₀	39	42
14	S/BMA	2	PS-CH ₂ NMe ₃ BF ₄	PEG ₁₆₅₀	67	78
15	S/BMA	2	PS-CH ₂ NMe ₃ BF ₄	PEG ₁₆₅₀	83	84

(a) organic phase, 1-octene and *n*-nonanal (1:1) (100 mmol), aqueous phase (15 mL), latex 100 mg + water; 80°C, 700 rpm (b) 5 mol% has been applied instead of 2 mol%; (c) percentage of organic compounds left in the organic phase determined by GC

These results can be rationalized by the fact that for the latexes prepared with the shorter chain PEG-surfactants, the surface coverage with hydrophilic units is decreased. The lipophilic core of the particles is less isolated with respect to the organic compounds and the transfer of 1-octene and nonanal proceeds efficiently.^[47]

The partitioning experiment using latex 7 differs from the observed trend. Although the short surfactant PEG₃₆₀ was used, the partitioning of 1-octene and nonanal was similar to the results for latex 3. For latex 7 a much higher surfactant concentration (2.5 times)

was used in the emulsion polymerization. Thus, more surfactant was present to stabilize the particles and the particle surface is more densely covered.

Latexes prepared with different monomers, MMA and BMA (latex 13-15) showed variation in the transport of the organic substrates. In the latex prepared with a styrene/MMA mixture (1:1) (latex 13) the transfer of 1-octene and nonanal into the aqueous phase is rather low with respect to latex 14 and 15. The transfer of the organic compounds into the lipophilic core of the latex particles enhances with increasing lipophilicity of the latex particle core. The lipophilicity increases from MMA to BMA. Thus, latex 14 styrene/BMA (1:1) can transfer more 1-octene and nonanal into the aqueous phase than latex 13 containing the styrene/MMA mixture (1:1).

Furthermore, the latex particle size has an impact on the behavior as a phase transfer agent. Latexes consisting of small particles have a higher interphase area between the lipophilic core and the hydrophilic shell. Thus, more 1-octene and nonanal can be transferred into the aqueous phase.

For instance, latex 15 styrene/BMA (1:9) has an average particle size of 53 nm and it transports 83% of 1-octene and 84% of nonanal into the aqueous phase. In contrast, latex 14 styrene/BMA (1:1) has an average particle size of 78 nm and it transfers only 67% of 1-octene and 78% of nonanal into the water phase.

Only slight differences were observed for latexes with different degree of cross-linker (mol% DVB). A minor increase of phase transfer is detected with an increase of cross-linking (1-5 mol% DVB). The increase of crosslinking in the lipophilic core results in smaller particles and hence, the total interphase area increases. Consequently more 1-octene and nonanal can be transferred into the water phase.

2.5 Conclusion

Several polystyrene-based latexes were synthesized by means of emulsion polymerization. The latex composition was varied with respect to surfactants, monomers, crosslinker concentration, and styrylsalts. The latexes were characterized by TEM, DLS, and zeta potential and their stability was proven. Furthermore, the presented latexes were applied as phase transfer agents in partitioning experiments.

From these results it was concluded that the stability of the latex particles is assured up to 80°C and up to a stirring rate of 700 rpm. Thus, latexes are applicable as phase transfer agent in catalytic reactions such as biphasic hydroformylation of higher alkenes at 80°C and a mechanical stirring rate of 700 rpm. The transfer of the organic compounds into the aqueous phase depends on the composition of the latexes. Consequently, the behavior of the latexes as phase transfer agents in the biphasic hydroformylation of higher alkenes can differ considerably.

2.6 Experimental Section

All chemicals were purchased from Aldrich, Acros or Merck and used as received unless stated otherwise. Solvents were purified using basic alumina columns after degassing. 1-octene, nonanal, monomers, and external standards were purified by flash chromatography (Al_2O_3) followed by distillation over CaH_2 and degassing using the freeze-pump-thaw method.

Synthesis of p-vinylbenzyltrimethylammonium tetrphenylborate (c)

This compound was synthesized from p-vinylbenzyltrimethylammonium chloride according to a literature procedure.^[48]

Synthesis of 4-vinylbenzylstyrene PEG_n (1-3)

The surfactants (surfmer) were synthesized according to a literature procedure.^[49]

Emulsion polymerization of polystyrene-based latexes^[37]

The emulsion polymerization was carried out under an inert atmosphere of argon using standard Schlenk techniques. The glassware was heated in an oven and subjected to three consecutive vacuum- argon cycles prior to use.

A solution of internal styrene salt (12 mmol) in de-gassed de-ionized water (80 mL) was placed into an autoclave equipped with a mechanical stirrer. The solution was heated to 80°C and stirred at 100 rpm. After this temperature was reached, styrene (49 mmol), divinylbenzene (1.85 mmol) and initiator (0.48 mmol) were added. The stirring rate was increased to 300 rpm. The macromonomer functional PEG₃₀₀₀ (1.23 mmol) in water (20 mL) was added. After 10 minutes the mixture became milky, indicating formation of the micro-emulsion. The suspension was stirred for 4 hours. During the reaction several samples were taken to measure the solids content and to monitor the conversion. Finally, the latex was cooled to room temperature and stored at 4°C. The latexes were purified by dialysis during 3-4 days using a cellulose hydrate membrane with a pore size of 25-30 Å. In case of big particles, ultracentrifugation was performed. The particles were analyzed by means of TEM, DLS and zeta potential measurement.

Partitioning experiments

A mixture of 1-octene and *n*-nonanal (1:1) (15 mL; 100 mmol) was treated with a latex-water emulsion (15 mL; 100mg solid content of latex diluted in water) under hydroformylation conditions (80 -100°C; stirring rate from 600 rpm to 1000 rpm) for at least 12 hours. The distribution between the phases was determined after cooling to room temperature by means of GC-analysis (external standard: dodecane).

GC analysis

GC	:	Shimadzu GC 17A
Column	:	HP Pona (crosslinked Me Siloxane), 50 m, inner Ø 0.20 mm, film thickness 0.5 µm
Carrier gas	:	Helium 208.0 kPa (total flow 69 ml/min)
Temperature program	:	60°C (hold: 10 min), 1°C/min to 65°C, 15°C/min to 250°C (hold: 3 min)
Injector	:	250°C
Detector (FID)	:	270°C
Split ratio	:	50
Injection volume	:	1.0 µL

Table 2.6 Selected retention times of the organic compounds and the external standard

Compound	Retention time (min)
1-octene	14.9
<i>n</i> -nonanal	23.8
dodecane	25.4

Characterization of the particle size by means of TEM^[39]

TEM images were taken using a Fei Tecnai 20 after deposition and drying a droplet of the latex dispersion on a carbon-coated copper grid.

Characterization of the particle size by means of DLS

Sample preparation

3-5 droplets of latex were diluted in 5 mL distilled water followed by ultrasonication for 5 min. Then the resulting solution was analyzed via Nanotracs DLS Particle Size Analyser.

DLS measurement

DLS	:	Nanotracs Particle Size Analyser
Samples	:	in wet state (0.001g/L)
Number of measurements	:	1 (180 s)
Temperature	:	25°C
Refractive index	:	1.331 for water

Characterization by means of zeta potential^[43]

The samples were diluted by a factor of 30 with distilled water in a cuvette. The measurements were performed on a Malvern Zetasizer ZS.

Instrument	:	Malvern
Name	:	Zetasizer Nano ZS
Laser	:	Laser Doppler Electrophoresis
Scattering angle	:	173 °
Wave length	:	633 nm
Number of measurements	:	6
Dilution	:	by a factor 30
Temperature	:	20°C
Cell	:	disposable zeta potential cell

2.7 References

- [1] A. Corma, H. Garcia, *Top. Catal.* **2008**, *48*, 8-31.
- [2] I. Horvath, *Acc. Chem. Res.* **1998**, *31*, 641-650.
- [3] S. Kainz, D. Koch, W. Baumann, W. Leitner, *Angew. Chem.* **1997**, *109*, 1699-1701.
- [4] D. Koch, W. Leitner, *J. Am. Soc.* **1998**, *120*, 13398-13404.
- [5] S. Bektesevic, T. Tack, M.R. Mason, M.A. Abraham, *Ind. Eng. Chem. Res.* **2005**, *44*, 4973-4981.
- [6] W. Leitner, *Acc. Chem. Res.* **2002**, *35*, 746-756.
- [7] P. Stephenson, B. Kondor, P. License, K. Scovell, S. K. Ross, M. Poliakoff, *Adv. Synth. Catal.* **2006**, *348*, 1605-1610.
- [8] B. Sueur, L. Leclercq, M. Sauthier, Y. Castanet, A. Mortreux, H. Bricout, S. Tilloy, E. Monflier, *Chem. Eur. J.* **2005**, *11*, 6228-6236.
- [9] G. Fremy, E. Monflier, J.-F. Carpentier, Y. Castanet, A. Mortreux, *J. Mol. Catal. A: Chem.* **1998**, *129*, 35-40.
- [10] S. Tilloy, E. Genin, F. Hapiot, D. Landy, S. Fourmentin, J.-P. Genet, V. Michelet, E. Monflier, *Adv. Synth. Catal.* **2006**, *348*, 1547-1552.
- [11] N. Sieffert, G. Wipff, *J. Phys. Chem. B* **2006**, *110*, 4125-4134.

- [12] T. Mathivet, C. Méliet, Y. Castanet, A. Mortreux, L. Carbon, S. Tilloy, E. Monflier, *J. Mol. Catal. A: Chem.* **2001**, *176*, 105-116.
- [13] L. Leclercq, M. Sauthier, Y. Castanet, A. Mortreux, H. Bricout, E. Monflier, *Adv. Synth. Catal.* **2005**, *347*, 55-59.
- [14] F. M. Menger, A. R. Elrington, *J. Am. Chem. Soc.* **1991**, *128*, 265-271.
- [15] J. F. Rusling, *Pure Appl. Chem.* **2001**, *73*, 1895-1905.
- [16] C. K. Niue, J. F. Rusling, *Electrochem. Commun.* **2002**, *4*, 340-343.
- [17] L. Caron, V. Nardello, J. Mugge, E. Hoving, P. L. Alsterds, J. M. Aubry, *J. Colloid Interface Sci.* **2005**, *282*, 478-485.
- [18] L. Caron, V. Nardello, J. Mugge, E. Hoving, P. L. Alsterds, J. M. Aubry, *J. Colloid Interface Sci.* **2005**, *282*, 478-485.
- [19] M. Haumann, H. Yildiz, H. Koch, R. Schomäcker, *Appl. Catal. A.* **2002**, *236*, 173-178.
- [20] P. Handa, M. Stierndahl, K. Holmberg, *Microporous Mesoporous Mater.*, **2007**, *100*, 146-153.
- [21] W. T. Ford, *Reactive and Functional Polymers* **1997**, *33*, 147-158.
- [22] S. Mecking, R. Thomann, *Adv. Mater.* **2000**, *12*, 953-956.
- [23] J. H. Schulmann, J.A. Friend, *J. Colloid Interface Sci.* **1949**, *4*, 497-509.
- [24] P. Kumar, K.L. Mittal, *Handbook of Microemulsion Science and Technology*, Marcel Dekker, New York, **1999**.
- [25] K. Holmberg, *Eur. J. Org. Chem.* **2007**, 731-742.
- [26] M. S. EL-Aasser, E.D. Sudol, in *Emulsion Polymerization and Emulsion Polymers*, (Eds.: P.A. Lovell and M. S. El-Aasser), Chichester: Wiley, **1997**, Chapter 2.
- [27] A. M. van Herk, *Chemistry and Technology of Emulsion Polymerization*, (Eds.: A. M. van Herk), 1st ed., Blackwell Publishing Ltd: Oxford, Great Britain, **2005**, pp 46 -78.
- [28] J. M. Asua, H. A. S. Schoonbrood, *Acta Polym.* **1998**, *49*, 671-686.
- [29] W. J. Harkins, *J. Am. Chem. Soc.* **1947**, *69*, 1428-1444.
- [30] W. V. Smith, R.H. Ewart, *J. Chem. Phys.* **1948**, *16*, 592-599.
- [31] B. Jacobi, *Angew. Chem.* **1952**, *64*, 539-43.
- [32] W. J. Priest, *J. Phys. Chem.* **1952**, *56*, 1077-1092.
- [33] R. M. Fitch, in *Polymer Colloids: A Comprehensive Introduction*, London: Academic Press, **1997**, Chapter 7.
- [34] F. K. Hansen, J. Ugelstad, *J. Polym. Sci. Polym. Chem. Ed.* **1978**, *16*, 1953-1979.
- [35] W. D. Harkins, *J. Am. Chem. Soc.* **1947**, *69*, 1428-1444.
- [36] D. Tillier, PhD Thesis, University of Eindhoven, **2005**.

- [37] R. Sablong, J. I. van der Vlugt, R. Thomann, S. Mecking, D. Vogt, *Adv. Synth. Catal.* **2005**, 347, 633-636.
- [38] D. F. Nicoli, P. Toumbas, US 6794671, **2004**.
- [39] All TEM pictures were taken by Dr. J. Loos, Laboratory of Materials and Interface Chemistry, Laboratory of Polymer Technology and Soft Matter Cryo-TEM Research Unit, Department of Chemical Engineering and Chemistry, Eindhoven University of Technology
- [40] O. J. Karlsson, B. E. H. Schade, A. M van Herk, in *Chemistry and Technology of Emulsion Polymerization*, (Ed.: A. M. van Herk), 1st ed., Blackwell Publishing Ltd: Oxford, Great Britain, **2005**, pp 210-222.
- [41] H. R. Sheu, M. S. El-Aasser, J. W. Vanderhoff, *J. Polym. Sci. Polym. Chem.* **1990**, 28, 629-651.
- [42] H. R. Sheu, M. S. Aasser, J. W. Vanderhoff, *Polym. Mat. Sci. Eng.* **1987**, 57, 911-915.
- [43] All zeta potentials were determined by Dr. J. Laven, Laboratory of Materials and Interface Chemistry, Department of Chemical Engineering and Chemistry, Eindhoven University of Technology
- [44] P. Stenius, B. Kromberg, in G. W. Poehlein, R.H. Ottewill, J. W. Goodwin (eds), *Science & Technology of polymer Colloids. Surface Characterization of Latexes*, Martinus Nijhoff Publishers, The Hague, 1983, II, 68, 449-479.
- [45] R. J. Hunter (eds), *Introduction to Modern Colloid Science*, Oxford University Press Inc., New York, United States, **1993**, 262-298.
- [46] F. Kuntz et al., Rhône -Poulenc Ind., Patent FR 2.230.654, **1983**, Patent FR 2.314910, **1975**, Patent FR 2.338.253, **1976**, Patent FR 2.349.562, **1976**, Patent FR 2.366.237 **1976**, Patent FR 2.473.505, **1979**, Patent FR 2.478.078, **1980**, Patent FR 2.550202, **1983**, Patent FR 2.561.650 **1984**
- [47] T. Aslamazova, K. Tauer, *Colloids and Surfaces A: physicochem. Eng. Aspects* **2004**, 239, 3-10.
- [48] J. Tang, H. Tang, W. Sun, H. Plancher, M. Radosz, Y. Shen, *Chem. Commun.* **2005**, 3325-3327.
- [49] K. Ito, S. Yokohama, F. Arakawa, Y. Yukawa, T. Iwashita, Y. Yamasaki, *Polym. Bull.* **1986**, 16, 337-344.

Latexes as Phase-Transfer Agents and Supports for Electrostatic Immobilization: Biphasic Hydroformylation of Higher Alkenes

One of the most important homogeneously catalyzed reactions in industry is the hydroformylation of alkenes.

A biphasic hydroformylation offers a feasible way to efficiently separate the catalyst from the reaction mixture. For water-soluble alkenes, this concept has been commercialized in the Ruhrchemie/Rhône-Poulenc process. In order to enable the use of this concept for water insoluble alkenes, the application of polystyrene-based latexes as phase-transfer agents was investigated for higher alkenes. The influence of latex compositions and mass transfer limitation will be discussed.

3.1 Introduction

The application of soluble transition metal complexes as selective homogeneous catalysts has increased significantly during the last decades. A number of large-scale processes, such as the production of adiponitrile, α -olefins (SHOP process), acetic acid and butanal are nowadays based on homogeneous catalysts.^[1-3] Nevertheless, the recovery from the reaction mixture and the reuse of the (expensive) catalyst remains a challenge. Therefore, it is of very high interest to develop feasible ways to solve this recycling problem.

Several concepts for the immobilization of homogeneous catalysts have been developed and investigated^[4] such as the use of solid supports,^[5] supramolecular architectures or the application in *sc*CO₂.^[6-11]

Another methodology utilizes biphasic (aqueous and organic) systems. The catalyst is located in one phase (e.g. aqueous), while the products remain in the other phase (e.g. organic). This two-phase system has already been commercialized by Ruhrchemie/Rhône-Poulenc^[12] for the conversion of propylene into *n*-butyraldehyde (Figure 3.1). However, a major issue of this process is the solubility of the reactants. The process is not suitable for the hydroformylation of higher alkenes, because of their poor solubility in water. A number of strategies have been proposed to overcome this problem.

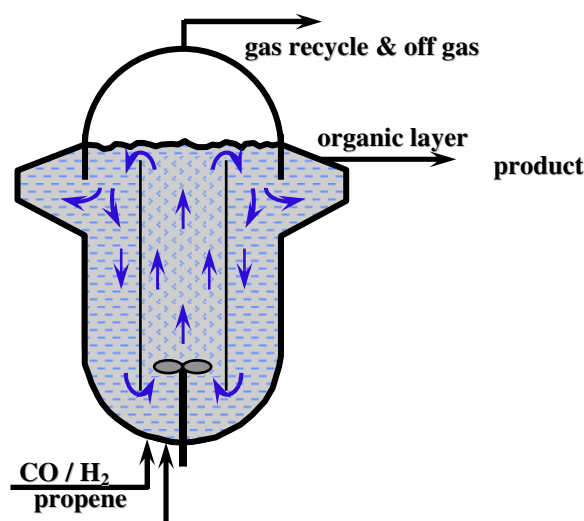


Figure 3.1 Product separation in the Ruhrchemie/Rhône-Poulenc process

Among those are the application of surfactants,^[13-18] co-solvents,^[19-21] supported aqueous phase catalysts,^[22-26] complexes of amphiphilic phosphine ligands,^[27-29]

thermoregulated phase-transfer catalysts,^[30-34] fluorous phase catalysts,^[35-37] and the application of catalysts in ionic liquids.^[38-43] These systems provide accelerated reaction rates by circumventing the limitations caused by the substrate insolubility in water.

Another possibility to enhance the reaction rate is to utilize phase-transfer agents, such as cyclodextrins,^[44-49] microemulsions or latexes.^[50] These agents should transfer the lipophilic substrate into the aqueous phase containing the catalyst.

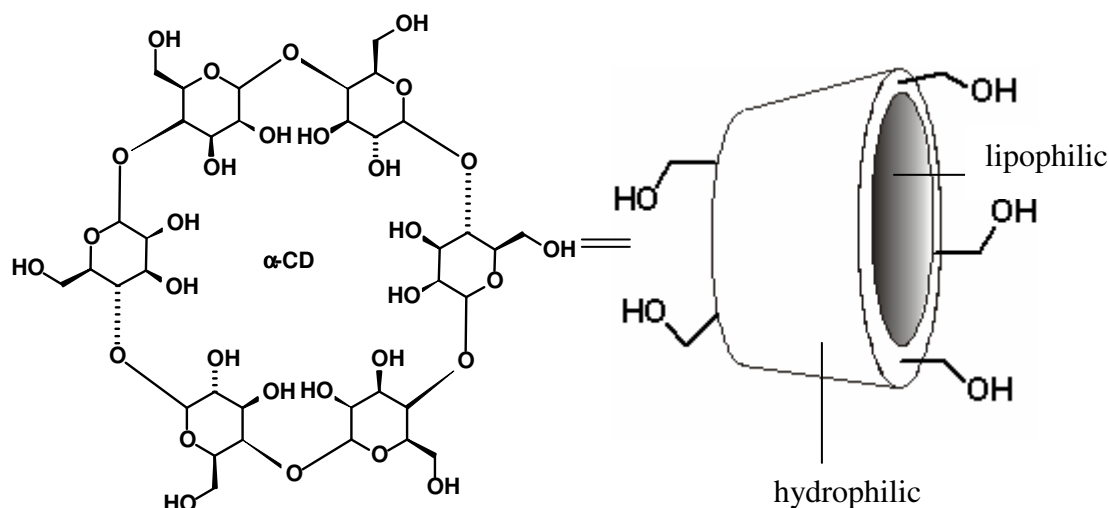


Figure 3.2 Structure of α -cyclodextrin (six membered sugar ring molecule)

Typical cyclodextrins consist of 6-8 glucopyranoside units (α - γ cyclodextrins) and can be topologically represented as truncated cones (Figure 3.2). The larger and the smaller openings of the truncated cone expose secondary and primary hydroxyl groups to the solvent. Because of this arrangement, the interior of the truncated cone is not hydrophobic, but considerably less hydrophilic than the aqueous environment and thus able to host other hydrophobic compounds. In contrast, the exterior is sufficiently hydrophilic and results in water solubility of cyclodextrins.

The application of cyclodextrins as phase-transfer agents is well documented.^[51-56] Cyclodextrins are most often chemically modified in order to act as phase-transfer agents. However, these additives are rather expensive, a significant drawback for larger scale application.

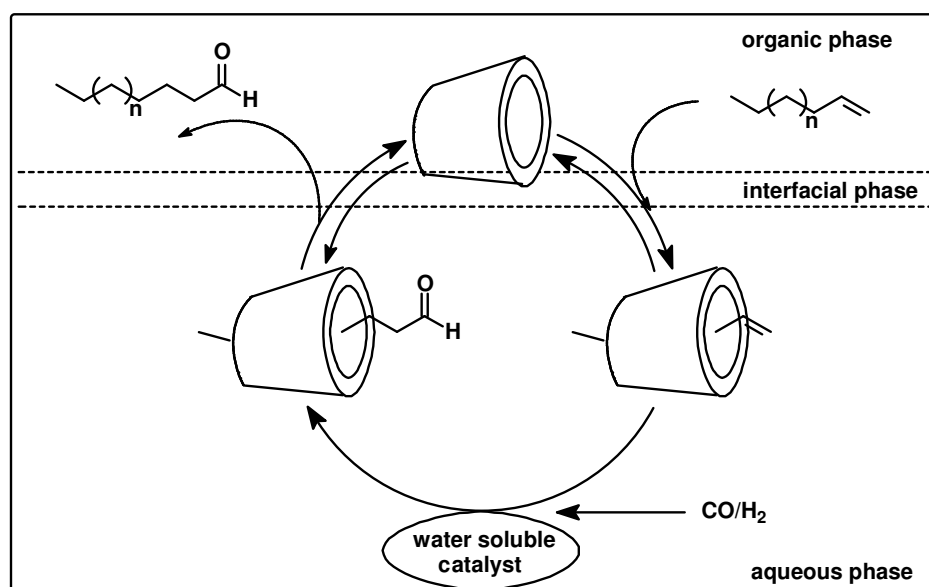


Figure 3.3 Biphasic hydroformylation of water-insoluble alkenes using cyclodextrins as phase-transfer agents. The truncated cone schematically represents the cyclodextrin

The combination of a lipophilic core and a hydrophilic shell is also present in microemulsion droplets and latex particles. For that reason we became interested in microemulsions and latexes as phase-transfer agents for lipophilic compounds. By definition, microemulsions are thermodynamically stable dispersions of oil, water, and a surfactant. Latexes are thermodynamically stable dispersions of a polymer and a surfactant in water. Thus, the only difference is the composition of the lipophilic core. The core of latexes contains polymers while the core of microemulsions contains organic compounds such as alkanes, alkenes, styrene, etc. (Figure 3.4).

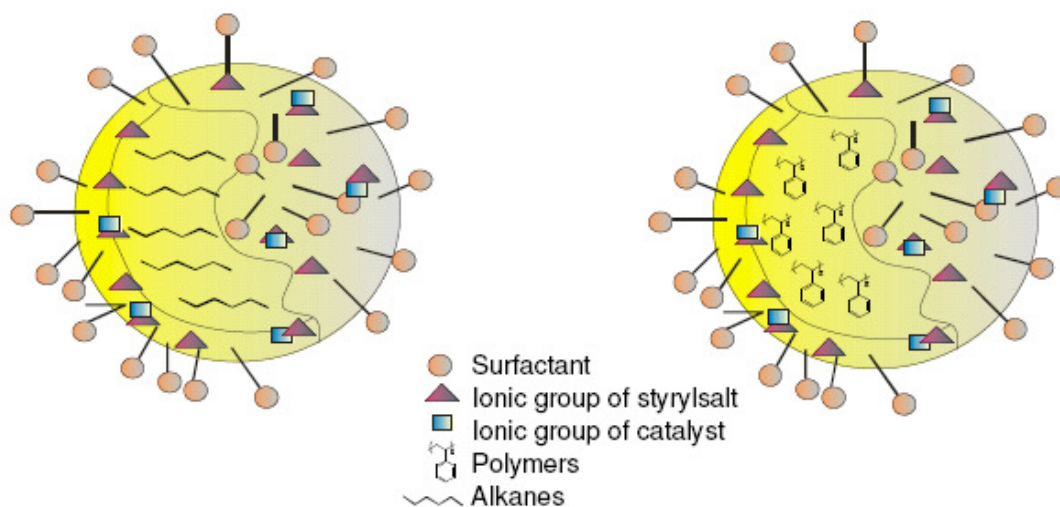
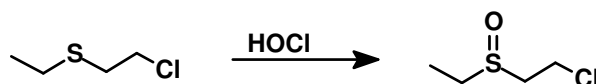


Figure 3.4 Structure of an oil-in-water microemulsion droplet (A) and latex particle (B)

The use of microemulsions as media for organic synthesis has attracted considerable interest in recent years.

Menger and Elrington were among the pioneers to explore microemulsions as media for organic reactions and to overcome reactant incompatibility.^[57] The authors demonstrated that a well-formulated microemulsion could effectively detoxify mustard gas. Although, it is less toxic than nerve agents, mustard gas is more persistent in the environment which is due to the low solubility in water.

Menger explored microemulsions as media for the oxidation (deactivation) of half mustard gas, which was used as model substrate in order to reduce the toxicity. The oxidation with hypochlorous acid turned out to be extremely fast in the microemulsions applied going to completion in less than 15 s. This is much shorter than a similar reaction performed in a two-phase system (20 min) (Scheme 3.1).



Scheme 3.1 Oxidation of half-mustard sulfide to sulfoxide

Furthermore, Egger *et al.* reported on the use of microemulsions based on glycoside surfactants as media for the epoxidation of alkenes using Mn-based catalysts.^[58] However, the obtained stereoselectivity was rather different when compared to the two-phase system. For instance, epoxidation of styrene in a biphasic system gave 40% enantiomeric excess while in a microemulsion the *ee* was only 27%.

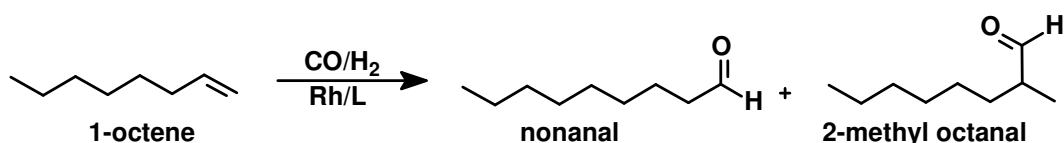
A number of other organic reactions, which were successfully performed in microemulsions, such as electroorganic synthesis,^[59] cyclization^[60] or oxidation^[61] have recently been reviewed. The application of microemulsions in catalysis has also found attention.^[62-65] For instance, Häger *et al.*^[66] reported on microemulsions acting as catalyst to enhance nucleophilic substitution reactions. Furthermore, Haumann *et al.*^[67] reported on the biphasic hydroformylation of internal alkenes in microemulsions based on fatty alcohol ethoxylates that result in high reaction rates as well as high regioselectivities. The benefit of this particular method is that the product layer is easily separated from the reaction mixture and the expensive catalyst can be reused. The same concept has been applied in Heck-type C-C coupling reactions.^[68]

Only few approaches to use latexes in catalysis have been reported previously.^[69-72]

In order to show that latexes can be effectively used as phase-transfer agents, different polystyrene-based latexes were investigated in the biphasic hydroformylation of higher alkenes. The synthesis and characterization of these latexes is described in Chapter 2. Mass transfer limitation in the biphasic hydroformylation using polystyrene-based latexes is discussed in detail.

3.2 General procedure for the biphasic hydroformylation of higher alkenes by means of polystyrene-based latexes

In order to evaluate the applicability of polystyrene-based latexes (Figure 3.5) as phase-transfer agents, the rhodium-catalyzed aqueous phase hydroformylation of 1-octene was investigated (Scheme 3.2). The water-soluble phosphines TPPTS and TPPTB^[73] were applied as monodentate ligands (Figure 3.6).



Scheme 3.2 The hydroformylation of 1-octene

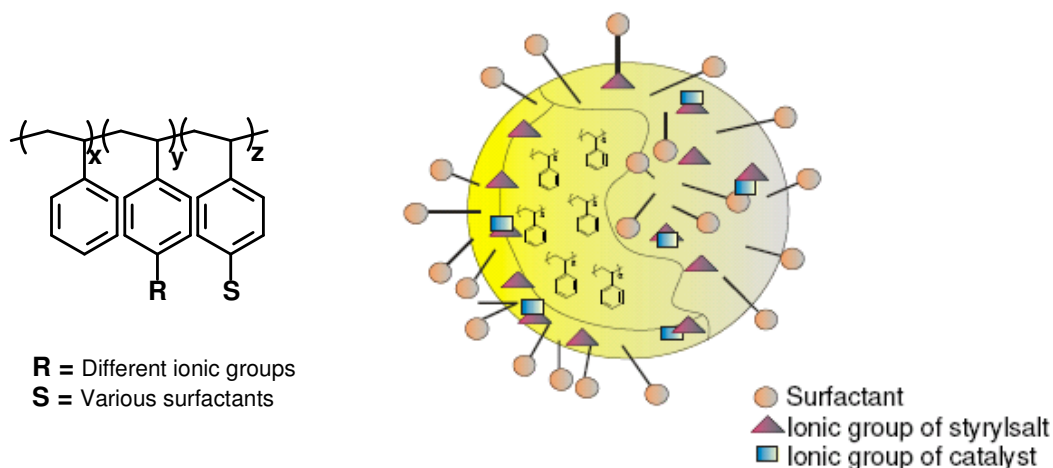


Figure 3.5 Schematic structure of the applied latexes and composition of a latex particle

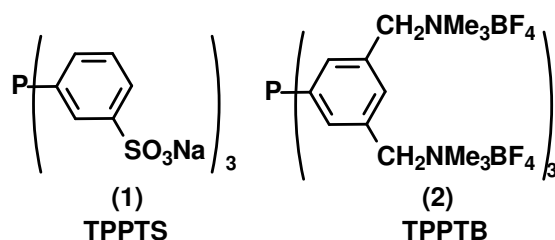


Figure 3.6 Water-soluble ligands applied in the biphasic hydroformylation Tris(3sulfophenyl)phosphine trisodium salt TPPTS (1), tris-(3,5-((trimethylammonio)methyl)phenyl)phosphine hexa-(tetrafluoroborate) (TPPTB) (2)

The polystyrene-based latexes (Chapter 2, Table 2.1) contain the hydrophobic monomer styrene, DVB as crosslinking agent, a non-ionic surfactant, and a styrylsalt. The combination of the non-ionic surfactant and styrylsalts provides an efficient stabilization of the latex particles.

Due to its properties, the polystyrene-based latex is supposed to transfer the water-insoluble alkene into the aqueous phase and consequently, facilitates the contact of the substrate with the catalyst (Figure 3.7).

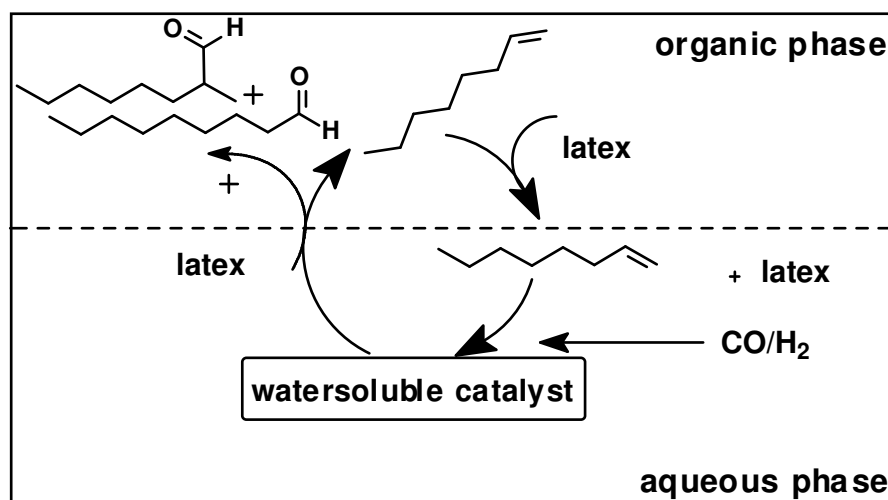


Figure 3.7 Schematic representation of the biphasic hydroformylation of 1-octene using latexes as phase-transfer agents

The biphasic hydroformylation experiments were performed at 80°C and a stirring rate of 700 rpm. These conditions were chosen because the latexes tend to coagulate under harsher reaction conditions, i.e. at higher temperature and higher stirring rates (Chapter 2, Section 2.4). Prior to the addition of the substrate, the catalyst was preformed at 80°C

and 20 bar CO/H₂ (1:1) for 3 h in order to activate the catalyst (resting state). Hydroformylation experiments were performed at different synthesis gas pressures (ranging from 20 bar to 160 bar).

In order to measure the ratios of the hydroformylation reaction, the gas uptake was followed automatically during the course of the reaction. The turnover frequencies were determined at 20% conversion of the alkene. The organic phases were analyzed by means of GC-analysis for conversion and regioselectivity and by ICP-AES in order to determine possible leaching.

3.3 Biphasic hydroformylation of higher alkenes using latexes

In the following sections the results of the biphasic hydroformylation reactions using latexes are presented. Various parameters that might have an influence on the activity and selectivity of the reaction were examined. In particular, the influence of the latex composition on the mass transfer was investigated.

3.3.1 Influence of the ionic character (non-ionic, anionic and cationic) of latexes using TPPTS

In order to evaluate the influence of the ionic character of the latex particles, differently charged latexes were applied as phase-transfer agents in the hydroformylation of 1-octene using Rh(acac)(CO)₂ as catalyst precursor (Figure 3.8). The results are shown in Table 3.1.

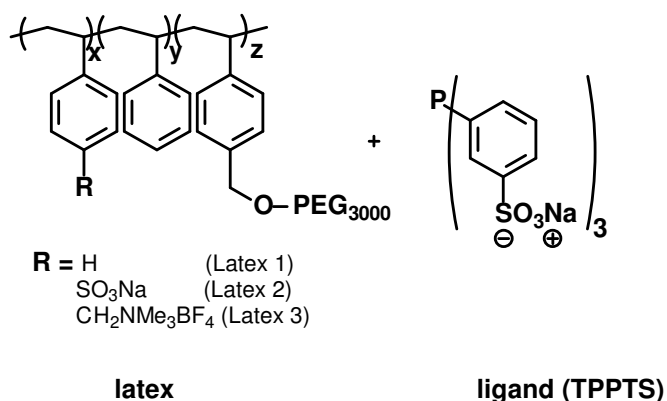


Figure 3.8 Schematic structures of latex and the applied ligand system

Table 3.1 Biphasic hydroformylation of 1-octene using TPPTS and latexes containing different ionic groups

Entry	Latex	Ionic group	Time [h]	Conversion [%]	Ratio l/b	TOF [h ⁻¹]
1	/	/	140	/	/	/
2	1	/	140	9.0	1.9	n.d.
3	2	SO ₃ Na	140	11.0	2.0	n.d.
4	3	CH ₂ NMe ₃ BF ₄	140	99	2.9	150

(a) Reaction conditions: 80°C, 700 rpm, 20 bar CO/H₂ (1:1), aqueous layer (15 mL), latex (solid amount 500 mg, 15 mL), Rh:L:S (1:6:3500), Rh(acac)(CO)₂ (7.2 mg, 0.0276 mmol, 0.92 mmol/L), TPPTS (95 mg, 0.166 mmol, 5.56 mmol/L), 1-octene (15 mL, 95 mmol, 3.17 mol/L)

In the absence of any latex no conversion was observed, caused by the negligible solubility of 1-octene in water.

A series of experiments showed a threshold amount of 1-octene for the biphasic hydroformylation using latexes to take place.

Below a 1-octene concentration of 0.4 mol/L no reaction occurred using a latex amount of 500 mg dispersed in 20 mL H₂O. Above 0.4 mol/L the reaction took place. Moreover, the yield observed by analyzing the organic phase by gas chromatography was not equal to the conversion observed by the gas uptake of CO/H₂. Perpetual the observed yield was lower (2-5%) compared to the conversion. Thus, we assume that a small amount of substrate/product remains in the latex phase after the reaction, resulting in a lower yield in the organic phase. Dynamic exchange of 1-octene with the environment, hence also catalysis, only occurs at a reasonable rate after the latex is completely loaded.

The addition of non-ionic latex did not significantly enhance the reaction rate either. A conversion of only 9% was obtained (Entry 2). Similar results were obtained for the sulfonated latex (Entry 3). However, with the ammonium-functionalized latex, the reaction rate was enhanced dramatically (Entry 4) and a turnover frequency of up to 150 h⁻¹ was observed (Figure 3.9).

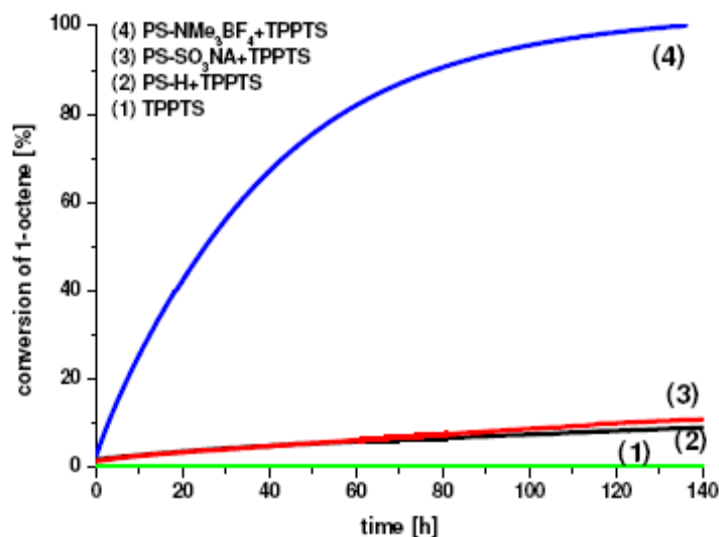


Figure 3.9 Conversion of 1-octene based on the gas uptake CO/H₂ versus the reaction time

Even though latex 1 (Table 3.1, Entry 2) transferred the substrate into the aqueous phase (Chapter 2), it seems that the 1-octene does not reach the Rh-complex. Our interpretation is that there is little interaction of the sulfonated catalyst dissolved in the aqueous phase with the non-ionic latex particles, resulting in a very low reaction rate.

The same argument holds for latex 2 (Table 3.1, Entry 3), containing sulfonated groups located in the interface of the particles. Although one might expect an increased interaction of the sulfonated catalyst with the charged double layer of the latex particles, this seems to play only a marginal role.

The ammonium groups of latex 3 form a positively charged shell, which seemingly leads to an efficient interaction with the negatively charged rhodium complex. Thus, the catalyst concentration at the interface increases and the reaction rate is dramatically enhanced (Table 3.1, Entry 4, Figure 3.9 (4) and Figure 3.10).

Apparently, the dramatic differences in 1-octene conversion can be attributed to electrostatic interaction between the ammonium-functionalized latex particles and the sulfonated groups of the catalyst complex.

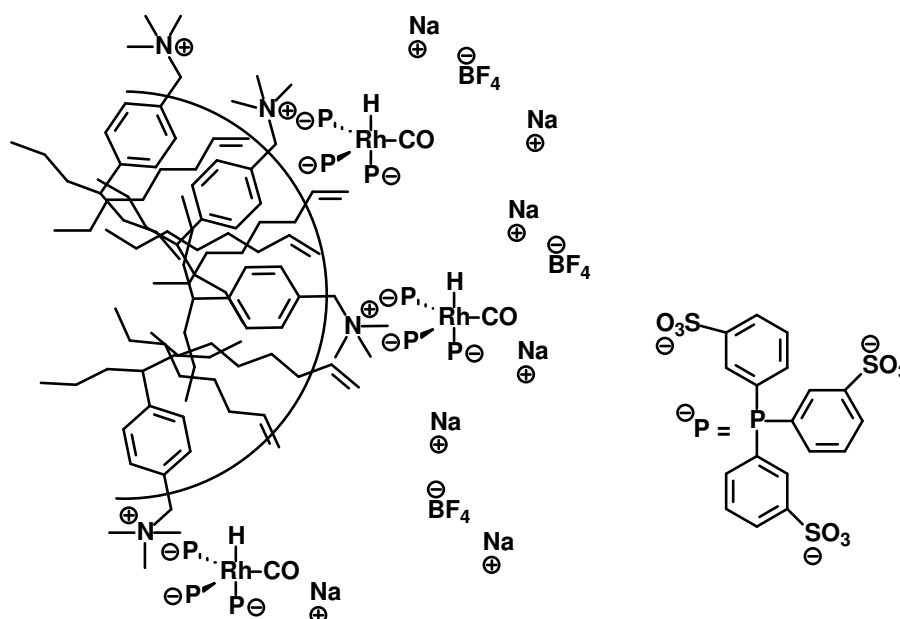


Figure 3.10 Schematic representation of the interaction between the ammonium-functionalized latex and the sulfonated catalyst

Similar effects were observed by Li *et al.*^[74] The authors demonstrated that the ionic character of different surfactants used as phase-transfer agents can dramatically influence the reaction rate of a biphasic hydroformylation. Non-ionic or anionic surfactants did not enhance the rate of the biphasic hydroformylation of 1-dodecene. In contrast, the reaction was dramatically accelerated using cationic surfactants. It was proposed that this enhancement is due to the fact that the cationic ends of the surfactants form a positively charged layer. This layer can interact with the anionic rhodium complex, $[\text{HRh}(\text{CO})(\text{TPPTS})_3]^{3-}$. Consequently, the catalyst accumulates at the interface and can readily react with the substrate.

3.3.2 Influence of the ionic character (non-ionic, anionic and cationic) of latexes using TPPTB

In order to put our previous explanation to the test, different charged latexes were applied under the same conditions but using a positively charged catalyst complex, bearing ammonium groups in the ligand $[\text{HRh}(\text{CO})(\text{TPPTB})_3]^{6+}$ (Figure 3.11). All results are summarized in Table 3.2.

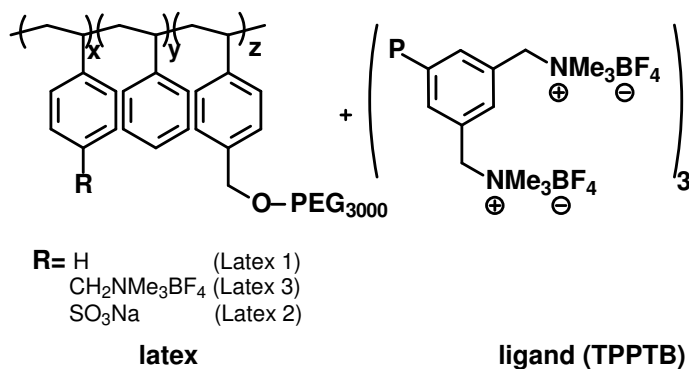


Figure 3.11 Schematic structures of latexes and the applied cationic ligand system

Table 3.2 Biphasic hydroformylation of 1-octene using TPPTB and latexes containing different ionic groups

Entry	Latex	Ionic group	Time [h]	Conversion [%]	Ratio l/b	TOF [h^{-1}]
1	1	/	140	8.0	1.9	n.d.
2	2	SO_3Na	140	35	2.6	85
3	3	$\text{CH}_2\text{NMe}_3\text{BF}_4$	140	13.0	2.0	n.d.

(a) Reaction conditions: 80°C , 600rpm, 20 bar CO/H_2 (1:1), aqueous layer (15 mL), latex (solid amount 500 mg, 15-20 mL), Rh:L:S (1:6:3500), $\text{Rh}(\text{acac})(\text{CO})_2$ (7.2 mg, 0.0276 mmol, 0.92 mmol/L), TPPTB (202 mg, 0.0166 mmol, 5.56 mmol/L), 1-octene (15 mL, 95 mmol, 3.17 mol/L)

The addition of non-ionic latex does not significantly enhance the reaction rate. Only a conversion of 8% was obtained.

In the case of ammonium-functionalized latex the reaction was not accelerated either (Entry 2).

However, with the sulfonated latex the reaction rate was enhanced dramatically (Entry 3) and a turnover frequency of up to 85 h^{-1} was observed.

Apparently, a similar effect as for the biphasic hydroformylation using TPPTS (Section 3.3.1) is responsible for the enhanced activity.

3.3.3 Phase-transfer mode of operation for latexes

Based on our observations we sketch the following picture for the mode of operation in latex-mediated phase-transfer hydroformylation.

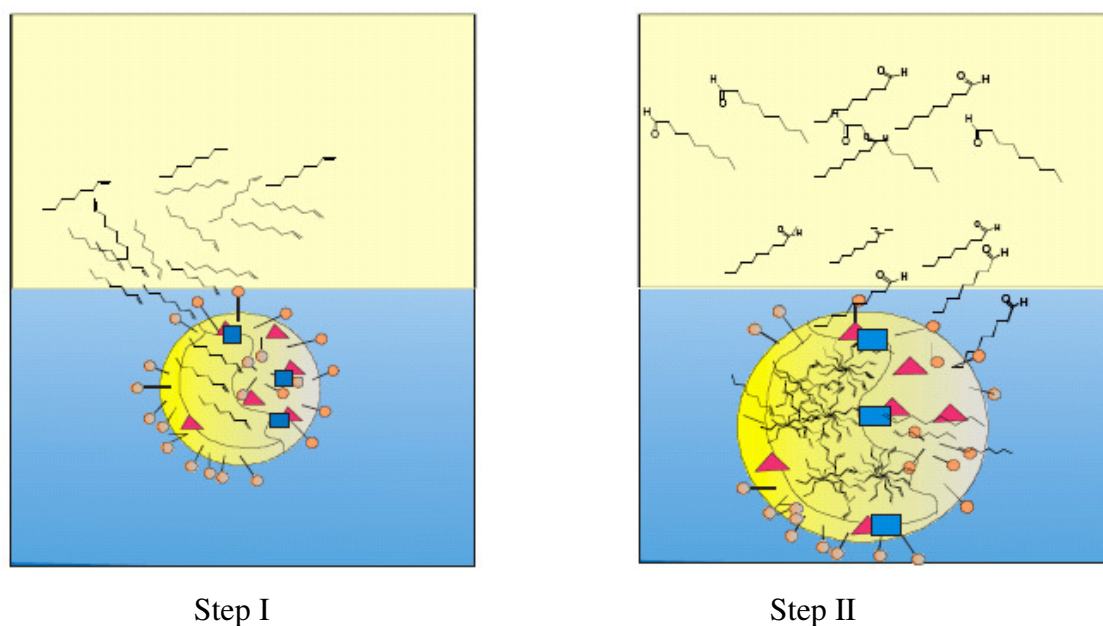


Figure 3.12 Phase-transfer mode of operation for latexes

The apolar alkene is transferred into the lipophilic core of the latex particles, which swell with the incorporation of substrate (Figure 3.12, Step I). Once the uptake capacity of the particles is reached, the alkene can be converted by the Rh-species at the particle core-shell interface. This nicely fits with our observation that there is a threshold amount of 1-octene needed for the hydroformylation to take place (Figure 3.12, Step II).

3.3.4 *Influence of different amounts of phase-transfer agents*

In multiphase systems, the reaction rate can be reduced by mass transfer limitations. In the systems described in this thesis, the phase-transfer of the substrate depends on the interphase area between the organic and the aqueous layer, generated by the latex.

Increasing amounts of latex increase the interphase area, reducing the liquid-liquid mass transfer limitation and ultimately overcome this limitation completely.

Therefore, different latex concentrations were used in the biphasic hydroformylation reaction. The optimal latex concentration was determined by comparing the corresponding reaction rates based on the gas uptake curves. All results are summarized in Table 3.3 and depicted in Figure 3.13.

Table 3.3 Biphasic hydroformylation of 1-octene using TPPTS and different amounts of latex 3

Entry	Solid amount [mg]	Time [h]	Conversion [%]	Ratio l/b	TOF [h^{-1}]
1	100	140	70	1.9	53
2	500	140	99	2.4	150
3	750	140	99	2.0	145
4	1000	140	93	2.6	120

(a) Reaction conditions: 80°C, 700 rpm, 20 bar CO/H₂ (1:1), aqueous layer (15 mL), latex 3 (15 mL), Rh:L:S (1:6:3500), Rh(acac)(CO)₂ (7.2 mg, 0.0276 mmol, 0.92 mmol/L), TPPTS (95mg, 0.166 mmol, 5.56 mmol/L), 1-octene (15 mL, 95 mmol, 3.17 mol/L)

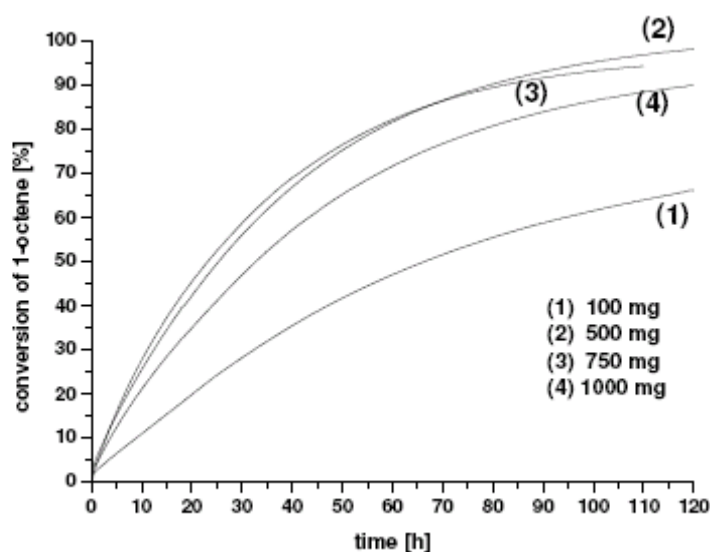


Figure 3.13 Conversion of 1-octene based on the gas uptake CO/H₂ versus the reaction time, conditions see Table 3.3

A clear trend can be observed when comparing the reaction rates. The TOF increased considerably when the amount of latex (given in dry matter) was increased from 100 to 500 mg. This implies that more substrate is transported into the interface area.

On the other hand, by further increasing the amount of latex to 750 and 1000 mg, respectively, the TOF decreased. One possible explanation for this decrease might be the resulting different molar ratio of Rh-catalyst and latex particles.

Therefore, the molar ratio of catalyst to latex particles was estimated for different particle sizes and latex amounts of 500 and 1000 mg. The amount of particles in solution n_p , was calculated according to Equation 1 for different average particle sizes, assuming spherical particles. For the latex particles the density of polystyrene was used.

$$n_p = \frac{6m_L}{\pi d^3 \rho_{PS} N_A} \quad (1)$$

n_p = amount of particles in solution [mol]
 m_L = amount of applied latex [g]
 d = average diameter of the particles [cm]
 ρ_{PS} = density of polystyrene (1.05 g/cm³)
 N_A = 6.022 × 10²³ mol⁻¹

The calculated estimates for the molar ratios are given in Table 3.4 and visualized in Figure 3.14.

Table 3.4 Rh-loading per latex particle

D _p [nm]	Solid amount 500 mg		Solid amount 1000 mg	
	n _p [μmol]	Molar ratio Rh ^a /latex	n _p [μmol]	Molar ratio Rh ^a /latex
5	12.08	2.3	24.16	1.14
10	1.51	18.3	3.02	9.14
20	0.19	145.2	0.38	72.6
40	0.023	1200	0.047	600
70	0.0044	6272	0.0088	3136

(a) n_{Rh} = 27.6 μmol

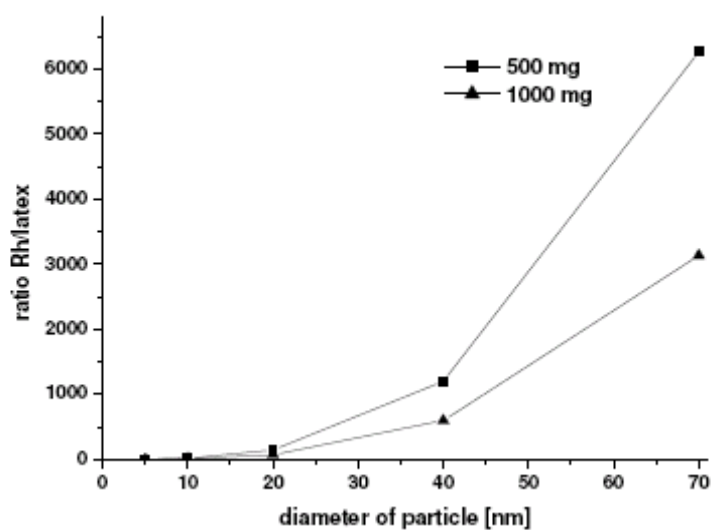


Figure 3.14 Calculated molar ratio Rh/particles for different average particle sizes

From Table 3.4 it is clear that by increasing the solid amount of latex a decrease in the molar ratio Rh/particle results. With increasing particle diameter a dramatic increase in the ratio Rh/particle occurs. The decrease in the Rh/particle ratio could result in a reduced reactivity. This limitation has to be considered mainly for systems which contain a large fraction of small particles (very low average Rh/particle ratio). For

instance, at an average particle size of 5 nm the molar Rh/particle ratio for 1000 mg of latex is only 1.14 compared to 3136 for a system with an average particle size of 70 nm. Furthermore, it should be kept in mind that the Rh- catalyst can be freely dispersed in the aqueous phase which could alter these ratios. Especially for the larger particles it may be assumed that more than one Rh-complex will be associated per particle. One may further assume is that not all Rh is in its active form at the same time. Although these considerations are made under a number of assumptions and can give only a rough estimation, one can draw conclusions and get a better feeling for the situation:

For latexes with a broad particle size distribution containing a large fraction of small particles and at a high loading of latex in the system, given the low Rh-concentration under catalytic conditions, it may well be that an increasing number of latex particles is not associated by a Rh-catalyst complex.

For these reasons it can be expected that there will be an optimum ratio of Rh-concentration and m_{latex} for each different latex polymer, depending on the individual particle size distribution. In the case examined here (Figure 3.13) this optimum ratio for $n_{\text{Rh}} = 27.6 \mu\text{mol}$ is reached at $m_{\text{latex}} = 500 \text{ mg}$.

3.3.5 Influence of surfactants

The role of the molecular weight of non-ionic surfactants on the behavior of latexes as phase-transfer agents in the biphasic hydroformylation of 1-octene was investigated.

In the case of the hydroformylation reaction using TPPTS, ammonium-functionalized latexes containing different surfactants were used (Figure. 3.15) and the results are depicted in Table 3.5.

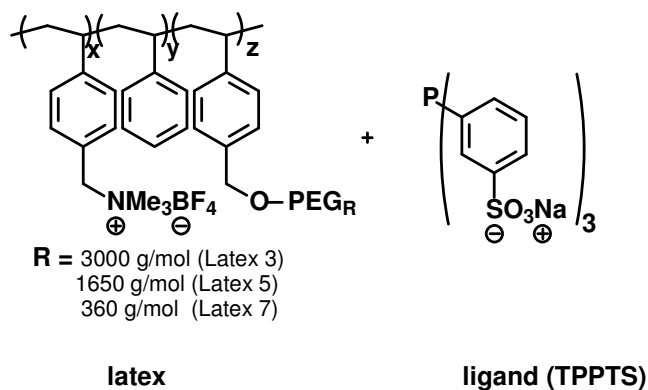


Figure 3.15 Schematic structures of the latexes and the applied ligand system

Table 3.5 Biphasic hydroformylation of 1-octene using TPPTS and latexes containing different surfactants

Entry	Latex	Surfactant [g/mol]	Time [h]	Conversion [%]	Ratio l/b	TOF [h^{-1}]
1	3	3000	140	99	2.4	150
2	5	1650	140	99	2.2	200
3	7	360	140	99	2.2	80

(a) Reaction conditions: 80°C, 700 rpm, 20 bar CO/H₂ (1:1), aqueous layer (15 mL), latex (solid amount 500 mg, 15-20 mL), Rh:L:S (1:6:3500), Rh(acac)(CO)₂ (7.2 mg, 0.0278 mmol, 0.922 mmol/L), TPPTS (95 mg, 0.1667 mmol, 5.56 mmol/L), 1-octene (15 mL, 95 mmol, 3.17 mol/L)

The highest rates were observed for latex 5 (PEG₁₆₅₀). Apparently, the latex with a shorter surfactant length (latex 5) has a lower surface coverage compared to the latex with a longer surfactant length (latex 3). For a higher surface coverage, the movement of 1-octene and nonanal across the particle interface is restricted. Therefore, the catalysis is largely limited by liquid-liquid mass transfer. Another possibility is that the longer surfactants can hinder the catalyst to interact with the styrylsalts due to their surface coverage. Consequently, the catalyst is not located in close proximity of the substrate and the reaction rate decreases (Figure 3.16).

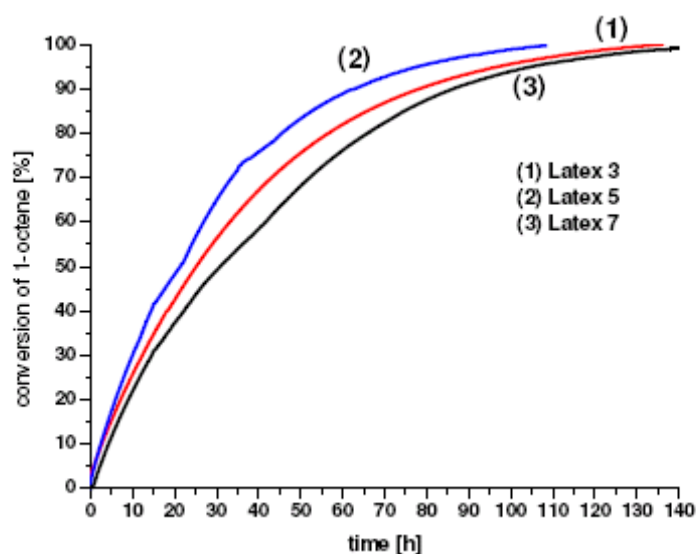


Figure 3.16 Conversion of 1-octene based on the gas uptake CO/H₂ versus the reaction time

Latex 7 (PEG₃₆₀) showed the lowest rate. Besides the shorter PEG surfactant, this latex contains 5 mol% of surfactant instead of 2 mol% as for the other latexes. For this short chain PEG surfactant, particle coagulation occurred for surfactant amounts lower than 5

mol%. The higher amount of surfactant also enlarges the particle coverage, which might lead to a decrease in reaction rate.

Another reason for the decrease of the reaction rate could originate from the molar ratio of Rh per latex particle. In comparison to latex 3 (d= 90 nm) and latex 5 (d= 37 nm), the average particle diameter of latex 7 is d = 25 nm. Assuming that latex 7 contains a high fraction of small particles, the Rh/latex molar ratio (Section 3.3.4) might be quite low, resulting in a decrease of the reaction rate.

For latex 3 and 5 the molar ratio of Rh/latex particles seems to play only a marginal role, which can be due to the higher average particle size. Here, the effect of surface coverage due to the surfactants seems to be predominant.

In case of the hydroformylation using TPPTB as ligand, sulfonated latexes were used (Figure. 3.17). The results obtained are shown in Table 3.6.

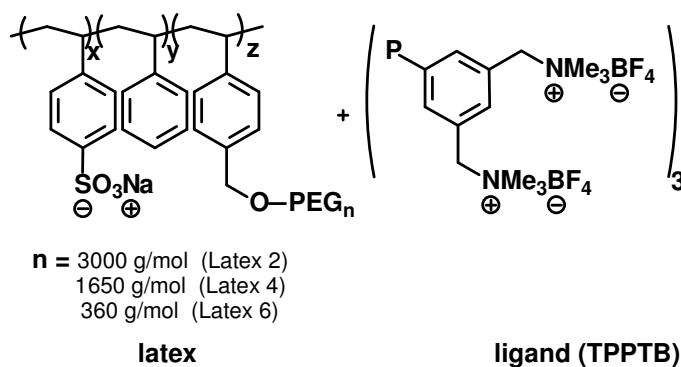


Figure 3.17 Schematic structures of latexes and the applied ligand system

Table 3.6 Biphasic hydroformylation of 1-octene using TPPTB and latexes containing different surfactants

Entry	Latex	Surfactant [g/mol]	Time [h]	Conversion [%]	Ratio l/b	TOF [h ⁻¹]
1	2	3000	140	25	2.4	85
2	4	1650	140	99	2.2	100
3	6	360	140	99	2.2	250

(a) Reaction conditions: 80°C, 700 rpm, 20 bar CO/H₂ (1:1), aqueous layer (15 mL), latex (solid amount 500 mg, 15-20 mL), Rh:L:S (1:6:3500), Rh(acac)(CO)₂ (7.2 mg, 0.0278 mmol, 0.922 mmol/L), TPPTB (202 mg, 0.1667 mmol, 5.56 mmol/L), 1-octene (15 mL, 95 mmol, 3.17 mol/L)

By decreasing the surfactant molecular weight, an increase in reaction rate was noticed. The highest reaction rate was observed for latex 6 (PEG₃₆₀), which contains the shortest surfactant (Figure 3.18). This latex also contains only 2 mol% of surfactant, just like all other latexes. Apparently, latex 6 has a lower surface coverage compared to the latexes

with a longer surfactant chain (latexes 2 and 4). For a higher surface coverage, the transport of 1-octene and nonanal across the particle interface might be restricted. Therefore, catalysis might be limited by mass transfer. Furthermore, assuming that the longer surfactants might hinder the catalyst to interact with the styrylsalts due to the higher surface coverage, the catalyst is not located in close proximity of the substrate and the reaction rate decreases.

The decrease of Rh/latex molar ratio by decreasing the particle size from latex 2 to latex 6 seems to have only a marginal effect. Although the average particle size decreases, the reaction rate increased from latex 2 to latex 6.

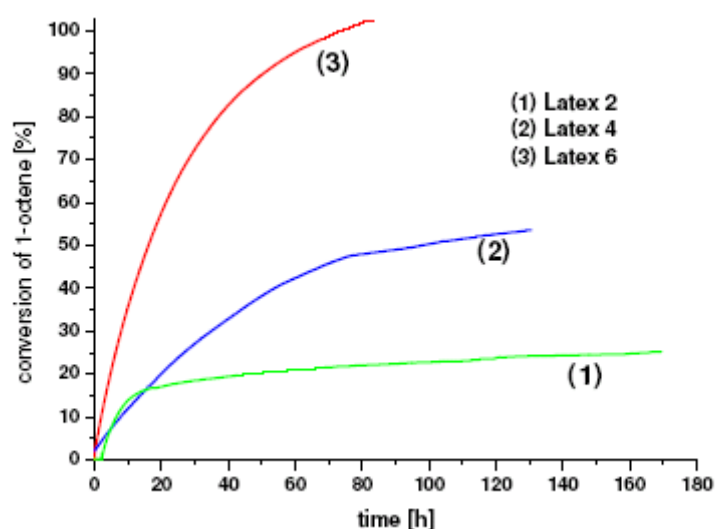


Figure 3.18 Conversion of 1-octene based on the gas uptake CO/H₂ versus the reaction time

In summary, the best results were obtained for the combinations of latex 5 with TPPTS, and latex 6 with TPPTB. Therefore, these systems were used for further investigations.

3.3.6 Influence of the synthesis gas solubility

Deshpande *et al.*^[75] showed that the CO partial pressure can influence the hydroformylation rate in a biphasic system, depending on the CO solubility in the solvent applied. The kinetics of the biphasic hydroformylation of 1-octene were studied using water-soluble Rh/TPPTS as catalyst and ethanol as cosolvent. It was observed that the reaction rate first increased with increasing the partial pressure of CO and passed through a maximum, with substrate-inhibited kinetics at higher P_{CO} . The initial

increase of P_{CO} enhances the formation of the active catalytic complex. Any further increase of the P_{CO} will favour the preferential formation of inactive di- and tricarbonylacylrhodium species. The maximum in their investigations was already passed at a P_{CO} of 5 bar, which is due to the fact that in an ethanol-water mixture (1:1) the solubility of CO is relatively high ($0.0157 \text{ mol/cm}^{-3}$ at $T=80^\circ\text{C}$).

Miyagawa *et al.*^[76] reported on the influence of various parameters such as temperature, pressure, substrate concentration, and catalyst concentration on the rhodium-catalyzed hydroformylation of higher alkenes in microemulsions and micellar media using TPPTS as ligand. They examined the influence of the CO partial pressure on the rate of the hydroformylation reaction up to 60 bar (CO:H₂, 3:1). At 45 bar P_{CO} , the reaction rate was still enhanced. It was claimed that no CO-inhibition was observed due to the low CO solubility in aqueous medium as compared to ethanol-water mixtures or organic solvents. For this reason, it seems likely that a change in reaction rate with an increasing P_{CO} will be observed in biphasic catalysis reactions using latexes.

In order to predict at which P_{CO} reasonable reaction rates can be expected for a biphasic system containing latexes, a control system was evaluated first. As a reference system, the homogeneous hydroformylation using triphenylphosphine as ligand in toluene was chosen. This reaction is typically performed at 15-20 bar CO/H₂ (1:1) and at a reaction temperature of 80°C . In order to extrapolate this system to the biphasic system, the solubility of CO in toluene is calculated and compared to water.

The calculations were carried out according to Henry's law as described by Delmas *et al.* (Equation 2).^[77]

$$K_H = \frac{P}{c_2} \quad \begin{array}{l} P = \text{partial pressure [MPa]} \\ c_2 = \text{dissolved gas concentration [kmol/m}^3\text{]} \\ K_H = \text{Henry's law constant [MPa m}^3\text{/kmol]} \end{array} \quad (2)$$

From the K_H and the known partial pressure it is possible to calculate the dissolved gas concentration in the solvents at 80°C . The K_H for CO proposed by Delmas *et al.* is $11.61 \pm 0.18 \text{ MPa m}^3\text{/kmol}$ in toluene, while it is $128.79 \pm 2.01 \text{ MPa m}^3\text{/kmol}$ in water.

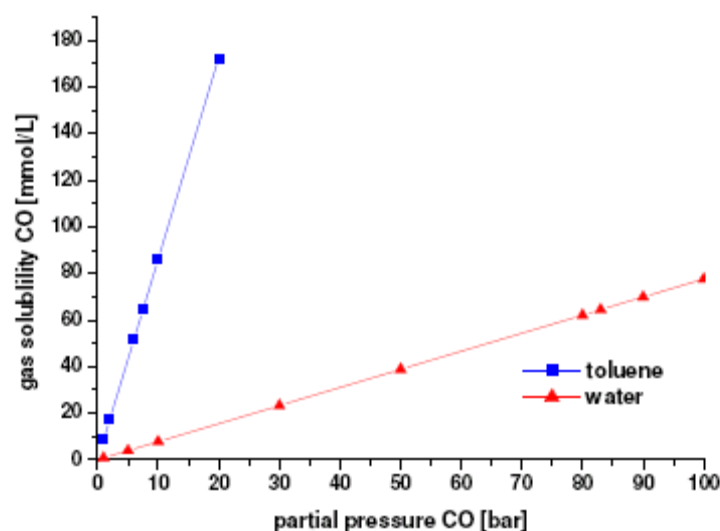


Figure 3.19 Pressure dependence of CO solubility in water and toluene according to Delmas et al.

The large difference in gas-solubility for toluene and water is visualized in Figure 3.19, in which the partial pressure is plotted *versus* the concentration of dissolved CO. At a partial pressure of $P_{CO} = 7.5$ bar (15 bar synthesis gas 1:1) the concentration of dissolved CO is approximately 64.5 mmol/L in toluene.

In water, the same concentration is reached at a partial pressure of CO $P_{CO} = 83$ bar and 166 bar synthesis gas (1:1), respectively.

The biphasic hydroformylation of 1-octene using latexes as phase-transfer agents were therefore performed at different CO/H₂ pressures ranging from 20 bar to 170 bar, at $T = 80^{\circ}\text{C}$ and a stirring rate of 700 rpm.

All results using TPPTS are summarized in Table 3.7 and the corresponding conversions are depicted in Figure 3.20.

Table 3.7 Biphasic hydroformylation of 1-octene at different pressures using TPPTS and latex 5

Entry	Pressure CO/H ₂ [bar]	Time [h]	Conversion [%]	Ratio l/b	TOF [h ⁻¹]
1	20	140	99	2.1	600
2	80	50	99	2.3	1500
3	115	50	99	2.4	1800
4	140	50	99	2.2	2000
5	160	50	99	2.2	1650

(a) Reaction conditions: 80°C , 700 rpm, 140 bar CO/H₂ (1:1), aqueous layer (20 mL), latex 5 (solid amount 500 mg, 15 mL), Rh:L:S (1:6:22300), Rh(acac)(CO)₂ (1.44 mg, $5.5 \cdot 10^{-3}$ mmol, 0.278 mmol/L), TPPTS (19 mg, 0.033 mmol, 1.668 mmol/L), 1-octene (20 mL, 124 mmol, 0.5 mol/L)

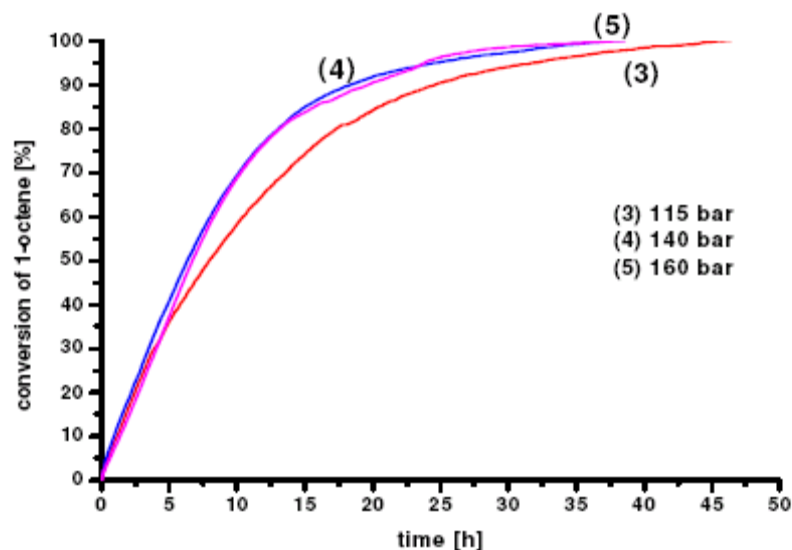


Figure 3.20 Conversion of 1-octene based on the gas uptake CO/H₂ versus the reaction time

The TOF increased from 600 h⁻¹ to 2000 h⁻¹ by increasing the pressure from 20 bar to 140 bar CO/H₂. At a pressure of 160 bar a decrease in TOF was observed again (Figure 3.20).

With TPPTB the highest turnover frequency (1800 h⁻¹) was already reached at 115 bar, which is significantly lower compared to the biphasic hydroformylation of 1-octene with TPPTS.

Table 3.8 Biphasic hydroformylation of 1-octene at different pressures using TPPTB and latex 7

Entry	Pressure [bar]	Time [h]	Conversion [%]	Ratio l/b	TOF [h ⁻¹]
1	20	140	99	2.1	650
2	80	50	99	2.4	1700
3	115	50	99	2.2	1800
4	135	50	99	2.2	1700

(a) Reaction conditions: 80°C, 700 rpm, 140 bar CO/H₂ (1:1), aqueous layer (20 mL), latex 7 (solid amount 500 mg, ~15-20 mL), Rh:L:S (1:6:22300), Rh(acac)(CO)₂ (1.44 mg, 5.5·10⁻³ mmol, 0.278 mmol/L), TPPTB (40 mg, 0.033 mmol, 1.668 mmol/L), 1-octene (20 mL, 124 mmol, 0.5 mol/L)

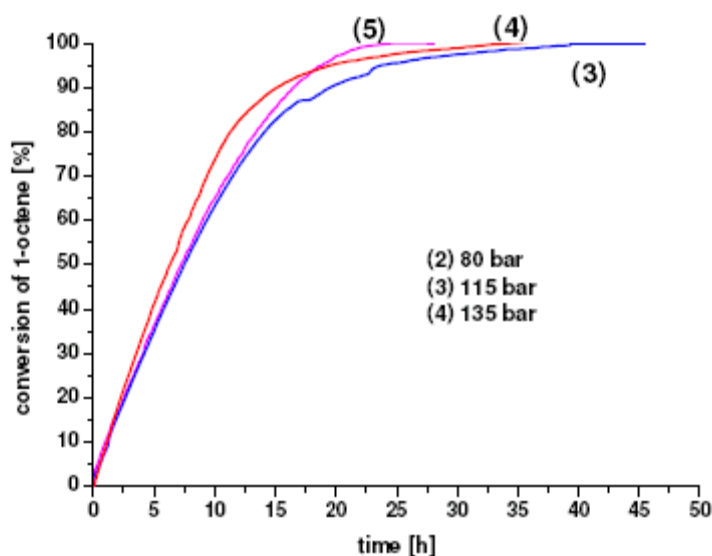


Figure 3.21 Conversion of 1-octene based on the gas uptake CO/H₂ versus the reaction time

In summary, the best reaction rates were observed at a synthesis gas pressure of 140 bar using TPPTS and 115 bar using TPPTB, respectively. It seems that the catalytic systems are not limited by the CO solubility at these pressures.

In the following sections (Section 3.3.6 and 3.3.7) several latexes, which vary in composition, were examined as phase-transfer agents in the biphasic hydroformylation reaction. Consequently, catalysis was carried out at a pressure of 140 bar CO/H₂ (1:1) based on the findings described above.

3.3.7 *Influence of different polymers in the lipophilic core of the latex particles*

Latexes with different core compositions were used in the biphasic hydroformylation of 1-octene. Different mixtures of polymers such as polystyrene/poly(methyl methacrylate) (PS/PMMA= 1:1), polystyrene/poly(*n*-butyl methacrylate) (PS/PBMA= 1:1 and 1:9) were investigated (Figure 3.22). The results are summarized in Table 3.9.

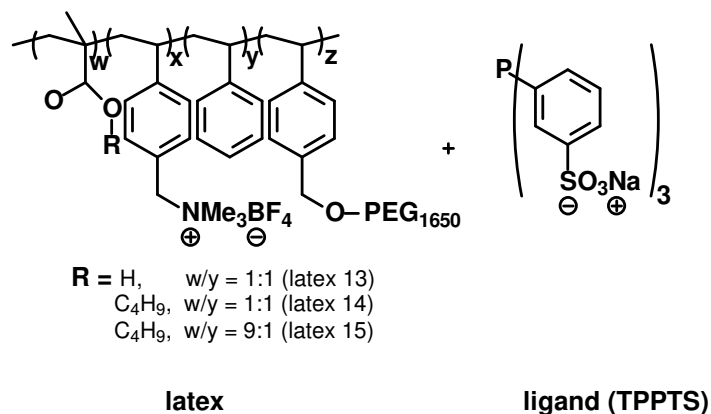


Figure 3.22 Schematic structures of latexes and the applied ligand system

Table 3.9 Results of biphasic hydroformylation of 1-octene using latexes containing different polymer compositions

Entry	Latex	Time [h]	Conversion [%]	Ratio l/b	TOF [h^{-1}]
1	5 (PS)	50	99	2.4	2000
2	13 (PS/PMMA)(1:1)	50	99	2.2	1150
3	14 (PS/PBMA)(1:1)	50	99	2.2	1400
4	15 (PS/PBMA)(1:9)	50	99	2.5	1150

(a) Reaction conditions: 80°C, 700 rpm, 140 bar CO/H_2 (1:1), aqueous layer (20 mL), latex (solid amount 500 mg, 15-20 mL), $\text{Rh}:\text{L}:\text{S}$ (1:6:22300), $\text{Rh}(\text{acac})(\text{CO})_2$ (1.44 mg, $5.5 \cdot 10^{-3}$ mmol, 0.278 mmol/L), TPPTS (19 mg, 0.033 mmol, 1.668 mmol/L), 1-octene (20 mL, 124 mmol, 0.5 mol/L)

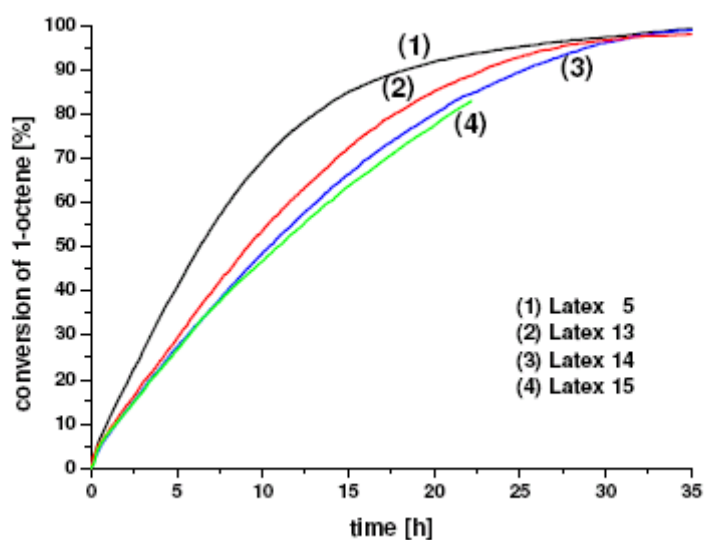


Figure 3.23 Conversion of 1-octene based on the gas uptake CO/H_2 versus the reaction time

As shown in Table 3.9 and Figure 3.23 the composition of the lipophilic core of the latex has an influence on the reaction rate. The highest TOF (2000 h^{-1}) was observed for latex 5. The activity decreased using the latexes 13-15. This decrease is most probably due to the higher hydrophilicity of their core compared to latex 5 (PS), caused by the use of the more polar polymers PMMA and PBMA. The dielectric constant of PS ($\epsilon_{25} = 2.55$) is slightly lower than for polyacrylates ($\epsilon_{25} = 2.6- 2.8$). Furthermore, the lipophilic core of latex 14 and 15 are softer due to a lower glass transition temperature (T_g) of PBMA ($T_g = 40-45^\circ\text{C}$) compared to PS ($T_g = 100^\circ\text{C}$). Thus, at higher temperature these latexes might begin to flow, resulting in fused structures. These factors might cause a lower substrate concentration in the particles and hence a lower reaction rate. Furthermore, the more polar product nonanal might accumulate in the latex core.

3.3.8 *Influence of different amounts of DVB cross-linker in the latex particles*

Another important feature in the biphasic hydroformylation is the degree of crosslinking of the polystyrene. Latexes, differing in the amount of DVB were synthesized and their performances were compared. The hydroformylation experiments were performed at 140 bar, 80°C and a stirring rate of 700 rpm. The results are summarized in Table 3.10 and in Figure 3.24.

Table 3.10 Biphasic hydroformylation of 1-octene using TPPTS and latexes containing different amount of DVB

Entry	Latex	DVB [mol%]	Time [h]	Conversion [%]	Ratio l/b	TOF [h^{-1}]
1	8	0	50	99	2.2	1250
2	9	1	50	99	2.4	1700
3	5	2	50	99	2.4	2000
4	10	3	50	99	2.3	1500
5	11	4	50	99	2.2	1700
6	12	5	50	99	2.1	1600

(a) Reaction conditions: 80°C , 700 rpm, 140 bar CO/H_2 (1:1), aqueous layer (20 mL), latex (solid amount 500 mg, 15-20 mL), Rh:L:S (1:6:22300), $\text{Rh}(\text{acac})(\text{CO})_2$ (1.44 mg, $5.5 \cdot 10^{-3}$ mmol, 0.278 mmol/L), TPPTS (19 mg, 0.033 mmol, 1.668 mmol/L), 1-octene (20 mL, 124 mmol, 0.5 mol/L)

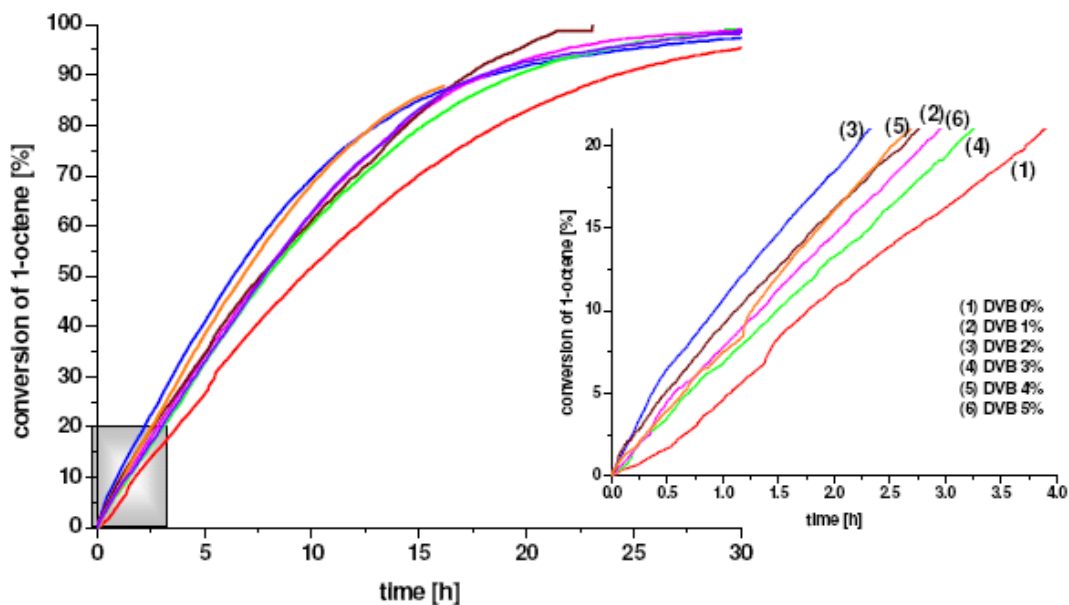


Figure 3.24 Conversion of 1-octene based on the gas uptake CO/H_2 versus the reaction time

As can be seen from Table 3.10 and Figure 3.24, the turnover frequencies vary from 1250 to 2000 h^{-1} . The reaction rate increased up to 2000 h^{-1} (Entry 3) by increasing the degree of crosslinking to 2%. This appears to be the optimal value. Further increase of crosslinking leads to a decrease in TOF to 1500-1700 h^{-1} .

Latex 5 with a degree of crosslinking of 2 mol% is the optimal polystyrene-based latex.

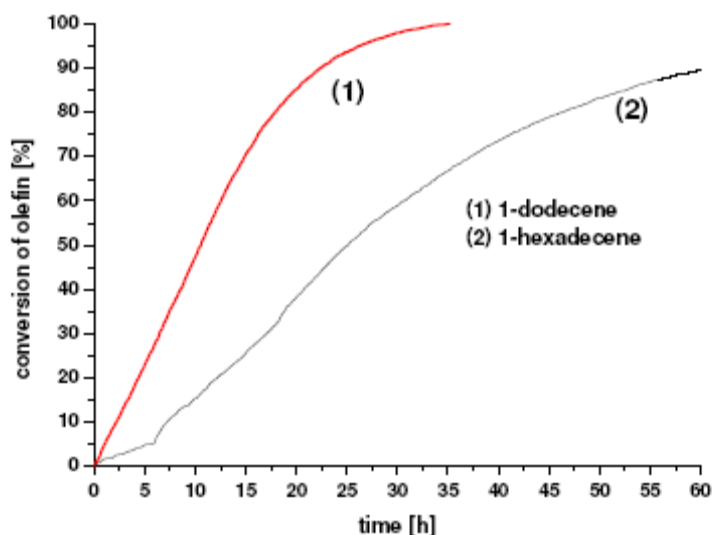
3.3.9 *Biphasic hydroformylation of higher alkenes using latexes as phase-transfer agents*

In order to illustrate the ability of polystyrene latexes to act as phase-transfer agents in the biphasic hydroformylation of alkenes higher than 1-octene, hydroformylation of 1-dodecene and 1-hexadecene was investigated. The reactions were carried out at 140 bar CO/H_2 (1:1), 80°C and a stirring rate of 700 rpm using latex 5 as phase-transfer agent. The catalytic results are listed in Table 3.11 and the gas uptake curves are depicted in Figure 3.25.

Table 3.11 Biphasic hydroformylation of higher alkenes using latex 5

Entry	Substrate	Time [h]	Conversion [%]	Ratio l/b	TOF [h ⁻¹]
1	1-dodecene	50	99	2.0	1400
2	1-hexadecene	80	99	2.5	250

(a) Reaction conditions: 80°C, 700 rpm, 140 bar CO/H₂ (1:1), aqueous layer (20 mL), latex 5 (solid amount 500 mg, 15mL), Rh:L:S (1:6:22300), Rh(acac)(CO)₂ (1.44 mg, 5.5·10⁻³ mmol, 0.278 mmol/L), TPPTS (19 mg, 0.033 mmol, 1.668 mmol/L), alkene (124 mmol, 0.5 mol/L)

**Figure 3.25** Conversion of higher 1-alkenes based on the gas uptake CO/H₂ versus the reaction time

As can be seen from Table 3.11, latex 5 also acts as phase-transfer agent for 1-dodecene and 1-hexadecene and relatively high turnover frequencies were observed. As expected the phase-transfer of the higher C₁₆ alkene seems to be more hindered.

3.4 Comparison of PPh₃ and TPPTS in the hydroformylation of 1-octene

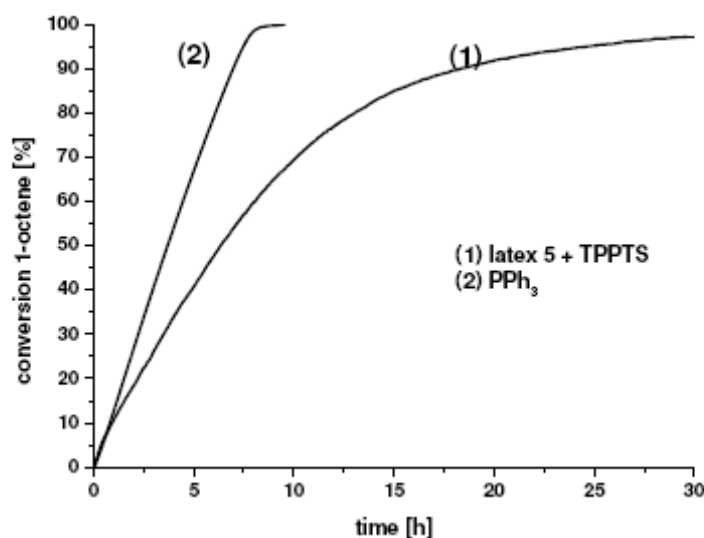
Among all biphasic hydroformylation experiments carried out, the combination of TPPTS and latex 5 was the best performing system.

In a bench mark experiment the biphasic hydroformylation of 1-octene using latex 5 and TPPTS was compared to the homogeneous single-phase hydroformylation with triphenylphosphine in toluene.

Table 3.12 Hydroformylation of 1-octene using latex and PPh₃^a

Entry	Ligand	Latex	Time [h]	Conversion [%]	Ratio l/b	TOF [h ⁻¹]
1 ^b	TPPTS	5	50	99	2.4	2000
2 ^c	PPh ₃	none	20	99	2.6	3000

(a) Reaction conditions: 80°C, 700 rpm, Rh:L:S (1:6:22300), Rh(acac)(CO)₂ (1.44 mg, 5.5·10⁻³ mmol, 0.278 mmol/L), 1-octene (20 mL, 124 mmol, 0.5 mol/L); (b) biphasic hydroformylation: 140 bar CO/H₂ (1:1), aqueous layer (20 mL), latex 5 (solid amount 500 mg, 15 mL), TPPTS (19 mg, 0.033 mmol, 1.668 mmol/L); (c) homogeneous hydroformylation: 15 bar CO/H₂ (1:1), toluene (20 mL), PPh₃ (9 mg, 0.033 mmol, 1.668mmol/L)

**Figure 3.26** Conversion of 1-octene based on the gas uptake CO/H₂ versus the reaction time

The rate in the aqueous biphasic hydroformylation of 1-octene, using latex 5/TPPTS (TOF= 2000 h⁻¹) was found to be in the same range as in the single phase hydroformylation in toluene using PPh₃ as ligand (TOF= 3000 h⁻¹).

No significant Rh-loss was detected (<0.9%) and the amount of isomerization was negligible for all biphasic hydroformylation reactions. The small difference in rates (factor 1.5) is more than compensated by the easy and efficient catalyst and product separation using the latex phase-transfer system.

3.5 Conclusions

The possibility of polystyrene-based latexes to act as phase-transfer agents in the biphasic hydroformylation of higher alkenes was investigated. It was found that the

combination of anionic modified catalyst (sulfonated ligand) and cationic modified latex (ammonium), *vice versa*, led to significantly increased performance. This was attributed to an electrostatic aggregation of the catalyst to the latex particles.

Furthermore, it was possible to minimize limitations due to mass transfer and CO solubility by variation of the nature of the latex and by increasing the synthesis gas pressure. A phase-transfer agent was found (latex 5), which leads to an overall reaction rate in the Rh-catalyzed aqueous-phase hydroformylation of 1-octene of up to 2000 h^{-1} using TPPTS as ligand. This TOF is only gradually lower (factor 1.5) than in the organic-phase hydroformylation using PPh_3 . More polar polymers (PS/acrylate copolymers) in the lipophilic core of the latex led to decrease overall rates ($\sim 1150 \text{ h}^{-1}$). The degree of crosslinking proved to be of importance as well. The best results were obtained for an amount of 2% of cross-linking agent (DVB).

3.6 Experimental section

All chemicals were purchased from Aldrich, Acros, Strem, or Merck and used as received unless stated otherwise. All preparations were carried out under an atmosphere of dry argon using standard Schlenk techniques. Solvents were distilled under argon atmosphere and dried by standard procedures. All glassware was dried by heating under vacuum. The synthesis gas [CO (99.997%)/ H_2 (99.997%) 1:1] was purchased from Linde gas.

Synthesis of TPPTB

Tris-(4-((trimethylammonio)methyl)phenyl)phosphine tris(tetrafluoroborate) was provided by MSc.D. Snelders in cooperation between the groups.^[73]

General procedure for biphasic hydroformylation experiments

The reactor was charged with water, $\text{Rh}(\text{acac})(\text{CO})_2$ ligand and latex (15 mL/ 20 mL). The ratio rhodium/ligand was 1:6. The catalyst was preformed for 3h at 700 rpm at

80°C and the desired pressure CO/H₂ (1:1). Subsequently, the substrate was added by dropping funnel and the conversion was measured *via* gas uptake of CO/H₂. After 200 h the reaction was stopped by cooling the reactor to room temperature and the pressure was released. The organic layer was analyzed by gas chromatography.

GC-Analysis

GC analysis

GC	:	Shimadzu GC 17A
Column	:	HP Pona (crosslinked Me Siloxane), 50 m, inner Ø 0.20 mm, film thickness 0.5 µm
Carrier gas	:	Helium 208.0 kPa (total flow 69 ml/min)
Temperature program	:	60°C (hold: 10 min), 1°C/min to 65°C 15°C/min to 250°C (hold: 3 min)
Injector	:	250°C
Detector (FID)	:	270°C
Split ratio	:	50
Injection volume	:	1.0 µL

Table 3.13 Selected retention times of the organic compound and the external standard

Compound	Retention time (min)
1-octene	14.9
linear nonanal	23.0
branched nonanal	23.8
dodecane	25.4

ICP- AES

The analytical principle used in the SPECTRO ICP systems is optical emission spectroscopy. A liquid is nebulized and then vaporized with in the Argon plasma.

The atoms and ions contained in the plasma vapor are excited into a state of radiated light (photon) emission. The radiation emitted can be passed to the spectrometer optic, where it is dispersed into its spectral components. From the specific wavelengths emitted by each element, the most suitable line for the application is measured by means of a CCD (charge coupled device).

The radiation intensity, which is proportional to the concentration of the element in the sample, is recalculated internally from a stored set of calibration curves and can be shown directly as percent or measured concentration.^[78]

Sample preparation

The volatiles from the organic sample were removed under vacuum. Afterwards the sample was calcinated at 500°C overnight in order to remove all organic compounds. After the sample had cooled down to room temperature sulphuric acid (2 mL) was added to the residue and heated until SO₃ fumes arisen out of the solution. The solution was cooled down again and H₂O₂ (2 mL) was slowly added. After the reaction, the solution was transferred into a volumetric flask of 25 mL and analyzed.

ICP instrumentation:

Spectrometer: SPECTRO CIROS^{CCD}
Technique: Inductively Coupled Plasma Optical Emission Spectrometry (ICP-OES)

Operating conditions:

Generator:	Free-running at Power	27,12 MHz 1400 W
Sample introduction:	Nebulizer Spray chamber Sample uptake rate	Cross-flow (SPECTRO) Double pass, Scott type (SPECTRO) 2 ml/min
Gas flows:	Outer gas Intermediate gas Nebulizer gas	12 l/min 1 l/min 1.00 l/min
Gas:	Argon	

3.7 References

- [1] B. Cornils, W. A. Herrmann, *Applied Homogeneous Catalysis with Organometallic Compounds*, 2nd Ed. Wiley-VCH, **2002**.
- [2] D. Vogt, in *Aqueous Phase Organometallic Catalysis- Concepts and Applications* (Eds.: B. Cornils, W.A. Herrmann) 2nd Ed., Wiley-VCH **2004**, 541-547.
- [3] W. Keim, *Chem. Ing. Techn.* **1984**, *56*, 850-853.
- [4] D. Cole-Hamilton, R. Tooze, *Catalyst Separation, Recovery and Recycling Chemistry and Process Design*, Springer, **2006**.
- [5] A. Corma, H. Garcia, *Top. Catal.* **2008**, *48*, 8-31.
- [6] I. Horvath, *Acc. Chem. Res.* **1998**, *31*, 641-650.
- [7] S. Kainz, D. Koch, W. Baumann, W. Leitner, *Angew. Chem.* **1997**, *109*, 1699-1701.
- [8] D. Koch, W. Leitner, *J. Am. Soc.* **1998**, *120*, 13398-13404.
- [9] S. Bektsev, T. Tack, M.R. Mason, M.A. Abraham, *Ind. Eng. Chem. Res.* **2005**, *44*, 4973-4981.
- [10] W. Leitner, *Acc. Chem. Res.* **2002**, *35*, 746-756.
- [11] P. Stephenson, B. Kondor, P. License, K. Scovell, S. K. Ross, M. Poliakoff, *Adv. Synth. Catal.* **2006**, *348*, 1605-1610.
- [12] F. Kuntz et al., Rhone-Poulenc Ind., Patent FR 2.230.654, **1983**, Patent FR 2.314910, **1975**, Patent FR 2.338.253, **1976**, Patent FR 2.349.562, **1976**, Patent FR 2.366.237 **1976**, Patent FR 2.473.505, **1979**, Patent FR 2.478.078, **1980**, Patent FR 2.550202, **1983**, Patent FR 2.561.650 **1984**.
- [13] A. Riisager, B. E. Hanson, *J. Mol. Catal. A: Chem.* **2002**, *189*, 195-202.
- [14] C. C. Miyagawa, J. Kupka, A. Schumpe, *J. Mol. Catal. A: Chem.* **2005**, *234*, 9-17.
- [15] H. Fu, M. Li, H. Chen, X. Li, *J. Mol. Catal. A: Chem.* **2006**, *259*, 156-160.
- [16] L. Tinucci, E. Platone, US Patent 4.996.366, **1991**.
- [17] M. Gimenez-Pedro, A. Aghmiz, C. Claver, A. M. Masdeu-Bulto, D. Sinou, *J. Mol. Catal. A: Chem.* **2003**, *200*, 157-163.
- [18] T. Bartik, B. Bartik, B. E. Hanson *J. Mol. Catal.* **1994**, *88*, 43-56.
- [19] R. M. Deshpande, P. Purwanto, H. Delmas, R. V. Chaudhari, *Ind. Eng. Chem. Res.* **1996**, *35*, 3927-3933.
- [20] R. M. Deshpande, H. Delmas, R. V. Chaudhari, *J. Mol. Catal. A: Chem.* **1997**, *126*, 133-140.
- [21] P. Purwanto, H. Delmas, *Catal. Today* **1995**, *24*, 135-140.
- [22] J. Horn, F. Michalek, C. C. Tzschucke, W. Bannwarth, *Top. Curr. Chem.* **2004**, *242*, 43-75.
- [23] U. J. Jauregui-Haza, E. Pardillo-Fontdevila, P. Kalck, A. M. Wilhelm, H. Delmas, *Catal. Today* **2003**, *79-80*, 409-417.

- [24] Q. Shi, Y.-J. Lee, M.-J. Kim, M.-K. Park, K. Lee, H. Song, M. Cheng, B.-S. Jeong, H.-g. Park, S. S. Jew, *Tetrahedron Lett.* **2008**, *49*, 1380-1383.
- [25] U. J. Jauregui-Haza, A. M. Wilhelm, H. Delmas, *Lat. Am. Appl. Res.* **2002**, *32*, 131-136.
- [26] J. P. Arhanchet, M. E. Davis, J. S. Merola, B. E. Hanson, *Nature* **1989**, *339*, 454-455.
- [27] R. Chen, R. P. J. Bronger, P. C. J. Kamer, P. W. N. M. Van Leeuwen, J. N. H. Reek *J. Am. Chem. Soc.* **2004**, *126*, 14557-14566.
- [28] B. E. Hanson, H. Ding, C. W. Kohlpaintner, *Catal. Today* **1998**, *42*, 421-429.
- [29] M. S. Goedheijt, B. E. Hanson, J. N. H. Reek, P. C. J. Kamer, P. W. N. M. van Leeuwen, *J. Am. Chem. Soc.* **2000**, *122*, 1650-1657.
- [30] C. Liu, J. Jiang, Y. Wang, F. Cheng, Z. Jin, *J. Mol. Catal. A: Chem.* **2003**, *198*, 23-27.
- [31] R. Chen, X. Liu, Z. Jin, *J. Organomet. Chem.* **1998**, *571*, 201-204.
- [32] Y. Wang, J. Jiang, R. Zhang, X. Liu, Z. Jin, *J. Mol. Catal.* **2000**, *157*, 111-115.
- [33] Z. Jin, X. Zheng, B. Fell, *J. Mol. Catal. A: Chem.* **1997**, *116*, 55-58.
- [34] B. Fell, *Tenside Surf, Det.* **1998**, *35*, 326-337.
- [35] I. T. Horvath, *Acc. Chem. Res.* **1998**, *31*, 641-650.
- [36] I. T. Horvath, J. Rabai, *Science* **1994**, *266*, 72-75.
- [37] I. T. Horvath, G. Kiss, R. A. Cook, J. E. bond, P. A. Stevens, J. Rabai, E. J. Mozeleski *J. Am. Chem. Soc.* **1998**, *120*, 3133-3143.
- [38] T. Welton, *Chem. Rev.* **1999**, *99*, 2071-2083.
- [39] P. Wasserscheid, T. Welton, *Ionic Liquids in Synthesis*, Wiley-VCH, Weinheim, Germany, **2003**.
- [40] B. Hamers, P. S. Bäuerlein, C. Müller, D. Vogt, *Adv. Syn. Catal.* **2008**, *350*, 332-342.
- [41] P. Wasserscheid, W. Keim, *Angew. Chem.* **2000**, *112*, 3926-3945.
- [42] A. Riisager, R. Fehrmann, M. Haumann, B. S. K. Gorle, P. Wasserscheid, *Ind. Eng. Chem. Res.* **2005**, *44*, 9853-9859.
- [43] L. Leclercq, I. Suisse, F. Agbossou-Niedercorn, *Chem. Commun.* **2008**, 311-313.
- [44] B. Sueur, L. Leclercq, M. Sauthier, Y. Castanet, A. Mortreux, H. Bricout, S. Tilloy, E. Monflier, *Chem. Eur. J.* **2005**, *11*, 6228-6236.
- [45] G. Fremy, E. Monflier, J.-F. Carpentier, Y. Castanet, A. Mortreux, *J. Mol. Catal. A: Chem.* **1998**, *129*, 35-40.
- [46] S. Tilloy, E. Genin, F. Hapiot, D. Landy, S. Fourmentin, J.-P. Genet, V. Michelet, E. Monflier, *Adv. Synth. Catal.* **2006**, *348*, 1547-1552.
- [47] N. Sieffert, G. Wipff, *J. Phys. Chem. B* **2006**, *110*, 4125-4134.

- [48] T. Mathivet, C. Méliet, Y. Castanet, A. Mortreux, L. Carbon, S. Tilloy, E. Monflier, *J. Mol. Catal. A: Chem.* **2001**, *176*, 105-116.
- [49] L. Leclercq, M. Sauthier, Y. Castanet, A. Mortreux, H. Bricout, E. Monflier, *Adv. Synth. Catal.* **2005**, *347*, 55-59.
- [50] W. T. Ford, *Reactive and Functional Polymers* **1997**, *33*, 147-158.
- [51] B. Sueur, L. Leclercq, M. Sauthier, Y. Castanet, A. Mortreux, H. Bricout, S. Tilloy, E. Monflier, *Chem. Eur. J.* **2005**, *11*, 6228-6236.
- [52] G. Fremy, E. Monflier, J.-F. Carpentier, Y. Castanet, A. Mortreux, *J. Mol. Catal. A: Chem.* **1998**, *129*, 35-40.
- [53] S. Tilloy, E. Genin, F. Hapiot, D. Landy, S. Fourmentin, J.-P. Genet, V. Michelet, E. Monflier, *Adv. Synth. Catal.* **2006**, *348*, 1547-1552.
- [54] N. Sieffert, G. Wipff, *J. Phys. Chem. B* **2006**, *110*, 4125-4134.
- [55] T. Mathivet, C. Méliet, Y. Castanet, A. Mortreux, L. Carbon, S. Tilloy, E. Monflier, *J. Mol. Catal. A: Chem.* **2001**, *176*, 105-116.
- [56] L. Leclercq, M. Sauthier, Y. Castanet, A. Mortreux, H. Bricout, E. Monflier, *Adv. Synth. Catal.* **2005**, *347*, 55-59.
- [57] F. M. Menger, A. R. Elrington, *J. Am. Chem. Soc.* **1991**, *113*, 265-271.
- [58] H. Egger, T. Sottmann, R. Strey, C. Valero, A. Berkessel, *Tenside Surfactants Deterg.* **2002**, *39*, 17-22.
- [59] J. F. Rusling, *Pure Appl. Chem.* **2001**, *73*, 1895-1905.
- [60] C. K. Niue, J. F. Rusling, *Electrochem. Commun.* **2002**, *4*, 340-343.
- [61] L. Caron, V. Nardello, J. Mugge, E. Hoving, P. L. Alsterds, J. M. Aubry, *J. Colloid Interface Sci.* **2005**, *282*, 478-485.
- [62] S. Kanagasabapathy, Z. Xia, G. Papadogianakis, B. Fell, *J. Prakt. Chem.* **1995**, *337*, 446-450.
- [63] B. Fell, D. Leckel, C. Schobben, *Fat Sci. Technol.* **1995**, *97*, 219-228.
- [64] A. Kumar, G. Oehme, J. P. Roque, M. Schwarze, R. Selke, *Angew. Chem.* **1994**, *106*, 2272-2275.
- [65] G. Oehme, I. Grassert, S. Ziegler, R. Meisel, H. Fuhrmann, *Catal. Tod.* **1998**, *42*, 459-470.
- [66] M. Häger, K. Holmberg, *Chem. Eur. J.* **2004**, *10*, 5460-5466.
- [67] M. Haumann, H. Yildiz, H. Koch, R. Schomäcker, *Appl. Catal. A.* **2002**, *236*, 173-178.
- [68] P. Handa, M. Stierndahl, K. Holmberg, *Microporous Mesoporous Mater.* **2007**, *100*, 146-153
- [69] A. M. van Herk, K. H. van Streun, J. van Welzen, A. L. German, *Br. Polymer J.* **1989**, *21*, 125-132.
- [70] W. T. Ford, *Reactive and Functional Polymers* **1997**, *33*, 147-158.
- [71] W. T. Ford, *Reactive and Functional Polymers* **2001**, *48*, 3-13

- [72] S. Mecking, R. Thomann, *Adv. Mater.* **2000**, *12*, 953-956.
- [73] R. Kreiter, R. J. M. Klein Gebbink G. van Koten, *Tetrahedron* **2001**, *59*, 3989-3997. provided by D. J. M. Snelders, Chemical Biology & Organic Chemistry, Faculty of Science, Utrecht University.
- [74] H. Chen, Y. Li, J. Chen, P. Cheng, Y.-E. He, X. Li, *J. Mol. Catal. A: Chem.* **1999**, *149*, 1-6.
- [75] R. M. Deshpande, P. Purwanto, H. Delmas, R. V. Chaudhari, *Ind. Eng. Chem. Res.* **1996**, *35*, 3927-3933.
- [76] C. C. Miyagawa, J. Kupka, A. Schumpe, *J. Mol. Catal. A: Chem.* **2005**, *234*, 9-17.
- [77] Jáuregui-Haza U.J. Pardillo-Fontedvila E.J., A.M. Wilhelm, H. Delmas, *Latin American Appl. Research*, **2004**, 71-74.
- [78] Information from <http://www.spectro.com/pages/e/index.htm>

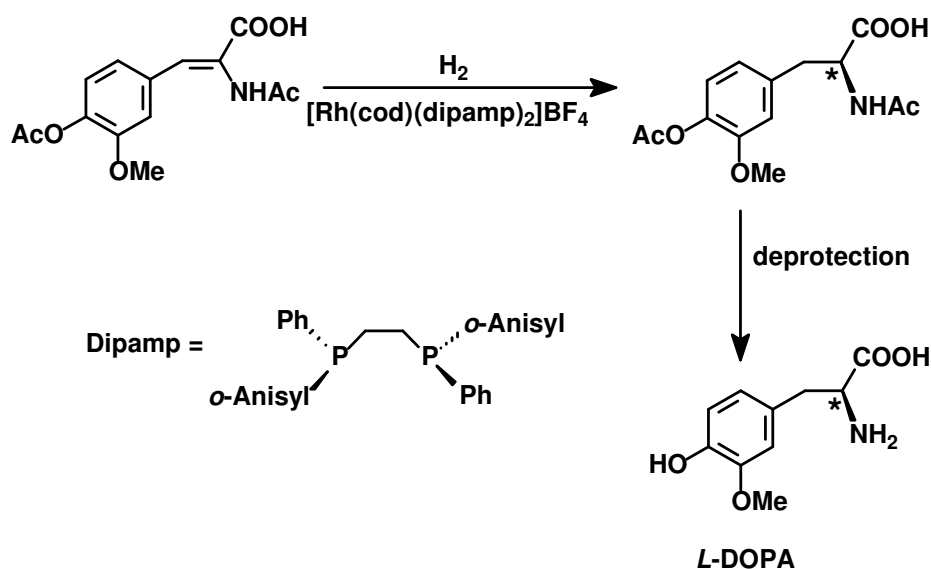
Immobilization of Cationic Hydrogenation Complexes *via* Electrostatic Interactions

Transition metal-catalyzed asymmetric hydrogenation is becoming increasingly important for the production of pharmaceuticals and agrochemicals. However, large-scale applications are often hampered by the difficulty of separation, recycling, and reuse of the homogeneous catalyst. A possible solution is the immobilization of hydrogenation catalysts *via* non-covalent interactions.

We investigated the concept of electrostatic immobilization of cationic Rh(I) complexes on a *p*-styryltriphenylborate-functionalized polymer. The application of the supported complexes in the asymmetric hydrogenation of enamines, α,β unsaturated ester and imines was examined. Furthermore, solvent effects and the influence of the counterions on the hydrogenation reaction are discussed.

4.1 Introduction

Transition metal-catalyzed asymmetric hydrogenation is becoming increasingly important for the production of pharmaceuticals and agrochemicals. One of the most prominent examples for the successful application of asymmetric hydrogenation is the Monsanto L-Dopa process, which has been developed by Knowles and coworkers.^{[1],[2]} The synthesis of L-3,4-dihydroxyphenylalanine (L-dopa), a drug used for the treatment of Parkinson's disease, has been developed and applied at an industrial scale (Scheme 4.1). For this achievement in asymmetric homogeneous catalysis W.S. Knowles was awarded the Nobel Prize in 2001 together with R. Noyori and H. B. Sharpless. However, large-scale applications of this reaction are often hampered by the difficulty of separation, recycling, and reuse of the homogeneous catalyst. For this reason, attention has recently focused on the design of immobilized catalysts in order to overcome these problems.



Scheme 4.1 Synthesis of L-DOPA

In general, there are two methods to immobilize catalysts, the physical immobilization and the chemical immobilization, which were already discussed in Chapter 1.

An attractive strategy for the immobilization of cationic complexes is the electrostatic immobilization *via* ionic interactions: This immobilization of cationic transition metal complexes by means of ion exchange is possible in several ways. For instance, the

complex can be anchored on inorganic or polymeric supports (a). Alternatively, the ligand can be electrostatically immobilized on supports (b) *via* ionic functional groups incorporated in the ligand (Figure 4.1).

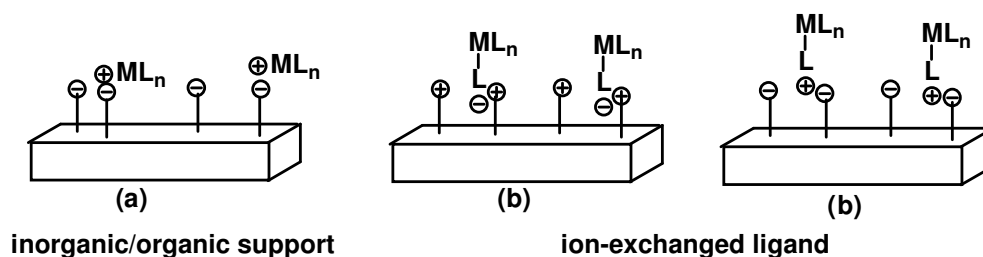


Figure 4.1 Immobilization methods for transition metal complexes *via* ionic interactions

Hydrogenation catalysts can be immobilized on solid inorganic supports, such as silica, alumina, active carbon and solid polymers. Inorganic supports are characterized by dimensionally stable pore sizes and higher temperature stabilities.

Several classes of inorganic supports, which are suitable for the direct exchange of positively charged hydrogenation complexes, such as smectite clay minerals, zeolite and heteropoly acids exist. The best example of polymeric supports for supporting cationic complexes is cation-exchange resins. Examples of the electrostatic immobilization of hydrogenation catalyst on these supports are described in detail in Chapter 1.

In this chapter, the electrostatic immobilization of hydrogenation catalyst on a functionalized polymer is presented. Furthermore, these modified systems were applied in the asymmetric hydrogenation of methyl (*Z*)- α -acetamidocinnamate, dimethylitaconate, and imines.

4.2 Concept

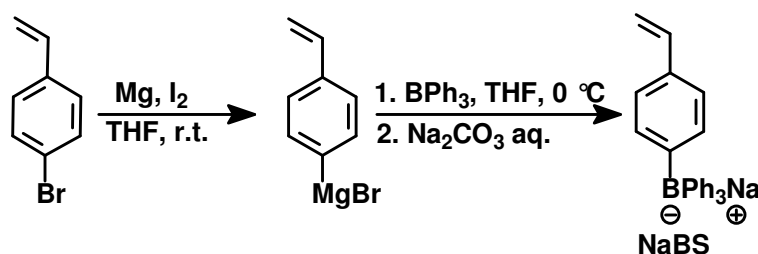
One example, which was already described in Chapter 1, is the electrostatic immobilization of a catalyst on functionalized polystyrene-based latexes. Sablong *et al.* reported on the successful immobilization of a cationic achiral Rh-diphosphine complex on latex particles, which are based on polymerizable *p*-styryl-triphenylborate anions.^[3] The heterogeneous achiral catalyst was successfully used and reused for several recycle runs in the hydrogenation of (*Z*)-2-acetamido-cinnamic acid.

Based on these results the possibility to prepare *p*-styryl-triphenylborate-functionalized polymers as support for cationic chiral catalysts and their application in asymmetric hydrogenations was investigated. A polystyrene polymer crosslinked with divinylbenzene was chosen as support due to its easy functionalization.^[4]

4.3 Synthesis of the immobilized cationic hydrogenation catalyst

4.3.1 Synthesis of sodium *p*-styryl-triphenylborate

In order to synthesize a polymer, which has the ability to interact electrostatically with cationic transition metal complexes, the functionalized monomer sodium *p*-styryl-triphenylborate (NaBS) (Scheme 4.2), which can be polymerized and provide the possibility to interact with the catalyst, was prepared.



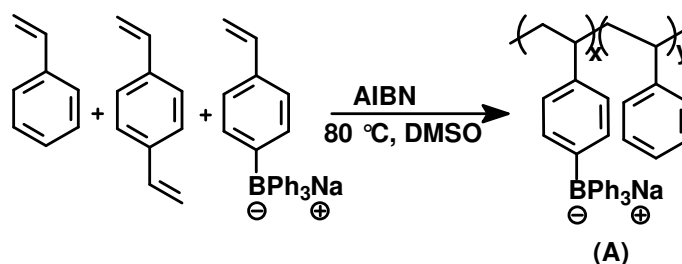
Scheme 4.2 Synthesis of sodium *p*-styryl-triphenylborate, which can electrostatically interact with the catalyst

The synthesis is a straightforward two-step method, following a modified literature procedure.^[5] *p*-Bromostyrene was first converted into the corresponding Grignard

reagent *p*-styrylMgBr, which was treated with one equivalent of triphenylborane (Scheme 4.2) at 0°C, yielding 60% of sodium *p*-styryltriphenylborate (NaBS) after workup.^[6]

4.3.2 Synthesis of polymeric support

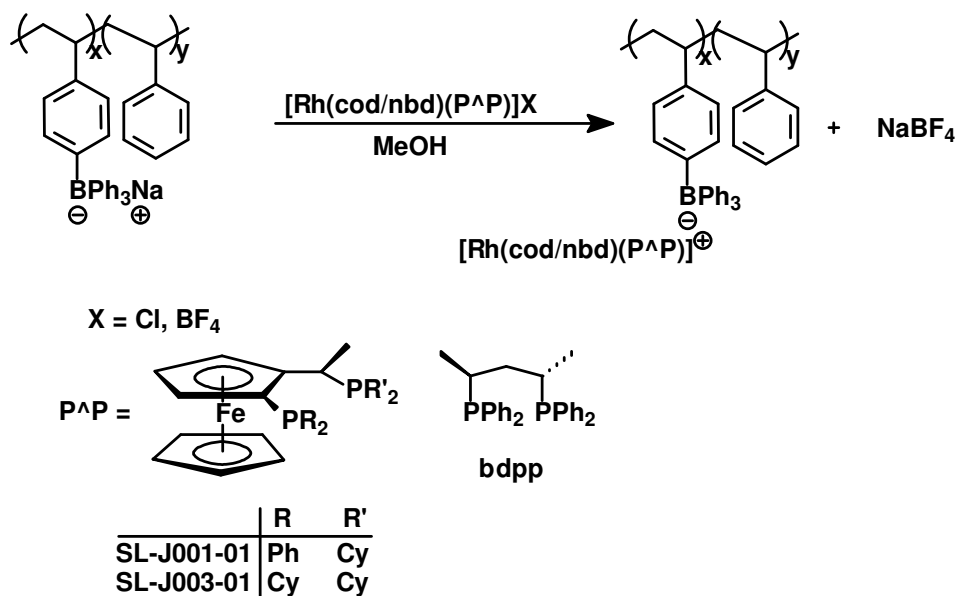
The functionalized polymer was synthesized using free radical polymerization with Azobisisobutyronitrile (AIBN) as radical initiator. The reactants, styrene, NaBS (5 mol%), DVB (1 mol%) and AIBN were dissolved in 2 mL of DMSO and heated to 80°C. After the solution became viscous and yellow, the mixture was cooled down and the polymer was obtained as a white powder by precipitation with MTBE. The functionalized polymer, depicted in Scheme 4.3 was used as support for the cationic Rh-complexes.



Scheme 4.3 Synthesis of sodium *p*-styryl-triphenylborate-functionalized polystyrene-based polymer A

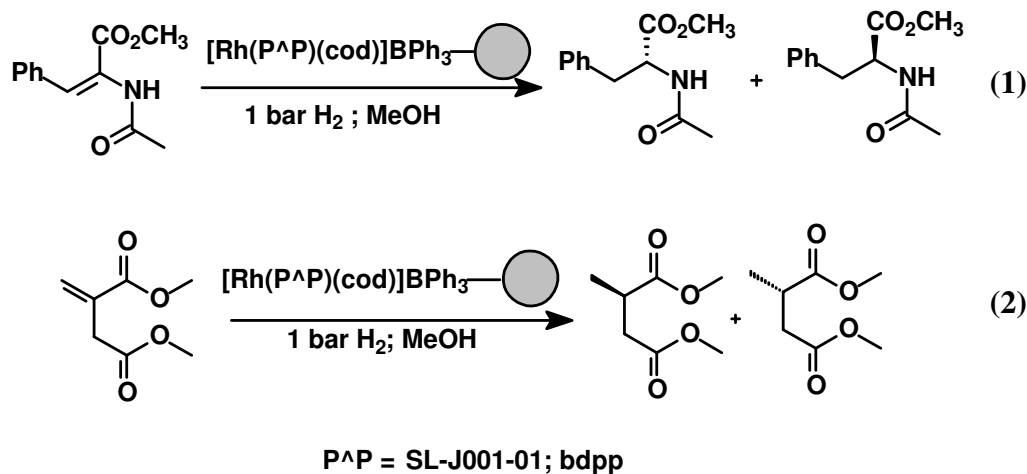
4.3.3 Immobilization of hydrogenation catalysts

The hydrogenation catalysts were anchored on the functionalized polymer according to the procedure described by Zhou *et al.*^[7] [Rh(cod)₂]BF₄ or [Rh(nbd)Cl]₂ and the ligand (P[^]P = bdpp, SL-J003-01, SL-J001-01) were dissolved in MeOH and stirred for 30 min. A suspension of polymer in MeOH was added to the solution and stirred for 30 min. The resulting precipitate was purified and analyzed by means of ICP-AES. The average catalyst loading was found to be 2-4 wt% (Scheme 4.4).



Scheme 4.4 Immobilization of $[\text{Rh}(\text{cod})(\text{P}^{\wedge}\text{P})]\text{BF}_4$ on the sodium *p*-styryl-triphenylborate-functionalized polystyrene-based polymer **A** via ion exchange

4.4 Application of immobilized Rh-based hydrogenation catalysts in the asymmetric hydrogenation of MAC and DMI



Scheme 4.5 Asymmetric hydrogenation of MAC (1) and DMI (2) catalyzed by an immobilized catalyst

The cationic transition metal complex $[\text{Rh}(\text{SL-J001-01})(\text{cod})]^+$ and $[\text{Rh}(\text{bdpp})(\text{cod})]^+$ immobilized on the functionalized polymer **A** were used in the asymmetric hydrogenation of (*Z*)- α -acetamidocinnamate (MAC, (1)) and dimethylitaconate (DMI, (2)) (Scheme 4.5).

The reaction was carried out in a glass apparatus where the immobilized catalyst was placed on an incorporated G4 frit (Figure 4.2). The substrate, dissolved in MeOH was added and H₂ bubbled through the solution. Afterwards the product was easily separated from the supported catalyst by simple filtration.

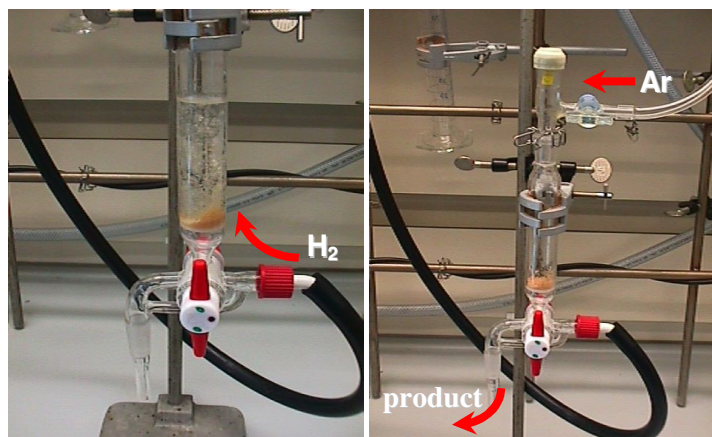


Figure 4.2 Equipment for hydrogenation of MAC and DMI at 1.3 bar H₂

The results of the asymmetric hydrogenation are shown in Table 4.1.

Table 4.1 Results of hydrogenation of MAC and DMI^a

Entry	Complex	MAC (1)		DMI (2)	
		Conversion [%]	<i>ee</i> [%]	Conversion [%]	<i>ee</i> [%]
1 ^b	[Rh(cod)(SL-J001-01)]BF ₄	100	98	100	99
2 ^b	[Rh(cod)(SL-J001-01)]BPh ₄	5	88	2	63
3 ^c	[Rh(cod)(SL-J001-01)]A	5	88	2	63
4 ^b	[Rh(cod)(bdpp)]BF ₄	100	88	100	80
5 ^b	[Rh(cod)(bdpp)]BPh ₄	2	60	2	50
6 ^c	[Rh(cod)(bdpp)]A	2	60	2	50

(a) Reaction conditions: 1.3 bar H₂, 25°C, MeOH (7 mL), 1h, Rh: substrate (1:100); (b) catalysts (0.022mmol, 3.14 mmol/L) substrate (2.2 mmol, 0.314 mol/L); (c) catalyst (3.6·10⁻³ mmol, 0.51 mmol/L), substrate (0.316 mmol, 51 mmol/L)

From these results, it can be concluded that the homogeneous [Rh(cod)(SL-J001-01)]BF₄ (Entry 1) and [Rh(cod)(bdpp)]BF₄ (Entry 4) are the most active catalysts compared to [Rh(cod)(bdpp/SL-J001-01)]BPh₄ or [Rh(cod)(bdpp/SL-J001-01)]A. The dramatic decrease in activity and selectivity of these systems can be due to the counterions. It has been shown by Zhou *et al.* that Rh-complexes containing

tetraphenylborate as counterion can be converted into $[\eta^6\text{-PhBPh}_3][\text{Rh}(\text{P}^{\wedge}\text{P})]^+$ complexes in the presence of H_2 (Figure 4.3).^[13]

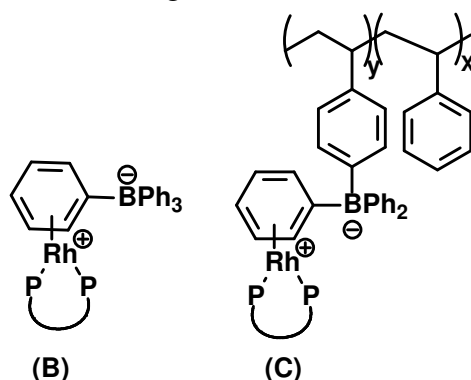
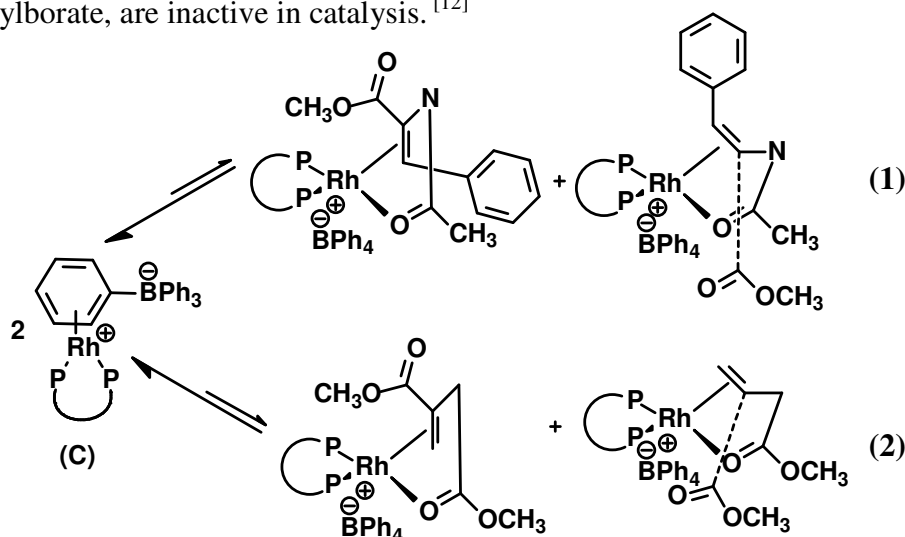


Figure 4.3 Schematic representation of η^6 -coordination of BPh_4^- **B** and BPh_3 polymer **C** to the cationic Rh complex through one phenyl group

The stability of such $\text{Rh}^{\text{I}}\text{-}\eta^6$ -arene complexes containing chelating diphosphine ligands has already been reported by Schrock and Osborn^[8] as well as by Halpern.^{[9],[10]}

Moreover, Heller *et al.*^[11] showed that complexes $[\eta^6\text{-PhBPh}_3][\text{Rh}(\text{P}^{\wedge}\text{P})]^+$ are not catalytically active for the asymmetric hydrogenation of $\text{C}=\text{C}$ bonds. Different substrates were hydrogenated in several solvents using $[\text{Rh}(\text{cod})(\text{P}^{\wedge}\text{P})]\text{BF}_4$. In solvents containing aromatic groups the activity was rather low and the formation of $\text{Rh}\text{-}\pi$ -arene complexes was observed, which are more stable than the diastereomeric substrate complexes. The $\text{Rh}\text{-}\pi$ -arene complexes that are formed with the aromatic groups of the triphenylborate, are inactive in catalysis.^[12]



Scheme 4.6 Schematic presentation of the equilibrium between the $\text{Rh}\text{-}\pi$ -arene complex and the diastereomeric substrate complexes (MAC (1); DMI (2))

Obviously, the equilibrium between Rh- π -arene complexes and the diastereomeric substrate complexes is shifted towards the Rh- π -arene complexes, as shown in Scheme 4.6.

This effect is most probably the reason for the low activity of [Rh(cod)(P^P)]BPh₄ and [Rh(cod)(P^P)]A (P^P = bdpp, SL-J001-01) in the asymmetric hydrogenation of MAC and DMI (Table 4.1; Entry 2, 3 and 5, 6).

In order to examine whether [Rh(cod)(P^P)]BPh₄ and [Rh(cod)(P^P)](A) (P^P = bdpp, SL-J001-01) complexes lead indeed to the formation of η^6 -arene complexes in the presence of H₂, the complexes were stirred for 2 h under H₂ atmosphere. The resulting complexes [Rh(cod)(P^P)]BPh₄ were analyzed by ¹H, and ³¹P- NMR spectroscopy.

[Rh(cod)(P^P)](A) (P^P = bdpp, SL-J001-01) complexes were analyzed by ³¹P- NMR spectroscopy.

The protons in η^6 -PhBPh₃ show significant high-field shifts compared to their non-coordinated analogs. In the ¹H-NMR *meta*, *ortho*, and *para* signals of η^6 -PhBPh₃ appear well separated at 4.96, 5.55 and 6.82 ppm, respectively.^[13]

The η^6 -PhBPh₃ coordination in **B** and **C** is clearly demonstrated by the ³¹P- NMR spectra.

The ³¹P-NMR signals of the coordinated ligand in the η^6 -PhBPh₃ complex shift downfield in comparison to the coordinated ligand in the cationic non-coordinated analogues (Table 4.2).

Table 4.2 ^{31}P NMR resonance peaks for coordinated ligand in $\eta^6\text{-PhBPh}_3$ complex and non-coordinated analogues (CDCl_3)

Complex	^{31}P NMR δ [ppm]
$[\text{Rh}(\text{cod})(\text{bdpp})]\text{BPh}_4$	27.0 (d, $J_{\text{P-Rh}} = 142$ Hz)
$[(\eta^6\text{-PhBPh}_3)][\text{Rh}(\text{bdpp})]^+$	39.24 ($J_{\text{P-Rh}} = 195$ Hz)
$[\text{Rh}(\text{cod})(\text{bdpp})]\mathbf{A}$	27.1 (d, $J_{\text{P-Rh}} = 144$ Hz)
$[(\eta^6\text{-PhBpolymer})][\text{Rh}(\text{bdpp})]^+$	39.24 ($J_{\text{P-Rh}} = 195$ Hz)
$[\text{Rh}(\text{cod})(\text{SL-J001-01})]\text{BPh}_4$	52.7 (dd, $J_{\text{P-P}} = 33$ Hz, $J_{\text{P-Rh}} = 140$ Hz) 20.5 (dd, $J_{\text{P-P}} = 29$ Hz, $J_{\text{P-Rh}} = 144$ Hz)
$[(\eta^6\text{-PhBPh}_3)][\text{Rh}(\text{SL-J001-01})]^+$	76.5 (dd, $J_{\text{P-P}} = 41$ Hz, $J_{\text{P-Rh}} = 202$ Hz) 32.5 (dd, $J_{\text{P-P}} = 40$ Hz, $J_{\text{P-Rh}} = 210$ Hz)
$[\text{Rh}(\text{cod})(\text{SL-J001-01})]\mathbf{A}$	52.5 (dd, $J_{\text{P-P}} = 31$ Hz, $J_{\text{P-Rh}} = 141$ Hz) 20.4 (dd, $J_{\text{P-P}} = 29$ Hz, $J_{\text{P-Rh}} = 144$ Hz)
$[(\eta^6\text{-PhBpolymer})][\text{Rh}(\text{SL-J001-01})]^+$	76.1 (dd, $J_{\text{P-P}} = 43$ Hz, $J_{\text{P-Rh}} = 202$ Hz) 32.4 (dd, $J_{\text{P-P}} = 39$ Hz, $J_{\text{P-Rh}} = 210$ Hz)

From these NMR data, it can be concluded that the *p*-styryl-triphenylborate-functionalized polymer **A** is not suitable as a support for the hydrogenation of C=C bonds.

4.4.1 Hydrogenation of MAC and DMI using a cation exchange resin **D**

Because only low conversions were reached in the asymmetric hydrogenation of MAC and DMI using the BPh_3 polymer **A** as support, the cation-exchange resin DOWEX 50 WX 8-400 **D** was used instead.^[14] The polystyrene-based resin **D** (Figure 4.4) contains no phenyl groups directly connected to the ionic group in contrast to polystyrene-based polymer **A** (Scheme 4.2). Therefore, it was possible to examine, whether the formation of the inactive Rh- π -complexes are mainly dependent on the ionic group or on the polymer support.

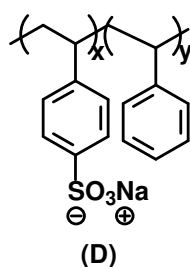
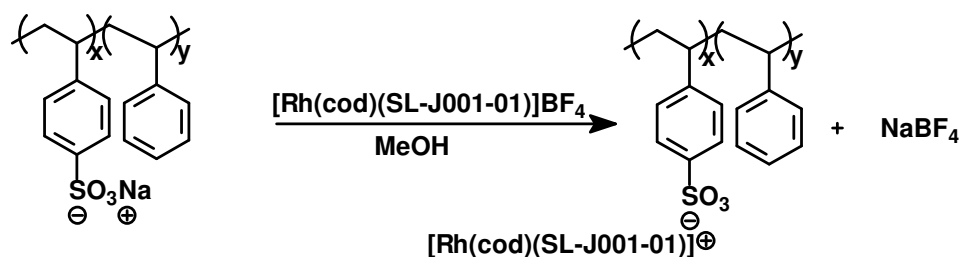


Figure 4.4 Schematic structure of the cation exchange resin **D**

The hydrogenation catalyst was immobilized on DOWEX 50 WX 8-400 according to the procedure described by Zhou *et al.*^[7] The support was suspended in MeOH and slowly added to a solution of $[\text{Rh}(\text{cod})(\text{SL-J001-01})]\text{BF}_4$ in MeOH. The resulting precipitate was purified and analyzed by means of ICP-AES. The average loading of $[\text{Rh}(\text{cod})(\text{SL-J001-01})]^+$ was found to be 4% (Scheme 4.7).



Scheme 4.7 Immobilization of $[\text{Rh}(\text{cod})(\text{P}^{\wedge}\text{P})]\text{BF}_4$ on cation exchange resin **D** via ion exchange

The immobilized complex $[\text{Rh}(\text{cod})(\text{SL-J001-01})]\text{D}$ was used in the hydrogenation of MAC and DMI.

Table 4.3 Hydrogenation results of MAC and DMI using **D** as support^a

Entry	Cycle	Complex	MAC (1)		DMI (2)	
			Conversion [%]	ee [%]	Conversion [%]	ee [%]
1	1	$[\text{Rh}(\text{cod})(\text{SL-J001-01})]\text{D}$	9	97	35	75
2	2	$[\text{Rh}(\text{cod})(\text{SL-J001-01})]\text{D}$	8.5	97	25	75
3	3	$[\text{Rh}(\text{cod})(\text{SL-J001-01})]\text{D}$	8	97	40	67
4	4	$[\text{Rh}(\text{cod})(\text{SL-J001-01})]\text{D}$	6	97	40	62
5	5	$[\text{Rh}(\text{cod})(\text{SL-J001-01})]\text{D}$	n.d.	n.d.	25	44

(a) Reaction conditions: 1.3 bar H_2 , 25°C, MeOH (7 mL), 30 min, Rh: substrate (1:100), immobilized catalyst ($3.6 \cdot 10^{-3}$ mmol, 0.51 mmol/L), substrate (0.316 mmol, 51 mmol/L)

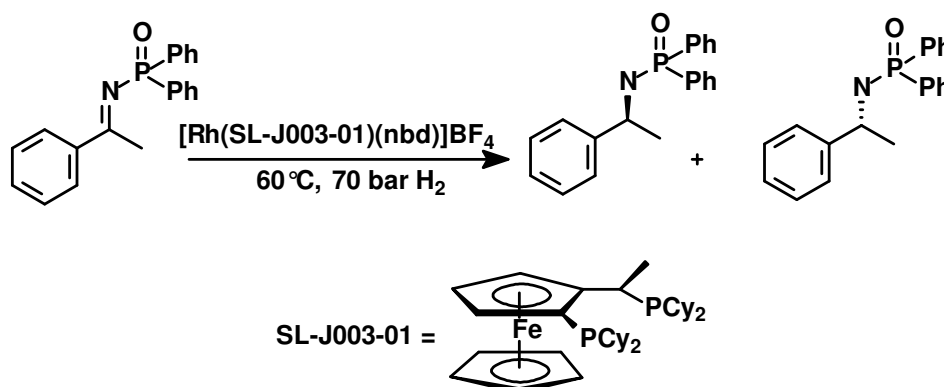
As can be seen from Table 4.3, the complex immobilized on the cation exchange resin **D** is more active and selective in the hydrogenation compared to the transition metal complex immobilized on polymer **A** (Table 4.1, Entry 3). Furthermore, $[\text{Rh}(\text{cod})(\text{SL-J001-01})]\text{D}$ could be reused in several cycles without significant Rh-loss, according to ICP-AES measurements. However, a decrease of activity in the hydrogenation of MAC was detected. In case of the hydrogenation of DMI both, the activity and enantioselectivity decreased. The higher activity of $[\text{Rh}(\text{cod})(\text{SL-J001-01})]\text{D}$ compared

to $[\text{Rh}(\text{cod})(\text{SL-J001-01})]\text{A}$ is most probably due to the tendency of **A** to act as η^6 -coordinating ligand through one or more phenyl groups of the borate.^[15-17] The tendency of **D** to act as a η^6 -coordinating ligand is presumably much lower caused by the fact that the phenyl groups of the resin are not directly part of the ionic group, which electrostatically interact with the cationic Rh complex.

4.5 Application of immobilized Rh-based catalyst in the hydrogenation of imines

In contrast to the hydrogenation of C=C bonds, Zhou *et al.*^[18] showed that Rh- π -complexes are active in the hydrogenation of C=N bonds. Therefore, polymer **A** was investigated as support for electrostatic immobilizations of cationic hydrogenation complexes in the hydrogenation of prochiral imines.

Spindler *et al.*^[19] investigated successfully the hydrogenation of *N*-(1-Phenylethyl)-*P,P*-diphenylphosphinimine using $[\text{Rh}(\text{nbd})(\text{SL-J003-1})]\text{BF}_4$ as catalyst (Scheme 4.8). Due to the good activity (500 h^{-1}) and selectivity (99% (*R*)) in this reaction, the recycling of $[\text{Rh}(\text{nbd})(\text{SL-J003-1})]^+$ complex immobilized on **A** was investigated.



Scheme 4.8 Asymmetric hydrogenation of *N*-(1-Phenylethyl)-*P,P*-diphenylphosphinimine reported by Spindler *et al.*

First, different solvents were tested in order to find the most suitable one for the recovery of the catalyst.

Hydrogenation catalysts containing different counterions were examined in order to investigate the influence of the anion on the selectivity and activity in the hydrogenation reaction. All results are shown in Table 4.4.

Table 4.4 Hydrogenation of *N*-(1-Phenylethyl)-*P,P*-diphenylphosphinimine using different catalytic systems and solvents^a

Entry	Catalyst	Time [h]	Solvent	Conversion [%]	ee [%]
1 ^b	[Rh(nbd)(SL-J003-01)]BF ₄	1	MeOH	99	98
2 ^b	[Rh(nbd)(SL-J003-01)]BAr ₄ ^F	16	MeOH	80	76
3 ^b	[Rh(nbd)(SL-J003-01)]BPh ₄	16	MeOH	81	82
4 ^c	[Rh(nbd)(SL-J003-01)]A	16	MeOH	14	91
5 ^b	[Rh(nbd)(SL-J003-01)]BPh ₄	16	MeOH/THF (1:9)	55	91
6 ^c	[Rh(nbd)(SL-J003-01)]A	16	MeOH/THF (1:9)	63	83
7 ^b	[Rh(nbd)(SL-J003-01)]BPh ₄	16	CH ₂ Cl ₂	0	/
8 ^c	[Rh(nbd)(SL-J003-01)]A	16	CH ₂ Cl ₂	0	/
9 ^b	[Rh(nbd)(SL-J003-01)]BPh ₄	16	MeOH/CH ₂ Cl ₂ (1:1)	0	/
10 ^c	[Rh(nbd)(SL-J003-01)]A	16	MeOH/CH ₂ Cl ₂ (1:1)	0	/
11 ^b	[Rh(nbd)(SL-J003-01)]BPh ₄	16	THF	24	86
12 ^c	[Rh(nbd)(SL-J003-01)]A	16	THF	20	86

(a) Reaction conditions: 70 bar H₂, 60°C, solvent (7 mL), Rh:S (1:100); (b) catalyst (4.77·10⁻³ mmol, 0.68 mmol/L), *N*-(1-Phenylethyl)-*P,P*-diphenylphosphinimine (100 mg, 0.477 mmol, 68 mmol/L), Rh:S (1:100); (c) Rh(nbd)(SL-J003-01)/A (50 mg, 1.9·10⁻³ mmol, 0.271 mmol/L), (60 mg, 0.19 mmol, 27 mmol/L)

It was found that the hydrogenation of the phosphine imine to the corresponding phosphine amine catalyzed by [Rh(nbd)(SL-J003-1)]BAr₄^F (Entry 2) or [Rh(nbd)(SL-J003-1)]BPh₄ (Entry 3) proceeds slower compared to [Rh(nbd)(SL-J003-1)]BF₄ (Entry 1). This observation suggests that the hydrogenation reaction depends on the nature of the counterion. In fact, the activity of [Rh(nbd)(SL-J003-1)]BAr₄^F and [Rh(nbd)(SL-J003-1)]BPh₄ are rather similar. Both complexes can form Rh- π -arene complexes in contrast to [Rh(nbd)(SL-J003-1)]BF₄. However, due to the conversions obtained in the hydrogenation of *N*-(1-Phenylethyl)-*P,P*-diphenylphosphinimine it seems that the equilibrium between the Rh- π -arene complex and diastereomeric substrate complexes shifts toward the substrate complexes, in contrast to the hydrogenation of MAC and DMI. In case of [Rh(nbd)(SL-J003-1)]BF₄, no Rh- π -arene complexes are formed, which results in a higher activity compared to the other systems.

By applying the immobilized catalyst (Entry 4) in MeOH the activity decreased dramatically, which is most likely due to the insolubility of the supported catalyst.

However, both, activity and selectivity, were much higher compared to the hydrogenation of MAC and DMI (Table 4.4)

The [Rh(nbd)(SL-JOO3-01)]**A** complex gave quite high activity and selectivity in the hydrogenation using the solvent mixture MeOH/THF (1:9) (Entry 6) in comparison to the results obtained in MeOH. Such difference is most likely due to the fact that the polymer-immobilized catalyst has a higher solubility in MeOH/THF (1:9).

Although [Rh(nbd)(SL-JOO3-01)]**A** is also soluble in THF as well as in MeOH/THF (1:9), the activity and the selectivity decreased in pure THF (Entry 12). In pure CH₂Cl₂ no conversion was observed (Entry 10).

Based on these results, the recovery experiments were performed in MeOH/THF (1:9).

4.5.1 *Recovery experiments in the hydrogenation of N-(1-Phenylethyl)-P,P-diphenylphosphinimine*

The recovery experiments were carried out in a stainless steel autoclave at 70 bar H₂ and 60°C. After the reaction, the solvent was evaporated and the immobilized catalyst was precipitated with MeOH. The solid was separated from the MeOH phase and the catalyst was used for the next recycling experiment. The results are given in Table 4.5.

Table 4.5 Recycling experiments of hydrogenation of *N*-(1-Phenylethyl)-*P,P*-diphenylphosphinimine^a

Entry	Catalyst	Run	Time [h]	Conversion [%]	ee [%]
1	[Rh(nbd)(SL-JOO3-01)] A	1	18	78	80
2	[Rh(nbd)(SL-JOO3-01)] A	2	18	36	56
3	[Rh(nbd)(SL-JOO3-01)] A	3	18	24	24
4	[Rh(nbd)(SL-JOO3-01)] A	4	18	10	rac.

(a) Reaction conditions: 70 bar H₂, 60°C, solvent (7 mL), Rh:S (1:100), [Rh(nbd)(SL-JOO3-01)]**A** (50 mg, 1.9·10⁻³ mmol, 0.271 mmol/L), (60 mg, 0.19 mmol, 27 mmol/L)

Clearly both, conversion and selectivity, decrease during the recycling experiments. Already after cycle 4 the conversion was rather low and no enantiomeric excess was observed anymore. These results suggest that with every recycling experiment the catalyst was partially deactivated by Rh-leaching, decomposition, or oxidation. In order to examine also possible leaching, the resulting MeOH solution was analyzed by ICP-AES. A Rh-loss of 10% was observed. Surprisingly, 20% Fe-loss was also detected,

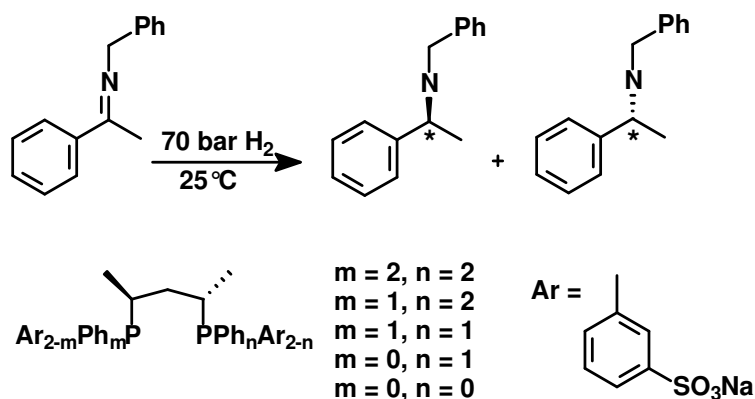
indicating that the ligand was also leaching. Thus, the immobilized catalyst is not suitable for recovery under these conditions.

One reason for the large Rh-loss in solution could be the use of MeOH as solvent and precipitation agent. Recently, Simons *et al.*^[20] applied mesoporous aluminosilicate AL-TUD-1 as support for different cationic Rh-based hydrogenation complexes with similar findings. By comparing different solvents in the hydrogenation of DMI they showed that the highest Rh-loss occurred using MeOH as reaction medium. The authors suggested that the high leaching is caused by the polarity and acidity of MeOH. The cationic transition metal complex can electrostatically interact with MeOH and is most probably stabilized in solution. They further observed that the ability to stabilize charged species in solution increased with increasing solvent polarity and acidity. The Rh-loss was rather high using the protic solvent MeOH. In aprotic solvents such as MTBE, the Rh-loss could be minimized.

Based on these results the hydrogenation of *N*-(1-Phenylethyl)-*P,P*-diphenylphosphinimine was performed in aprotic solvents, such as *n*-hexane or MTBE. Unfortunately, the hydrogenation of *N*-(1-Phenylethyl)-*P,P*-diphenylphosphinimine could not be carried out, due to the insolubility of *N*-(1-Phenylethyl)-*P,P*-diphenylphosphinimine in these solvents. Therefore, the hydrogenation of imines, rather than phosphine imines was investigated.

Bakos *et al.*^[21] successfully demonstrated the hydrogenation of *N*-benzyl-(1-phenylethylidene)-imine using [Rh(cod)(bdpp)]Cl as precatalyst. The conversion after 6 h was 96% and an enantiomeric excess of 84% (*R*) was reached (Scheme 4.9).

Based on these results, the use of [Rh(nbd)(bdpp)]**A** was investigated.



Scheme 4.9 Hydrogenation of *N*-benzyl-(1-phenylethylidene)-imine using sulfonated substituted bdpp ligands reported by Bakos *et al.*^[21]

Once again, the effect of different solvents on activity and selectivity in the asymmetric hydrogenation was examined first. The results are presented in Table 4.6.

Table 4.6 Asymmetric hydrogenation of *N*-benzyl-(-1-phenylethylidene)-imine using different catalyst and solvents^a

Entry	Catalyst	Solvent	Time [h]	Conversion [%]	<i>ee</i> [%]
1 ^b	[Rh(cod)(bdpp)]Cl	MeOH	6	96	84 <i>R</i>
2 ^c	[Rh(cod)(bdpp)]BF ₄	MeOH	18	99	71 <i>R</i>
3 ^c	[Rh(cod)(bdpp)]BPh ₄	MeOH	18	99	6 <i>R</i>
4 ^d	[Rh(nbd)(bdpp)] A	MeOH	18	77	11 <i>S</i>
5 ^c	[Rh(cod)(bdpp)]BF ₄	MTBE	18	--	--
7 ^d	[Rh(nbd)(bdpp)] A	MTBE	18	--	--
8 ^c	[Rh(cod)(bdpp)]BF ₄	hexane	18	--	--
10 ^d	[Rh(nbd)(bdpp)] A	hexane	18	--	--

(a) Reaction conditions: 25°C, 70 bar H₂, MeOH (7 mL), Rh:S (1:100); (b) asymmetric hydrogenation reported by Bakos *et al.*, (c) catalyst (4.77·10⁻³ mmol, 0.68 mmol/L), *N*-benzyl-(-1-phenylethylidene)-imine (100 mg, 0.477 mmol, 68 mmol/L); (d) [Rh(nbd)(bdpp)]**A** (50 mg, 1.9·10⁻³ mmol, 0.271 mmol/L), *N*-benzyl-(-1-phenylethylidene)-imine (40 mg, 0.19 mmol, 27 mmol/L)

The results indicate again that the activity as well as the enantioselectivity depends on the nature of the counterion. The enantiomeric excess decreased dramatically using [Rh(cod)(bdpp)]BPh₄ (Entry 3) as precatalyst compared to the systems [Rh(cod)(bdpp)]Cl (Entry 1) and [Rh(cod)(bdpp)]BF₄ (Entry 2). In case of the heterogeneous catalyst (Entry 4) the activity decreased with respect to the homogeneous ones (Entries 1-3). The decrease in activity is most probably due to the insolubility of the immobilized catalyst in MeOH. Surprisingly, the enantioselectivity obtained showed always the *R*-configuration using the homogeneous catalysts (Entries 1-3) while the immobilized catalyst gave the *S*-configured product.

The precatalysts [Rh(cod)(bdpp)]BF₄ and [Rh(nbd)(bdpp)]**A** were further used in the aprotic, apolar solvents MTBE and *n*-hexane. In both cases no activity was observed. In order to perform the recycling experiments, another method for catalyst recovery was investigated. Instead of performing the catalysis in aprotic solvents the catalysis was carried out in MeOH again but in contrast to the previous described recovery experiments, the catalyst was reused by precipitation with the aprotic solvent *n*-hexane. Thus, it should be possible to reach high activity and selectivity and it is possible to overcome the Rh-leaching.

4.5.2 Recovery experiments in the hydrogenation of *N*-benzyl-(-1-phenylethylidene)-imine

The hydrogenation of *N*-benzyl-(-1-phenylethylidene)-imine was carried out in MeOH, and the catalyst was recovered by precipitation with *n*-hexane. Therefore, the different solubility of catalyst and substrate/product was exploited. The immobilized catalyst is insoluble in *n*-hexane in contrast to the substrate and products.

Table 4.7. Recycling experiments of the hydrogenation of *N*-benzyl-(-1-phenylethylidene)-imine^a

Entry	Catalyst	Run	Time [h]	Conversion [%]	ee [%]
1	[Rh(nbd)(bdpp)] A	1	18	77	11(S)
2	[Rh(nbd)(bdpp)] A	2	20	77	6(S)
3	[Rh(nbd)(bdpp)] A	3	20	77	6(S)
4	[Rh(nbd)(bdpp)] A	4	20	70	2(S)

(a) Reaction conditions: 25°C, 70 bar H₂, MeOH (7 mL), Rh:S (1:100), [Rh(nbd)(bdpp)]**A** (50 mg, 1.9·10⁻³ mmol, 0.271 mmol/L), *N*-benzyl-(-1-phenylethylidene)-imine (40 mg, 0.19 mmol, 27 mmol/L)

All results of the recycling experiments are given in Table 4.7. After every cycle the activity and selectivity decreased. This is most probably caused by the oxidation and decomposition during the recovery process. However, it was possible to recover the immobilized catalyst without significant Rh-leaching (< 0.9%), according to the observed ICP-AES results. Thus, we could prove that the investigated polymer **A** is suitable as support for chiral cationic hydrogenation catalysts using ligands, such as bdpp, in the asymmetric hydrogenation of *N*-benzyl-(-1-phenylethylidene)-imine.

4.6 Conclusions

A sodium *p*-styryl-triphenylborate-functionalized polymer was synthesized by copolymerization of sodium *p*-styryl-triphenylborate with styrene. This polymer was used as support for the electrostatic immobilization of cationic transition metal complexes. The non-covalently supported catalysts were applied in the asymmetric hydrogenation of methyl (*Z*)-2-acetamido cinnamate, dimethylitaconate, *N*-(1-Phenylethyl)-*P,P*-diphenylphosphinimine and *N*-benzyl-(-1-phenylethylidene)-imine.

The supported catalysts were inactive in the hydrogenation of methyl (*Z*)-2-acetamido cinnamate and dimethylitaconate independent from the applied solvent. The inactivity is due to the formation of inactive $[(\eta^6\text{-PhBPh}_2\text{polymer})][\text{Rh}(\text{P}^{\wedge}\text{P})]^+$ ($\text{P}^{\wedge}\text{P} = \text{bdpp}$, SL-J001-01) complexes.

However, the supported catalyst $[\text{Rh}(\text{nbD})(\text{SL-J003-01})]\text{A}$ was active in the asymmetric hydrogenation of *N*-(1-Phenylethyl)-*P,P*-diphenylphosphinimine and *N*-benzyl-(-1-phenylethylidene)-imine.

When the hydrogenation of *N*-(1-Phenylethyl)-*P,P*-diphenylphosphinimine was carried out in MeOH/THF (1:9), high activity (63%) and enantioselectivity (83%) were reached. Unfortunately, a high catalyst leaching (10-20%) was observed in the recovery experiments using a MeOH/THF (1:9) mixture as solvent. Furthermore, the asymmetric hydrogenation could not be performed in aprotic solvents due to the insolubility of the substrate.

When the hydrogenation of *N*-benzyl-(-1-phenylethylidene)-imine with $[\text{Rh}(\text{nbD})(\text{bdpp})]\text{A}$ was performed in MeOH high activities (77%) were reached. Apparently, the counterion influenced the enantioselectivity dramatically which resulted in a change of absolute configuration from *R* to *S* (11%).

The supported catalyst was reused several times with only low Rh-leaching and only a slight decrease of activity and enantioselectivity was observed.

These results prove that sodium *p*-styryl-triphenylborate-functionalized polymers are suitable supports for cationic transition metal complexes. For further applications of *p*-styryl-triphenylborate-functionalized polymers suitable substrate/solvent combinations have to be found.

4.7 Experimental section

All chemicals were purchased from Aldrich, Acros, Strem, or Merck and used as received unless stated otherwise. All preparations were carried out under an atmosphere of dry argon using standard Schlenk techniques. Solvents were dried by standard procedures. All glassware was dried by heating under vacuum.

The NMR spectra were recorded on Varian Mercury 400, 200 MHz spectrometer (400 MHz for ^1H , and 200 MHz for ^{31}P and ^{19}F).

4.7.1 Synthesis of Sodium-*p*-styryltriphenylborate (NaBS)

The synthesis was carried out following a literature procedure.^[5] To a solution of Mg-turnings (0.7 g, 28.8 mmol, activated with I_2) was added dropwise 4-bromostyrene (5 g, 27 mmol) at room temperature. The solution was stirred for 2 h. The mixture was cooled to 0°C and triphenylborane in THF 0.25 mol/L (140 mL, 35 mmol) was added. The reaction mixture was stirred for 1 h. The ice bath was removed and the turbid solution was allowed to reach r.t. over 1 h period. Afterwards an aq. sat. Na_2CO_3 solution (30mL) was added and stirred at r.t. overnight. The solvent was evaporated and the residue was added to hot acetone.^[6] After filtration through a Celite pad, the filtrate was concentrated and the product precipitated with Et_2O . The obtained white precipitate was filtrated off and dried under vacuum. Yield: 60% (4 g, 10.8 mmol). ^1H NMR (CDCl_3) δ : 7.14- 6.77 (m, 20H, Ph), 6.64- 6.49 (m, 1H, CH), 5.60-5.50 (dd, 1H, CH_2), 4.99- 4.93 (dd, 1H, CH_2)

4.7.2 Synthesis of functionalized polymer A

The monomer NaBS (0.25 g, 0.68 mmol) dissolved in DMSO (0.5 mL), styrene (1.5 mL, 12.65 mmol), DVB (35.4 mg, 0.27 mmol) and AIBN (0.1 g, 0.6 mmol) were heated under stirring to 80°C . The solution changed from colorless to yellow within 1h, followed by formation of a viscous oil. The reaction mixture was cooled to r.t. and poured into MTBE. After the solution was stirred overnight, the white polymer was

formed. The polymer was filtered and dried under vacuum. Yield: 1 g GPC: $M_n = 2500$, $M_w = 4000$ und $PDI = 1.60$ (PS-calib.)

4.7.3 Immobilization on the polymer A

The synthesis was carried out following a literature procedure.^[7] $[\text{Rh}(\text{cod})_2]\text{BF}_4$ (0.043 mmol) and the ligand (0.043 mmol) were dissolved in MeOH and stirred for 30 min.. A suspension of polymer (700 mg, 0.087 mmol) in MeOH (2 mL) was added to the solution. The resulting precipitate was filtered and washed with MeOH (2.15 mL). The supported catalyst was dried under vacuum. Yield: 40% The resulting polymer was analyzed by ICP-AES: indicating a catalyst loading of 2-4%.

$[\text{Rh}(\text{cod})(\text{bdpp})]\text{A}$	^{31}P NMR (CDCl_3) δ : 27.1 (d, $J_{\text{P-Rh}} = 144$ Hz)
$[\text{Rh}(\text{cod})(\text{SL-J001-01})]\text{A}$	^{31}P NMR (CDCl_3) δ : 52.5 (dd, $J_{\text{P-P}} = 31$ Hz, $J_{\text{P-Rh}} = 141$ Hz), 20.4 (dd, $J_{\text{P-P}} = 29$ Hz, $J_{\text{P-Rh}} = 144$ Hz)
$[\text{Rh}(\text{cod})(\text{SL-J003-01})]\text{A}$	^{31}P NMR (CDCl_3) δ : 55.0 (dd, $J_{\text{P-P}} = 30$ Hz, $J_{\text{P-Rh}} = 158$ Hz); 18.7 (dd, $J_{\text{P-P}} = 32$ Hz, $J_{\text{P-Rh}} = 144$ Hz)

4.7.4 Synthesis of $[\text{Rh}(\text{cod})(\text{P}^{\wedge}\text{P})]\text{BPh}_4$

The synthesis was carried out following a literature procedure.^[7] $[\text{Rh}(\text{cod})_2]\text{BF}_4$ (100 mg, 0.217 mmol) and $\text{P}^{\wedge}\text{P}$ (0.434 mmol) were dissolved in MeOH. A solution of NaBPh_4 (150 mg, 0.434 mmol) in MeOH (2 mL) was added to the stirred red solution. The resulting precipitate was filtered and washed with MeOH/ H_2O (2 mL), Et_2O (4 mL), MeOH (2 mL). The red-orange crystals were dried under vacuum.

$\text{Rh}(\text{cod})(\text{SL-J001-01})\text{BPh}_4$

$\text{Rh}(\text{cod})(\text{SL-J001-01})\text{BPh}_4$ was synthesized analogue to the procedure 4.7.4.

Yield: 90% (464.1 mg, 0.39 mmol)

^{31}P NMR (CDCl_3) δ : 52.7 (dd, $J_{\text{P-P}} = 33$ Hz, $J_{\text{P-Rh}} = 140$ Hz), 20.5 (dd, $J_{\text{P-P}} = 29$ Hz, $J_{\text{P-Rh}} = 144$ Hz)

$^1\text{H NMR}$ (CDCl_3) δ : 8.25-8.30 (m, 2H, Ph); 6.89-7.67 (m, 28H, Ph); 5.45 (s, 1H, CH); 5.19 (s, 1H, CH); 4.58 (m, 1H, CH); 4.40 (s, 1H, CH); 4.20 (s, 1H, CH); 4.36 (s, 1H, CH); 3.7(s, 5H, CH); 3.49 (s, 1H, CH) 2.84 (m, 1H, CH); 0.8- 2.58 (m, 31H,)

[Rh(cod)(bdpp)]BPh₄

[Rh(cod)(bdpp)]BPh₄ was synthesized analogue to the procedure 4.7.4.

Yield: 90% (377.86 mg, 0.39 mmol)

$^{31}\text{P NMR}$ (CDCl_3) δ : 27.0 (d, $J_{\text{P-Rh}} = 142$ Hz)

$^1\text{H NMR}$ (CDCl_3) δ : 8.19 (m, 4H, Ph); 7.7 (m, 6H, Ph); 7.5 (m, 6H, Ph); 7.3 (m, 12H, Ph+B-Ph); 7.03 (t, 2H, $J = 7,3$ Hz, B-Ph); 6.89 (t, 2H, $J = 7,3$ Hz, B-Ph); 4.72 (m, 2H, CH); 3.91 (m, 2H, CH); 2.73 (m, 2H, CH); 2.52 (m, 4H, CH); 1.96 (m, 4H, CH₂); 1.70 (m, 2H, CH₂); 1.03 (m, 6H, CH₃)

4.7.5 Synthesis of $[(\eta^6\text{-PhBPh}_3)][\text{Rh}(\text{P}^\wedge\text{P})]^+$ and $[(\eta^6\text{-PhBPh}_2\text{polymer})][\text{Rh}(\text{P}^\wedge\text{P})]^+$

[Rh(cod)(P[∧]P)]BPh₄/[Rh(cod)(P[∧]P)]BPh₃polymer ($8.4 \cdot 10^{-3}$ mmol, 1.2 mmol/L) was dissolved in CH₂Cl₂ (10 mL) in a Schlenk tube. The system was flushed with Ar and purged 3 times with H₂. The mixture was stirred for 2h under H₂ (1.3 bar) atmosphere at r.t. The solution was concentrated and hexane was added to precipitate the product. The resulting polymer was washed with cold CH₂Cl₂ and dried under vacuum.

$[(\eta^6\text{-PhBPh}_3)][\text{Rh}(\text{SL-J001-01})]^+$

$[(\eta^6\text{-PhBPh}_3)][\text{Rh}(\text{SL-J001-01})]^+$ was synthesized analogue to the procedure 4.7.5.

$^{31}\text{P NMR}$ (CDCl_3) δ : 76.5 (dd, $J_{\text{P-P}} = 41$ Hz, $J_{\text{P-Rh}} = 202$ Hz); 32.5 (dd, $J_{\text{P-P}} = 40$ Hz, $J_{\text{P-Rh}} = 210$ Hz)

$^1\text{H NMR}$ (CDCl_3) δ : 7.9 (m, 2H, Ph); 6.96-7.67 (m, 28H, Ph); 6.12 (m, 1H, CH); 5.43 (s, 1H, CH); 4.38 (m, 1H, CH); 4.32 (s, 1H, CH); 4.20 (s, 1H, CH); 3.46 (s, 5H, CH); 3.01 (s, 1H, CH); 0.68- 2.18 (m, 33H,)

$[(\eta^6\text{-PhBPh}_2\text{polymer})][\text{Rh}(\text{SL-J001-01})]^+$

$[(\eta^6\text{-PhBPh}_2\text{polymer})][\text{Rh}(\text{SL-J001-01})]^+$ was synthesized analogue to the procedure 4.7.5.

^{31}P NMR (CDCl_3) δ : 76.1 (dd, $J_{\text{P-P}} = 43$ Hz, $J_{\text{P-Rh}} = 202$ Hz); 32.4 (dd, $J_{\text{P-P}} = 39$ Hz, $J_{\text{P-Rh}} = 210$ Hz)

$[(\eta^6\text{-PhBPh}_3)][\text{Rh}(\text{bdpp})]^+$

$[(\eta^6\text{-PhBPh}_3)][\text{Rh}(\text{bdpp})]^+$ was synthesized analogue to the procedure 4.7.5.

^{31}P NMR (CDCl_3) δ : 39.2 (d, $J_{\text{P-Rh}} = 195$ Hz)

^1H NMR (CDCl_3) δ : 6.97-8.19 (m, 35H, Ph+B-Ph); 6.87 (t, 1 H, $J = 6.5$ Hz, η -Ph-B); 5.55 (t, 2 H, $J = 6.2$ Hz, η -Ph-B); 4.96 (t, 2H, $J = 6.2$ Hz, η -Ph-B); 2.64 (m, 2H, CH); 1.74 (s, 2H, CH); 1.54 (s, CH); 1.03 (m, 6H, CH_3)

$[(\eta^6\text{-PhBPh}_2\text{polymer})][\text{Rh}(\text{bdpp})]^+$

$[(\eta^6\text{-PhBPh}_2\text{polymer})][\text{Rh}(\text{bdpp})]^+$ was synthesized analogue to the procedure 4.7.5.

^{31}P NMR (CDCl_3) δ : 39.7 (d, $J_{\text{P-Rh}} = 195$ Hz)

4.7.6 Synthesis of $[\text{Rh}(\text{nbd})(\text{SL-J003-01})]\text{BPh}_4$

The synthesis was carried out following a literature procedure.^[7] $[\text{Rh}(\text{nbd})\text{Cl}]_2$ (176 mg, 0.434 mmol) and SL-J003-01 (263 mg, 0.434 mmol) were dissolved in MeOH. A solution of NaBPh_4 (150 mg, 0.434 mmol) in MeOH (2 mL) was added to the stirred red solution. The resulting precipitate was filtered and washed with MeOH/ H_2O (2 mL), Et_2O (4 mL), MeOH (2 mL). The red-orange crystals were dried under vacuum. Yield: 90% (438 mg, 0.39 mmol)

^{31}P NMR (CDCl_3) δ : 55.0 (dd, $J_{\text{P-P}} = 34$ Hz, $J_{\text{P-Rh}} = 156$ Hz); 18.8 (dd, $J_{\text{P-P}} = 30$ Hz, $J_{\text{P-Rh}} = 150$ Hz)

^1H NMR (CDCl_3) δ : 7.4-6.9 (m, 20H, Ph); 4.98 (s, 1H, CH); 4.53 (m, 2H, CH); 4.29 (s, 5H, CH); 4.1 (s, 1H, CH); 3.9 (s, 1H, CH); 2.82 (m, 1H, CH); 0.9- 2.4 (m, 57H,)

4.7.7 Synthesis of $[Rh(nbd)(SL-J003-01)]BAr_4^F$

The synthesis was carried out following a literature procedure.^[22] $[Rh(nbd)Cl]_2$ (26,05 mg, 0.0565 mmol) and 2.5 eq. norbornadiene (30 mg, 0.325 mmol) were dissolved in CH_2CH_2 (10 mL). A solution of $NaBAr_4^F$ (100 mg, 0.113 mmol) in CH_2CH_2 (2 mL) was added to the stirred yellow solution. After the addition was complete, the red solution was stirred for at least 20 min followed by filtration. The solution was concentrated and *n*-hexane (30 mL) was added to give red crystals of the complex. The product was filtered and dried under vacuum. Yield: 77% (100 mg, 0.087 mmol).

To a solution of $[Rh(nbd)_2]BAr_4^F$ in MeOH (5 mL) was added SL-J003-01 in MeOH (2 mL) and during stirring the color changed. The solution was used without any further purification in the hydrogenation reactions.

^{31}P NMR ($CDCl_3$) δ : 54.9 (dd, $J_{P-P} = 30$ Hz, $J_{P-Rh} = 156$ Hz); 18.7 (dd, $J_{P-P} = 30$ Hz, $J_{P-Rh} = 150$ Hz) ^{19}F NMR ($CDCl_3$) δ : -62.41

1H NMR ($CDCl_3$) δ : 7.7-6.7 (m, 12H, Ph); 4.96 (s, 1H, CH); 4.50 (m, 2H, CH); 4.27 (s, 5H, CH); 4.05 (s, 1H, CH); 3.93 (s, 1H, CH); 2.76 (m, 1H, CH); 0.88- 2.77 (m, 57H.)

4.7.8 Synthesis of $[Rh(cod)(P^{\wedge}P)]BF_4$ (1a, 1b) and $[Rh(nbd)(P^{\wedge}P)]BF_4$ (1c)

To a solution of $[Rh(cod)_2]BF_4$ in the desired solvent (5 mL) was added ($P^{\wedge}P$) dissolved in the desired solvent (2 mL) and during stirring the color changed. The solution was used without any purification in the hydrogenation reactions.

1a $P^{\wedge}P = bdpp$ ((2*S*,4*S*)-2,4-bis(diphenylphosphino)pentane

^{31}P NMR ($CDCl_3$) δ : 27.0 (d, $J_{P-Rh} = 142$ Hz); ^{19}F NMR ($CDCl_3$) δ : -153.79

1b $P^{\wedge}P = SL-J001-01$ (*R*)-(1)-{[(*S*)-2diphenylphosphino]ferrocenyl}ethyl} dicyclohexylphosphine

^{31}P NMR ($CDCl_3$) δ : 52.7 (dd, $J_{P-P} = 33$ Hz, $J_{P-Rh} = 140$ Hz), 20.5 (dd, $J_{P-P} = 30$ Hz, $J_{P-Rh} = 144$ Hz); ^{19}F NMR ($CDCl_3$) δ : -154.09

1c $P^{\wedge}P = SL-J003-01$ (*R*)-(1)-{[(*S*)-2dicyclohexylphosphino]ferrocenyl}ethyl} dicyclohexylphosphine

^{31}P NMR (CDCl_3) δ : 54.9 (dd, $J_{\text{P-P}} = 30$ Hz, $J_{\text{P-Rh}} = 156$ Hz); 18.7 (dd, $J_{\text{P-P}} = 30$ Hz, $J_{\text{P-Rh}} = 150$ Hz); ^{19}F NMR (CDCl_3) δ : -154.0

4.7.9 Synthesis of methyl (Z)- α -acetamidocinnamate

Methyl (Z)- α -acetamidocinnamate was synthesized according to a literature procedure.^[23]

4.7.10 General hydrogenation procedure for MAC and DMI

A Schlenk tube was filled with substrate (2.2 mmol) and catalyst (0.022 mmol) dissolved in the desired solvent (7 mL), purged three times with H_2 . The reaction mixture was stirred under H_2 (1.3 bar) at 20°C. After the required time, the resulting solution was passed through a small alumina column prior to quantitative analysis by GC.

4.7.11 General hydrogenation procedure for MAC and DMI using immobilized catalyst

The supported catalyst precursor ($3.16 \cdot 10^{-3}$ mmol) was placed in a glass custom made filtration cell equipped with a G4 frit in methanol suspension (20 mL). Hydrogen was bubbled through the suspension for 2 h. The solvent was expelled from the cell and replaced by a solution of substrate (MAC or DMI (0.316 mmol)) in MeOH (7 mL). After the required time, the reaction mixture was filtered through the frit and the filtrate was analyzed by GC. The supported catalyst left in the frit was reused for several runs. The filtrates were combined, dried under vacuum, and the residue was analyzed by ICP-AES.

GC analysis**Conversion of methyl (Z)- α -acetamidocinnamate (MAC)**

GC	:	Shimadzu GC 17A
Column	:	HP Pona (crosslinked Me Siloxane), 50 m, inner \varnothing 0.20 mm, film thickness 0.5 μ m
Carrier gas	:	Helium 250.0 kPa (total flow 35 ml/min)
Temperature program	:	70°C (hold: 10 min), 7°C/min to 120°C, 14°C/min to 270°C (hold: 4 min)
Injector	:	250°C
Detector (FID)	:	270°C
Split ratio	:	21
Injection volume	:	1.0 μ L

Table 4.8 Selected retention times of substrate and product

Compound	Retention time (min)
methyl (Z)- α -acetamidocinnamate	20.9
hydrogenated product	19.5

Enantiomeric excess methyl (Z)- α -acetamidocinnamate (MAC)

GC	:	Shimadzu GC 17A
Column	:	Chirasil L-Val, 25 m, inner \varnothing 0.25 mm, film thickness 0.12 μ m
Carrier gas	:	Helium 120.0 kPa (total flow 69 ml/min)
Temperature program	:	170°C (hold: 25 min)
Injector	:	250°C
Detector (FID)	:	270°C
Split ratio	:	50
Injection volume	:	1.0 μ L

Table 4.9 Selected retention times of product enantiomers

Compound	Retention time (min)
enantiomer (<i>R</i>)	5.26
enantiomer (<i>S</i>)	5.59

Conversion of Dimethylitaconate (DMI)

GC	:	Shimadzu GC 2010
Column	:	Lipodex- E, 25 m, inner Ø 0.25 mm
Carrier gas	:	Hydrogen 113.6 kPa (total flow 154 ml/min)
Temperature program	:	90°C (hold: 15 min)
Injector	:	220°C
Detector (FID)	:	220°C
Split ratio	:	100
Injection volume	:	1.0 µL

Table 4.10 Selected retention times of substrate and products

Compound	Retention time (min)
enantiomer (<i>R</i>)	6.3
enantiomer (<i>S</i>)	6.6
dimethylitaconate	9.6

4.7.12 Synthesis of *N*-(1-Phenylethyl)-*P,P*-diphenylphosphinimine

N-(1-Phenylethyl)-*P,P*-diphenylphosphinimine was synthesized according to a literature procedure.^[24]

4.7.13 Synthesis of *N*-benzyl-(-1-phenylethylidene)-imine

N-benzyl-(-1-phenylethylidene)-imine was synthesized according to a literature procedure.^[25]

4.7.14 General hydrogenation procedure of imines using homogeneous catalysts

A stainless steel autoclave filled with substrate (0.4778 mmol) and catalyst ($4.778 \cdot 10^{-3}$ mmol) dissolved in the desired solvent (7 mL) was purged three times with H₂. The autoclave was pressurized with H₂ (70 bar) and heated to 60°C for *N*-(1-Phenylethyl)-*P,P*-diphenylphosphinimine and r.t. for benzyl-(-1-phenylethylidene)-amine. After the required time the solution was removed from the autoclave and passed through a small alumina column prior to quantitative analysis by HPLC.

4.7.15 General hydrogenation procedure for *N*-(1-Phenylethyl)-*P,P*-diphenylphosphinimine using immobilized catalyst

A stainless steel autoclave filled with substrate (0.19 mmol) and catalyst ($1.9 \cdot 10^{-3}$ mmol) dissolved in MeOH/ THF (1:9) (7 mL) was purged three times with H₂. The autoclave was pressurized with H₂ (70 bar) and heated to 60°C for *N*-(1-Phenylethyl)-*P,P*-diphenylphosphinimine. After the required time the resulting solution was transferred from the autoclave to a Schlenk tube and the solvent was evaporated under vacuum. Then MeOH was added to the residue and the resulting precipitate was filtered. The solid catalyst was reused for several cycles. The filtrate was analyzed by HPLC and ICP-AES.

4.7.16 General hydrogenation procedure for *N*-benzyl-(-1-phenylethylidene)-imine using immobilized catalyst

A stainless steel autoclave filled with substrate (0.19 mmol) and catalyst ($1.9 \cdot 10^{-3}$ mmol) dissolved in MeOH (7 mL) was purged three times with H₂. The autoclave was pressurized with H₂ (70 bar) at r.t. After the required time, the resulting solution was

transferred from the autoclave to a Schlenk tube and the solvent was evaporated. *N*-hexane was added to the residue and the precipitate was filtered. The solid catalyst was reused for several cycles. The filtrate was analyzed by HPLC and ICP-AES.

HPLC-Analysis for *N*-(1-Phenylethyl)-*P,P*-diphenylphosphinimine

HPLC-Pump	:	Shimadzu LC-20AD
Autosampler	:	Spark Holland Marathon
HPLC-Pump	:	Shimadzu LC-20AD
Oven	:	Self build 25°C
UV-Detector	:	Shimadzu SPP-20A
Column	:	OD-H, 25 cm, inner Ø 0.46 mm, particle size 5 µm
Solvents	:	10% <i>i</i> -PrOH/ hexane
Flow rate	:	0.5 mL/min
Detector set	:	254 nm
Injection volume	:	1.0 µL

Table 4.11 Selected retention times of substrate and product

Compound	Retention time (min)
major isomer (<i>R</i>)	13.5
<i>N</i> -(1-Phenylethyl)- <i>P,P</i> -diphenylphosphinimine	15.5
minor isomer (<i>S</i>)	16.7

HPLC-Analysis for benzyl-(-1-phenylethylidene)-amine

HPLC-Pump	:	Shimadzu LC-20AD
-----------	---	------------------

Autosampler	:	Spark Holland Marathon
HPLC-Pump	:	Shimadzu LC-20AD
Oven	:	Self build 25°C
UV-Detector	:	Shimadzu SPP-20A
Column	:	OD-H, 25 cm, inner Ø 0.46 mm, particle size 5 µm
Solvents	:	<i>n</i> -hexane
Flow rate	:	1 mL/min
Detector set	:	220 nm
Injection volume	:	1.0 µL

Table 4.12 Selected retention times of substrate and product

Compound	Retention time (min)
major isomer (<i>R</i>)	17.5
minor isomer (<i>S</i>)	20.5
benzyl-(-1-phenylethylidene)-amine	27.5

ICP- AES

The analytical principle used in the SPECTRO ICP systems is optical emission spectroscopy. A liquid is nebulized and then vaporized with in the Argon plasma.

The atoms and ions contained in the plasma vapor are excited into a state of radiated light (photon) emission. The radiation emitted can be passed to the spectrometer optic, where it is dispersed into its spectral components. From the specific wavelengths emitted by each element, the most suitable line for the application is measured by means of a CCD (charge coupled device).

The radiation intensity, which is proportional to the concentration of the element in the sample, is recalculated internally from a stored set of calibration curves and can be shown directly as percent or measured concentration.^[26]

Sample preparation

The volatiles from the organic sample were removed under vacuum. Afterwards the sample was calcinated at 500°C overnight in order to remove all organic compounds. After the sample had cooled down, sulphuric acid (2 mL) was added to the residue and heated until SO₃ fumes arised out of the solution. The solution was cooled down and H₂O₂ (2 mL) was slowly added. After the reaction, the solution was transferred into a volumetric flask of 25 mL and analyzed.

ICP instrumentation:

Spectrometer: SPECTRO CIROS^{CCD}
Technique: Inductively Coupled Plasma Optical Emission Spectrometry (ICP-OES)

Operating conditions:

Generator:	Free-running at Power	27,12 MHz 1400 W
Sample introduction:	Nebulizer Spray chamber Sample uptake rate	Cross-flow (SPECTRO) Double pass, Scott type (SPECTRO) 2 ml/min
Gas flows:	Outer gas Intermediate gas Nebulizer gas	12 l/min 1 l/min 1.00 l/min
Gas:	Argon	

4.8 References

- [1] W. S. Knowles, M. J. Sabacky, B. D. Vineyard, D. J. Weinkauff, *J. Am. Chem. Soc.* **1975**, *97*, 2567-2568.
- [2] W. S. Knowles, *Acc. Chem. Res.* **1983**, *16*, 106-112.
- [3] R. Sablong, J. I. van der Vlugt, R. Thomann, S. Mecking, D. Vogt, *Adv. Synth. Catal.* **2005**, *347*, 633-636.
- [4] I. Tóth, P. C. van Geem, in *Handbook of Homogeneous Hydrogenation* (Eds. J. G. de Vries, C. J. Elsevier) Ed. Wiley –VCH, **2007**, *3*, 1421-1467.
- [5] M. Ono, S. Hinokuma, S. Miyake, S. Inazawa, (Japan Polyolefins Co., Ltd.), *Eur. Patent Appl.* 710, 663, **1996**.
- [6] G. A. Molander, R. Figueroa, *Org. Lett.* **2006**, *8*, 75-78.
- [7] Z. Zhou, G. Facey, B. R. James, H. Alper, *Organometallics* **1996**, *15*, 2496-2503.
- [8] R. R. Schrock, J. A. Osborn, *Inorg. Chem.* **1970**, *9*, 2339-2343.
- [9] J. Halpern, D. P. Riley, A. S. C. Chan, J. S. Pluth, *J. Am. Chem. Soc.* **1977**, *99*, 8055-8057.
- [10] C. R. Landis, J. Halpern, *Organometallics* **1983**, *2*, 840-842.
- [11] D. Heller, H.-J. Drexler, A. Spannenberg, B. Heller, J. You, W. Baumann, *Angew. Chem., Int. Ed.* **2002**, *41*, 777-780.
- [12] D. Heller, A. H. M. de Vries, J. G. de Vries, in *Handbook of Homogeneous Hydrogenation* (Eds. J. G. de Vries, C. J. Elsevier) Ed. Wiley –VCH, **2007**, *3*, 1483-1516.
- [13] Z. Zhou, B. R. James, H. Alper, *Organometallics* **1995**, *14*, 4209-4212.
- [14] P. Barbaro, *Chem. Eur. J.* **2006**, *12*, 5666-5675.
- [15] S. H. Strauss, *Chem. Rev.* **1993**, *93*, 927-942.
- [16] J. van de Broeke, E. de Wolf, B.-J. Deelman, G. van Koten, *Adv. Synth. Catal.* **2003**, *345*, 625-635.
- [17] M. Aresta, E. Quaranta, I. Tommasi, *New J. Chem.* **1997**, *21*, 595-613.
- [18] Z. Zhou, B. R. James, H. Alper, *Organometallics* **1995**, *14*, 4209-4212.
- [19] F. Spindler, H.-U. Blaser, *Adv. Synth. Catal.* **2001**, *343*, 68-70.
- [20] C. Simons, U. Hanefeld, I. W. C. E. Arends, R. A. Sheldon, T. Maschmeyer, *Chem. Eur. J.* **2004**, *10*, 5829-5835.
- [21] J. Bakos, A. Orosz, B. Heil, M. Laghmari, P. Lhoste, D. Sinou, *J. Chem. Soc. Chem. Commun.* **1991**, 1684-1685.
- [22] M. N. Cheemala, P. Knochel, *Org. Lett.* **2007**, *9*, 3089-3092.
- [23] M. Alane, M. Jahjah, M. Berthod, M. Lemaire, V. Meille, C. de Bellefon, *J. Mol. Catal. A: Chem.* **2007**, *268*, 205-212.

- [24] T. Kobayashi, H. Kawate, H. Kakiuchi, H. Kato, *Bull. Chem. Soc. Jpn.* **1990**, *63*, 1937-1942.
- [25] J. S. M. Samec, J.-E. Bäckvall, *Chem. Eur. J.* **2002**, *8*, 2955-2961.
- [26] Information from <http://www.spectro.com/pages/e/index.htm>

Application of Latex-incorporated Nixantphos in the Biphasic Hydroformylation of Higher Alkenes: *Initial Results and Outlook*

Previous investigations focussed on the preparation and application of latexes as phase transfer agents and supports for electrostatic immobilization in the biphasic hydroformylation of higher alkenes and in the asymmetric hydrogenation.

In this chapter the covalent bonding of the ligand Nixantphos to polystyrene-based latex particles is investigated. The application of these functionalized latex particles in the biphasic hydroformylation of 1-octene is presented.

Furthermore, suggestions for alternative latex compositions are made.

5.1 Introduction

In Chapter 3, the application of polystyrene-based latexes as phase transfer agents in the biphasic hydroformylation of higher alkenes was presented. It was shown that especially efficient systems were obtained, combining the catalyst bearing a sulfonated ligand (TPPTS) with a latex bearing ammonium groups. The conclusion was that this combination leads to the aggregation of the catalyst with the latex particles, representing an electrostatic anchoring at the latex shell.

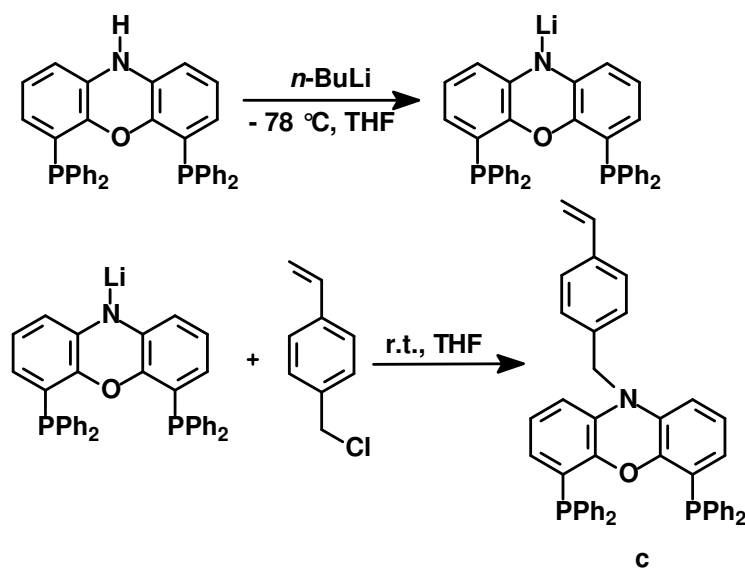
It has been proposed that the alkene was transferred into the lipophilic core of the latex particle. At the interface of the core and the hydrophilic shell, the catalysis takes place. Several polystyrene-based latexes, which vary in composition, were examined and excellent reaction rates were observed (TOF's of up to 2000 h⁻¹).

It was shown that the process can be limited by the mass transfer of the substrate from the organic phase into the lipophilic core of the particles and from the core to the interface of the particles (Chapter 3, Section 3.3.3).

Part of this mass transfer limitation might be avoided by placing the catalyst in the lipophilic core of the latex particle. Therefore, the bidentate phosphine ligand Nixantphos was decorated with a polymerizable group (styrene) and covalently incorporated into the polymer. The synthesis of latex-incorporated Nixantphos as well as its application is discussed. As an outlook for future work alternative latex compositions are suggested. The use of polymers that exhibit lower critical solution temperature (LCST) behaviour is also addressed.

5.2 Synthesis of latex-incorporated Nixantphos

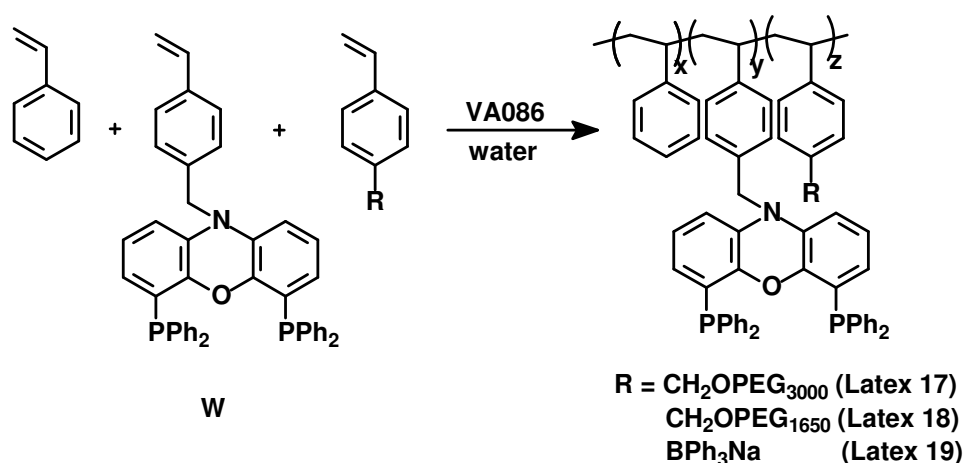
In order to introduce a polymerizable vinyl-group into nixantphos, the synthesis of *p*-vinylbenzylnixantphos, was considered.



Scheme 5.1 Synthesis of functionalized nixantphos

n-BuLi was added to a solution of Nixantphos in THF at $-78\text{ }^{\circ}\text{C}$. Subsequently, one equivalent of *p*-vinylbenzyl chloride was added leading to 42% yield of *p*-vinylbenzylnixantphos **c** after workup (Scheme 5.1).

Compound **c** was copolymerized with styrene and a polymerizable surfactant (surmfer) by means of emulsion polymerization according to the synthesis described by R. Sablong *et al.*^[1] Latexes with different surmfers were prepared. PEG₃₀₀₀ and PEG₁₆₅₀ were used for latex 17 and 18, respectively. Sodium *p*-vinylbenzyltriphenylborate was used for latex 19 (Scheme 5.2). The resulting latex particles were characterized by means of TEM and solid state NMR spectroscopy.



Scheme 5.2 Emulsion copolymerization of *p*-vinylbenzylnixantphos

The emulsion polymerization was successfully performed with 2 mol% of the reactive surfactants. The amount of functionalized Nixantphos **c** was 2-3 mol%. No

divinylbenzene (DVB) was used as cross-linker in order to avoid insufficient diffusion of the Rh-precursor into the ligand-containing core of the particles.

5.3 Characterization of latex-incorporated nixantphos

The average particle size distributions were determined by means of TEM (Table 5.1). With decreasing surfactant molecular weight, a decrease of the corresponding particle size was observed (Latex 17, 18). This is most likely due to the fact that for longer chain surfactants an increased number of hydrophobic monomer units is required in order to start the particle formation. This leads to fewer particles after the particle nucleation. Consequently, these particles are loaded with more monomer, leading to larger particles. In case of shorter polyethyleneglycol chains, the amount of monomer required before particle formation is lower. That leads to a higher number of particles with smaller sizes.

Table 5.1 Particle size average of the synthesized latexes

Latex	Surfactant	Particle size average [nm]
17	PEG ₃₀₀₀	100
18	PEG ₁₆₅₀	80
19	BPh ₄ Na	70

All latexes have a rather broad particle size distribution as it is shown in Figure 5.1.

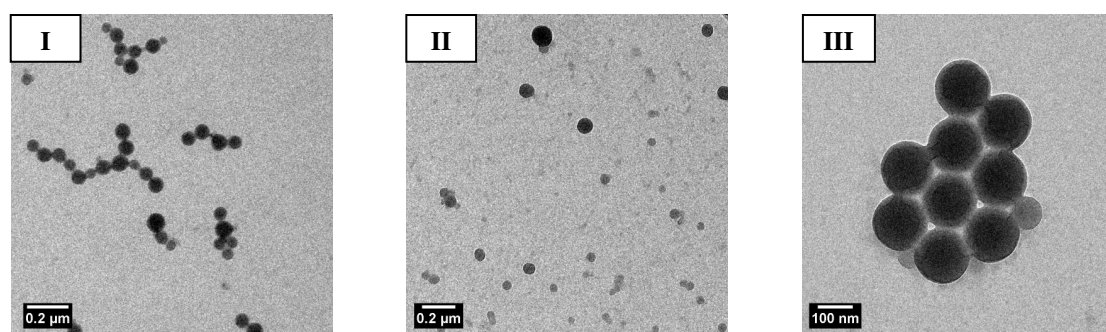


Figure 5.1 TEM pictures of latexes with different surfactants, (I) latex 17 PEG₃₀₀₀, (II) latex 18 PEG₁₆₅₀, (III) latex 19 BPh₄Na

All latexes were analyzed by solid state ³¹P-NMR spectroscopy in order to determine the amount of ligand content.^[2] For latex 1 and latex 3 no ³¹P-NMR signal was

detected. One possible explanation is that no ligand was incorporated within the latex particle. Even if small amounts of ligand were incorporated, this could still be below the NMR detection limit. Therefore, the emulsions were additionally analysed by means of ICP-AES (Figure 5.2, Table 5.3).

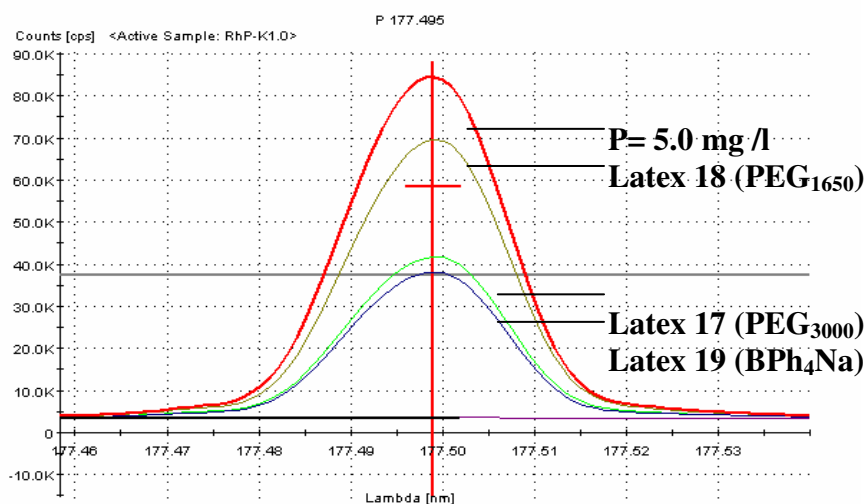


Figure 5.2 Phosphorus content measured by ICP-AES

Table 5.2 Calculated nixantphos concentration based on ICP-AES results

Latex	Surfactant	Nixantphos [mol/l]	Nixantphos-content [mol%]
17	PEG ₃₀₀₀	0.19	1.2
18	PEG ₁₆₅₀	0.32	2
19	BPh ₄ Na	0.17	1.1

The results are summarized in Figure 5.2 and Table 5.2. Phosphorus was detected in all latexes. For latex 17 and 19 an average loading of approximately 1 mol% was found while a loading of 2 mol% was found for latex 18. These results indicate that the amount of Nixantphos is below the detection limit of the solid state NMR for latex 17 and 18.

5.4. Application of Nixantphos as ligand in the one-phase hydroformylation

In order to evaluate this concept, reference hydroformylation experiments were first performed using Nixantphos as ligand. The reaction was carried out at 20 bar of synthesis gas (CO/H₂ 1:1), 80°C and a stirring rate of 700 rpm. The gas uptake was monitored during the course of the reaction and a TOF of 2000 h⁻¹ was calculated after 20% 1-octene conversion.

The conversion of alkene as well as the amount of linear and branched aldehyde formed was determined by GC. The resulting l/b ratio is 55 which is typical for bidentate phosphine ligands with relatively large bite-angles.^[3,4]

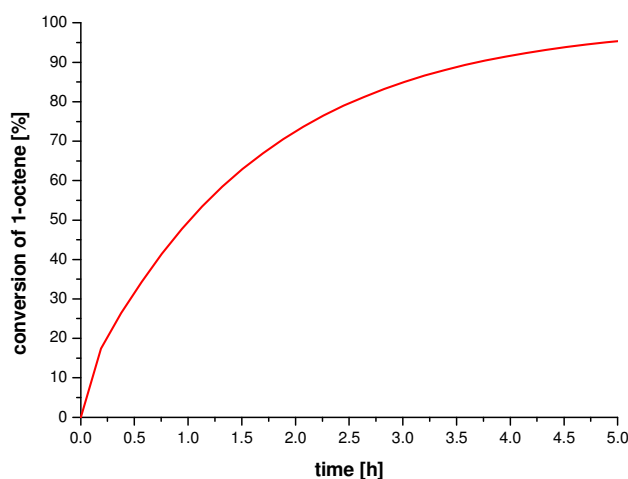


Figure 5.3 Conversion of 1-octene based on gas uptake CO/H₂ versus reaction time for Nixantphos

5.5. Application of latex-incorporated Nixantphos in the biphasic hydroformylation of 1-octene

In order to examine the catalytic performance of latex-incorporated Nixantphos, the latexes 17-19 were applied in the biphasic hydroformylation of 1-octene using Rh(acac)(CO)₂ as catalyst precursor.

The hydroformylation should take place in the lipophilic core of the latex particles. Therefore, the precursor was dissolved in different organic solvents, which are known to cause swelling of the lipophilic core of the particles, in order to achieve efficient

transport of the Rh-precursor to the incorporated phosphine-ligands. Before the addition of 1-octene, the catalyst solution was stirred with the latex for several hours. Subsequently, the reactor was pressurized with CO/H₂ (1:1) to 20 bar at 80°C to generate the catalytic resting state [Rh(H)(CO)₂(latex 17/18/19)]. The hydroformylation was carried out at 80 °C, 20 bar CO/H₂ and 600 rpm. All results are depicted in Table 5.3.

Table 5.3 Biphasic hydroformylation of 1-octene using latex-incorporated nixantphos

Entry	Precursor	Solvent for precursor	Pre-treatment [h]	Ratio l/b	Latex
1	Rh(acac)(CO) ₂	dodecane	16	1.5	latex 19
2	Rh(acac)(CO) ₂	dodecane	72	2.5	latex 19
4	Rh(acac)(CO) ₂	MeOH	72	1.5	latex 19
5	Rh(acac)(CO) ₂	MeOH	under CO/H ₂ 6	n.d.	latex 19 in MeOH
6	Rh(acac)(CO) ₂	hexane	under CO/H ₂ 6	1	latex 17
7	Rh(acac)(CO) ₂	hexane	under CO/H ₂ 6	40	latex 18
8	Rh(acac)(CO) ₂	hexane	under CO/H ₂ 6	1	latex 19

Reaction conditions: 20 bar CO/H₂ (1:1), 80°C, 700 rpm, Rh(acac)(CO)₂ (1.1 mg, 4.26·10⁻³ mmol, 0.142 mmol/L), latex-incorporated nixantphos (15 mL, 0.026 mmol, 0.852 mmol/L), 1-octene (15 mL, 95 mmol, 3.16 mol/L), Rh:L:substrate (1:3:22300)

After completion of the reaction the organic phase was analyzed by means of GC.

From Table 5.3 it is clear that in most cases no coordination of the Rh-center to the bidentate phosphine ligands occurred, because the observed l/b ratios of ~ 2 are typical for Rh-complexes containing monodentate phosphine ligands or phosphine free Rh-species. Apparently an efficient transport of the Rh-precursor to the incorporated ligand did not proceed.

In case of latex 18 dispersed in MeOH coagulation took place during the reaction and the organic phase could not be analyzed (Entry 5). However, in contrast to the other experiments a linear/branched ratio of 40 (Entry 7) was observed by applying latex 17 in hexane. This high ratio suggests an efficient transport of Rh into the particle core. A TOF of 780 h⁻¹ was reached compared to a TOF of up to 400 h⁻¹ for the other systems used.

In order to determine potential Rh-loss, the organic phases were analyzed by ICP-AES. For all samples 90% Rh-loss was detected! Only in the case of latex 18, a Rh-loss of 50% was detected, which implies that a certain amount of Rh was coordinated to the latex-incorporated nixantphos (Entry 7). This was also consolidated by the GC results. However, in order to prove that the ligand system did not leach from the lipophilic core

into the organic phase, the organic phase was also analyzed by ICP-AES for phosphorus. No significant ligand leaching was detected (< 1.0%).

Based on these results it can be concluded that the concept presented here can be successfully applied but other methods have to be invested to incorporate the Rh-complex into the latex.

5.6 Examples of variations of latexes nature

In Chapter 3 and 5 several parameters were discussed, which can influence the reaction rate of the biphasic hydroformylation of higher alkenes. These investigations provide ample opportunities in the field of continuous aqueous organometallic catalysis. Therefore several options for possible variations are presented.

5.6.1 Surfactants

In all the investigations presented here only reactive surfactants were used in the emulsion polymerization in order to stabilize the latex particles. One option would be the use of surfactants, which can stabilize the latex particle *via* electrostatic interactions. Examples are SDS (sodium dodecylsulfate), CTAB (hexadecyl-trimethyl-ammonium bromide) or CAPB {[3-(dodecanoylamino)propyl] (dimethyl)ammonio}acetate (Figure 5.4).

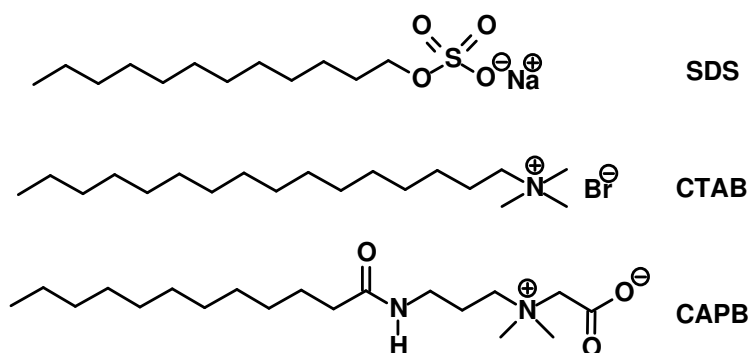


Figure 5.4 Surfactants which can electrostatically stabilize latex particles

The surface coverage of latex particles using electrostatically anchored surfactants might be lower compared to reactive surfactants, which are covalently anchored. Therefore the latex particles are more “open” for the transfer of organic compounds into the lipophilic core of the particles, eventually leading to higher reaction rates.

It was shown in Chapter 3 that the synthesis of charged particles is necessary in order to achieve an efficient interaction with the charged Rh-complexes. The charge was introduced by styrylsalts (Chapter 2, Figure 2.6). However, also these systems can stabilize the latex particles and cover the surface, which can hinder the transfer of lipophilic compounds between the organic phase and the particles.

In order to stabilize the particle and to introduce the charge at ones, surfactants containing ionic groups could be used. For instance, anionic surfactants or cationic surfactants, such as SDS or CTAB, as depicted in Figure 5.4.^[5]

5.6.2 *Organic polymers in the lipophilic core*

Latexes, which vary in their composition, were investigated in the hydroformylation of 1-octene as described in Chapter 3. Different PS-PBMA and PS-PMMA mixtures were used. The resulting reaction rates showed that the use of polymers, which are more hydrophilic compared to PS, lower the reaction rates. Therefore, it would be interesting to investigate latexes with a more lipophilic core compared to polystyrene-based latexes. Suitable monomers for this investigation are for instance isooctyl acrylate, isododecyl acrylate, *p*-vinylbenzyl chloride or butadiene (Figure 5.5).^[6]

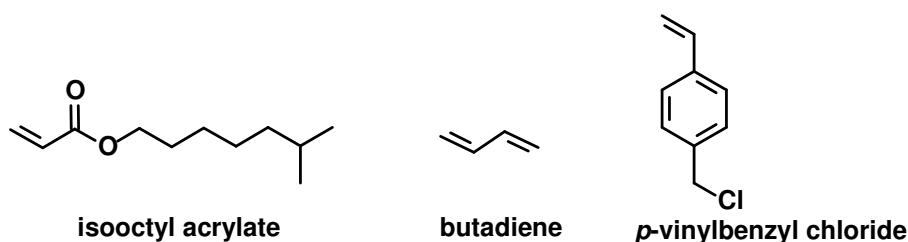


Figure 5.5 Suitable monomers for emulsion polymerization

Furthermore, only polystyrene-based latexes were used in these investigations as phase transfer agents. Another possibility is the application of poly(*N*-isopropylacrylamide)-

based latex particles (PNIPAM-based latex particles). These latexes are thermosensitive. In particular, PNIPAM-based latexes have a lower critical solution temperature (LCST).

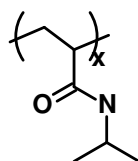


Figure 5.6 Schematic structure of Poly(*N*-isopropylacrylamide)

At temperatures below the LCST the PNIPAM-based latex particles can swell in water while above the LCST the particles collapse. This effect is due to the fact that the hydrogen bonds between the $-\text{CONH}(\text{Me}_3)_2$ groups (Figure 5.6) in the polymer chain and the water molecules are the major interactions below the LCST. Thus, the latex particles are rather hydrophilic. By increasing the temperature the hydrogen bonds break, resulting in a phase-separation above the LCST. The system separates into two phases, a polymer-rich phase and a water-rich phase.^[7]

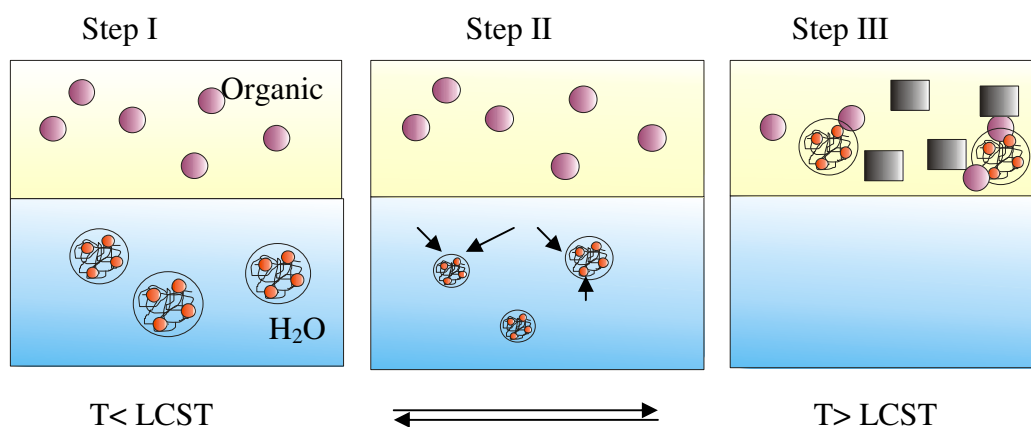





Figure 5.7 Effect of thermosensitive latex particles in catalysis,  represents latex particles containing catalyst;  substrate;  product

This effect could also be exploited in the biphasic catalysis. Crosslinked PNIPAM-based particles can be functionalized with a coordinating ligand. Then the Rh complexes can be introduced. At temperatures below the LCST, the PNIPAM-based particles are water-soluble, remain swollen and suspended in the aqueous phase (Figure 5.7, Step I). Increase of the temperature above the LCST results in the exclusion of water from the particle and subsequently in the collapse of the particles (Figure 5.7, Step II) At this stage the particles become hydrophobic and can move into the organic

phase in which they could swell and lead to a contact of the catalyst with the substrate (Figure 5.7, Step III). The decrease of temperature at the end of the catalytic reaction results in the inclusion of water into the particles. The particles become water-soluble again and move back into the aqueous phase. Thus, the catalyst coordinated in the particles can easily be separated from the product phase.

Experimental Section

All chemicals were purchased from Aldrich, Acros, Strem, or Merck and used as received unless stated otherwise. All preparations were carried out under an atmosphere of dry argon using standard Schlenk techniques. Solvents were distilled under argon atmosphere and dried by standard procedures. All glassware was dried by heating under vacuum. The synthesis gas [CO (99.997%)/H₂ (99.997%) 1:1] was purchased from Linde gas. The NMR spectra were recorded on Varian Mercury 400, 200 MHz spectrometer (400 MHz for ¹H, and 200 MHz for ³¹P).

Synthesis of *p*-vinylbenzylnixantphos c

Nixantphos (1g, 1.81 mmol) was dissolved in THF (50 mL) and cooled to -78 °C. *n*-BuLi (0.75 mL, 2.5 M in THF) was slowly added to the solution. The solution was warmed to room temperature and stirred further for 2h at room temperature. *p*-Vinylbenzyl chloride (0.28 mg, 1.81 mmol) was added to the turbid solution and the mixture was stirred overnight at room temperature. After the solution was washed with brine, the organic phase was collected, dried over Na₂SO₄ and concentrated. *p*-vinylbenzylnixantphos was obtained by precipitation with Et₂O. Yield: 42% (503 mg, 0.7602 mmol)

³¹P NMR (CDCl₃) δ: -19.02 ¹H NMR (CDCl₃) δ: 7.22-7.40 (m, 24H, Ph); 6.74 (dd, 1H, CH=CH); 6.58 (t, 2H, *J* = 7.3 Hz, *J* = 8.0 Hz, CH); 6.31 (t, 2H, *J* = 8.0 Hz, 2H);

6.03 (t, 2H, $J = 7.3$ Hz, CH); 5.7 (dd, 1H, $J = 17.0$ Hz); 5.28 (t, 1H, $J = 10.9$ Hz); 4.78 (s, 2H, CH₂)

Emulsion polymerization of latex-incorporated Nixantphos^[1]

A solution of surfactant (0.55 mmol) in de-gassed de-ionized water (30 mL) was placed in an autoclave equipped with a mechanical stirrer. The solution was heated to 80 °C and stirred at 100 rpm. After this temperature was reached, styrene (26.3 mmol), (c) (500 mg, 0.83 mmol) and initiator AIBN (0.48 mmol) were added. The stirring rate was increased to 300 rpm. After 10 minutes the mixture became milky, indicating formation of the microemulsion. The suspension was stirred for 4 hours. During the reaction several samples were taken to measure the solid content and to monitor the conversion. Finally, the latex was cooled to room temperature and stored at 4°C. The latexes were purified by dialysis during 3-4 days using a cellulose hydrate membrane with a pore size of 25-30 Å. In case of big particles, ultracentrifugation was performed. The particles were analyzed by means of TEM.

General procedure for biphasic hydroformylation experiments

The latex-incorporated nixantphos (15 mL, 0.026 mmol, 0.852mmol/L) was stirred with a solution of Rh(acac)(CO)₂ (1.1 mg, $4.26 \cdot 10^{-3}$ mmol, 0.142 mmol/L) in the desired solvent (1mL) for the required time. Subsequently, the reactor was charged with this solution and the dropping funnel was charged with 1-octene (15 mL, 95 mmol, 3.16 mol/L). The ratio rhodium/ligand was 1:6. Catalysis was performed at 80°C and 20 bar CO/H₂ for the desired time at 600 rpm. The substrate was added by the dropping funnel and the conversion was measured *via* gas uptake of CO/H₂. After 200 h the reaction was stopped by cooling the reactor to room temperature and the pressure was released. The organic layer was analyzed by gas chromatography and ICP-AES.

GC analysis

GC	:	Shimadzu GC 17A
Column	:	HP Pona (crosslinked Me Siloxane), 50 m, inner Ø 0.20 mm, film thickness 0.5 µm
Carrier gas	:	Helium 208.0 kPa (total flow 69 ml/min)
Temperature program	:	60°C (hold: 10 min), 1°C/min to 65°C 15°C/min to 250°C (hold: 3 min)
Injector	:	250°C
Detector (FID)	:	270°C
Split ratio	:	50
Injection volume	:	1.0 µL

Table 3.13 Selected retention times of the organic compound and the external standard

Compound	Retention time (min)
1-octene	14.9
linear nonanal	23.0
branched nonanal	23.8
dodecane	25.4

5. 4. References

- [1] R. Sablong, J. I. van der Vlugt, R. Thomann, S. Mecking, D. Vogt, *Adv. Synth. Catal.* **2005**, *347*, 633-636.
- [2] All solid state ³¹P-NMR spectra were taken by Dr. P.C.M.M. Magusin on a Bruker DMX 500 spectrometer, Molecular Heterogeneous Catalysis, Department of Chemical Engineering and Chemistry, Eindhoven University of Technology
- [3] P. W. N. M. Leeuwen, *Homogeneous Catalysis Understanding the Art* 1st Ed. Kluwer Academic Publishers, **2004**, 139-190.
- [4] L. A. Van der Veen, P. H. Keeven, G. C. Schoemaker, J. N. H. Reek, P. C. J. Kamer, P. W. N. M. Van Leeuwen, M. Lutz, A. L. Spek, *Organometallics* **2000**, *19*, 872-883.
- [5] S.-H. Yu, H. Cölfen, *J. Mater. Chem.* **2004**, *14*, 2124-2147.
- [6] X. S. Chai, F. J. Schork, A. DeCinque, K. Wilson, *Ind. Eng. Chem. Res.* **2005**, *44*, 5256-5258.
- [7] H. Yamauchi, Y. Maeda, *J. Phys. Chem. B.* **2007**, *111*, 12964-12968.

Catalyst Immobilization via Electrostatic Interactions: Polystyrene-based Supports

The recovery of homogeneous catalysts still remains a crucial feature for industrial applications. Over the years a range of concepts were developed to tackle this problem. The most elegant and successful approach with respect to industrial application so far has been the two-phase catalysis, exemplified by the Shell Higher Olefin Process (SHOP) for ethene oligomerization, and the Ruhrchemie/Rhône Poulenc process (RCH/RP) for propene hydroformylation. In both processes the catalyst, dissolved in a polar solvent, is easily recovered and separated from an apolar product phase by phase-separation and extraction in a non-destructive procedure. However, considerable solubility of the substrates in the polar catalyst phase is required.

In general it can be stated that for each and every homogeneous catalytic process that made its way into industrial application, an individual solution to the problem of catalyst recovery and recycling was developed. Therefore, a toolbox of generic methods, each with proven boundaries of applicability, would be highly desirable in order to speed up future process development.

The subject of this dissertation is the development of non-destructive methods that combine the advantages of homogeneous catalysis with easy separation and recycling, especially for substrates, which are insoluble in the catalyst supporting phase. More specific, it focuses on use of phase-transfer agents and on the electrostatic immobilization of catalysts.

Latexes display a number of features that make them very attractive for these purposes. First of all they can be produced on a large scale in a single step from cheap building blocks in relatively simple procedures. Their properties can be varied in a wide range by the proper choice of monomers and polymerization conditions. As core-shell particles, representing a kind of “macromolecular micelles”, their solubility and the polarity of their interior can be fine-tuned. This unique combination of features makes these nanomaterials superior candidates for our purposes.

Therefore, latexes were studied as phase-transfer agents and supports for homogeneous catalysts.

In **Chapter one**, the literature concerning the electrostatic immobilization of catalysts is reviewed. The immobilization on supports like zeolites, clays, heteropolyacids, ionic liquids, and dendrimers is reviewed. Their application in catalysis is presented and compared. One major conclusion of this survey is that latexes have hardly ever been considered as catalyst supports.

Chapter two focuses on the synthesis and characterization of polystyrene-based latexes. The latexes are prepared by free initial radical emulsion copolymerization. The polystyrene-based latexes contain the hydrophobic monomer styrene, DVB as cross-linking agent, a polymerizable non-ionic surfactant, and polymerizable styrylsalts. The combination of the non-ionic surfactant and a styrylsalt provides an efficient stabilization of the latex particles.

Polystyrene is chosen for the lipophilic core, because it is rather stable at higher temperatures and relatively rigid in comparison to other polymers. The latexes are characterized by means of Transmission Electron Microscopy, Dynamic Light scattering, and Zeta potential measurements. The average particle size is depending on the composition of the latexes and varies in the range of 25 - 80 nm. The coagulation stability and the ability of these latexes to act as phase-transfer agents are examined in partitioning experiments. The latexes are stable for extended time (6 days) at up to 80°C and stirring rates of up to 700 rpm, which makes their application in catalytic reactions feasible.

It is shown how the composition of the latexes affects the phase-transfer of lipophilic compounds. In the partitioning experiments, selectivity for 1-octene over n-nonanal (factor 2.5) is found. This is of great importance with view on the envisaged use in the two-phase hydroformylation of water-insoluble higher alkenes.

In **Chapter three** the polystyrene-based latexes are applied in the water-organic Rh-catalyzed hydroformylation of higher alkenes using water-soluble catalysts. The influence of latex concentration, latex composition, as well as of significant reaction parameters like the synthesis gas (CO/H₂) pressure on the performance of catalytic systems are discussed in detail. Very efficient catalysis is accomplished, with rates close to the organic-phase hydroformylation using PPh₃. 1-Octene can be converted with a Turnover Frequency of 2000 h⁻¹ using TPPTS as ligand.

The efficient phase transfer and the electrostatic aggregation of the catalyst with the latex are responsible for this outstanding performance. The catalyst and product phase separation after complete conversion of higher alkenes is instantaneous, providing an easy and efficient catalyst recycling technology.

These excellent results make polystyrene-based latexes feasible for industrial applications.

Chapter four comprises the synthesis and application of electrostatically immobilized transition metal catalysts in the asymmetric hydrogenation of C=C and C=N bonds. A sodium *p*-styryl-triphenylborate-functionalized polymer is synthesized by radical copolymerization of sodium *p*-styryl-triphenylborate and styrene. This polymer is used as support for cationic transition metal complexes. The supported catalysts are inactive in the hydrogenation of C=C bonds independently from the applied solvent but show moderate activities and enantioselectivities in the hydrogenation of C=N bonds. When the hydrogenation of *N*-benzyl-(-1-phenylethylidene)-imine with [Rh(nbd)(bdpp)]-functionalized polymer is performed in MeOH, good conversions (77%) are reached. The counterion dramatically influences the enantioselectivity, which can even result in a change of the absolute configuration of the product. The supported catalyst can be reused several times with very low Rh-leaching and only a slight decrease in activity and enantioselectivity.

In **Chapter five** the concept is extended to the incorporation of diphosphine ligands (Nixantphos) into polystyrene-based latexes. The phosphorus ligand is decorated with a polymerizable group (styrene) and covalently incorporated into the particles. Initial results on the application in the biphasic hydroformylation of higher alkenes are presented and discussed.

An outlook for the future development and prospect of the use of latexes for catalyst recycling is given.

Immobilisatie van katalysatoren via electrostatische interacties: Dragers gebaseerd op polystyreen

Het hergebruik van homogene katalysatoren blijft van cruciaal belang voor industriële toepassingen. In de loop der jaren zijn er verscheidene concepten ontwikkeld om dit probleem te omzeilen. De elegantste en meest succesvolle oplossing wat betreft industriële toepassing tot op heden is twee-fase katalyse, met het Shell Hogere Olefine Proces (SHOP) voor de oligomerisatie van etheen en het Ruhrchemie/Rhône Poulenc Proces (RCH/RP) voor hydroformylering van propeen als belangrijkste voorbeelden. Voor beide processen geldt dat de katalysator, die in een polair oplosmiddel is opgelost, eenvoudig kan worden hergebruikt en afgescheiden van de apolaire product fase door middel van fase scheiding en extractie waarin de katalysator intact blijft. De substraten moeten echter wel voldoende oplosbaar zijn in de polaire katalysator fase.

In het algemeen geldt dat voor elk homogeen gekatalyseerd proces dat in de industrie wordt toegepast, een aparte oplossing voor het hergebruik van de katalysator is ontwikkeld. Een gereedschapskist met allerlei algemeen toepasbare technieken voor katalysator recycling, elk met zijn eigen tekortkomingen, zou proces ontwikkeling in de toekomst kunnen versnellen en is daarom zeer gewenst.

Het onderwerp van dit proefschrift is de ontwikkeling van niet-destructieve methodes die de voordelen van homogene katalyse combineren met gemakkelijk scheiden en hergebruiken van de katalysator, vooral voor substraten die niet oplosbaar zijn in de katalysator fase. Het proefschrift richt zich in het bijzonder op het gebruik van fase transfer agents en op de electrostatische immobilisatie van katalysatoren.

Latexen hebben een aantal kenmerken die hen hiervoor heel aantrekkelijk maken. Ten eerste kunnen ze gemakkelijk in één stap op grote schaal geproduceerd worden uitgaand van goedkope uitgangsstoffen. Door de keuze van geschikte monomeren en polymerisatiecondities, kunnen hun eigenschappen breed gevarieerd worden. Aangezien latexen deeltjes zijn die bestaan uit een kern en een schil, een soort “macromoleculaire micellen”, kunnen hun oplosbaarheid en de polariteit van de binnenkant precies afgesteld worden. Deze unieke combinatie van eigenschappen maakt, dat deze nanomaterialen uitstekende kandidaten zijn voor onze toepassing.

Hierdoor zijn latexen onderzocht als fase transfer agents en als drager voor homogene katalysatoren.

In **hoofdstuk 1** wordt een literatuuroverzicht gegeven van electrostatische immobilisatie van katalysatoren. De immobilisatie op dragers als zeolieten, klei, heteropolyzuren, ionische vloeistoffen en dendrimeren en hun toepassing in katalyse wordt beschreven en vergeleken. De belangrijkste conclusie die uit dit literatuuroverzicht getrokken kan worden is dat latexen zelden als drager voor katalysatoren zijn overwogen.

Hoofdstuk 2 is gericht op de synthese en karakterisering van op polystyreen gebaseerde latexen. De latexen worden gesynthetiseerd door middel van vrij radicaal emulsie co-polymerisatie. De op polystyreen gebaseerde latexen bevatten het hydrofobe monomeer styreen, DVB als crosslinker, een polymeriseerbare non-ionische surfactant en polymeriseerbare styrylzouten. De combinatie van de non-ionische surfactant en een styrylzout zorgen voor een efficiënte stabilisatie van de latex deeltjes.

Polystyreen is gekozen als lipofiele kern, omdat het relatief stabiel is bij hogere temperaturen en tamelijk stug vergeleken met andere polymeren. De latexen worden gekarakteriseerd door middel van Transmissie Electronen Microscopie, Dynamische Lichtverstrooiing en Zeta potentiaal metingen. De gemiddelde deeltjes grootte hangt af van de samenstelling van de latex en varieert van 25 tot 80 nm. De coagulatie stabiliteit en de mogelijkheid van deze latexen om als fase-transfer agent te dienen wordt onderzocht in partitioning experimenten. De latexen zijn geruime tijd stabiel (6 dagen) bij 80°C en roersnelheden tot 700 rpm, wat hun toepassing in katalyse mogelijk maakt. Er wordt aangegeven hoe de samenstelling van de latexen de fase-transfer van lipofiele verbindingen beïnvloedt. In partitioning experimenten is een selectiviteit voor 1-octeen boven n-nonanal (factor 2.5) gevonden. Dit is erg belangrijk voor de beoogde toepassing van deze systemen in de twee-fase hydroformylering van niet in water oplosbare hogere alkenen.

In **hoofdstuk 3** worden de op polystyreen gebaseerde latexen toegepast in de twee-fase Rh-gekatalyseerde hydroformylering van hogere alkenen met water oplosbare katalysatoren. De invloed van de latex concentratie, latex samenstelling en belangrijke reactie parameters als synthese gas druk (CO/H_2) op de prestaties van de katalysator

worden in detail bediscussieerd. Efficiënte katalyse kan worden bereikt; reactiesnelheden benaderen die van PPh_3 in de organische fase. 1-Octeen kan met TPPTS als ligand worden omgezet met een Turnover Frequency van 2000 h^{-1} .

De efficiënte fase transfer en de electrostatische aggregatie van de katalysator met de latex zijn verantwoordelijk voor deze buitengewone prestatie. Na de conversie van hogeren alkenen scheiden de product fase en de katalysator fase zich instantaan, wat een gemakkelijke en efficiënte katalysator recyclingstechnologie oplevert.

Deze uitstekende resultaten maken industriële toepassingen van op polystyreen gebaseerde latexen mogelijk.

Hoofdstuk 4 omvat de synthese en toepassing van electrostatisch geïmmobiliseerde overgangsmetaal katalysatoren in de asymmetrische hydrogenering van C=C en C=N bindingen. Een natrium p-styryl-triphenylboraat gefunctionaliseerde polymeer wordt gesynthetiseerd door middel van radicaal co-polymerisatie van natrium p-styryl-triphenylboraat en styreen. Deze polymeer wordt gebruikt als drager voor kationische overgangsmetaal complexen. De geïmmobiliseerde katalysatoren zijn inactief in de hydrogenering van C=C bindingen in welk oplosmiddel dan ook, maar tonen gemiddelde activiteit en enantioselectiviteit in de hydrogenering van C=N bindingen. Wanneer de hydrogenering van *N*-benzyl-(1-phenylethylidene)-imine wordt uitgevoerd met de $[\text{Rh}(\text{nbd})(\text{bdpp})]$ gefunctionaliseerde polymeer in methanol, worden hoge conversies (77%) bereikt. Het tegenion heeft grote invloed op de enantioselectiviteit; dit kan zelfs leiden tot verandering van de absolute configuratie van het produkt. De geïmmobiliseerde katalysator kan verscheidene malen worden hergebruikt met slechts een kleine teruggang in activiteit en enantioselectiviteit en erg lage Rh-leaching.

In **hoofdstuk 5** wordt het concept uitgebreid naar de incorporatie van difosfine liganden (Nixantphos) in op polystyreen gebaseerde latexen. Het fosfor ligand wordt uigerust met een polymeriseerbare groep (styreen) en op covalente wijze in de latex ingebouwd. Voorlopige resultaten van de toepassing van deze latex in twee-fase hydroformylering van hogere alkenen wordt gepresenteerd en bediscussieerd.

Een vooruitzicht voor de toekomstige ontwikkeling en gebruik van latexen voor katalysator recycling wordt weergegeven.

K.Kunna, C. Müller, J. Loos and D. Vogt "Aqueous Phase Hydroformylation of 1-Octene: Styrene Latices as Phase-Transfer Agents" *Angew. Chem., Int. Ed.*, **2006**, *45*, 7289-7292

Katharina Kunna was born in Rostock, Germany on December 05, 1980. She finished her secondary school at the “Erasmus Gymnasium” in Rostock in 1999. In the same year she started studying chemistry at the University of Rostock, Department of Chemistry. She did her graduation project in the section of technical, analytical and environmental chemistry under the supervision of Prof. Dr. U. Kragl. The title of her project was



“Enzymatische Racematspaltung von Corollosporin *N*-Analoga”. In August 2004, she finished her graduation project and obtained the title of Chemist. In September 2004 she moved to the Netherlands to start her doctoral research in the Laboratory of Homogeneous Catalysis and Coordination Chemistry of Prof. Dr. D. Vogt. Her research was mainly focused on the immobilization of transition metal complexes via electrostatic interactions and their application in catalysis. The most important results of this research are described in this thesis.

Katharina Kunna werd op 5 december 1980 in Rostock (Duitsland) geboren. In 1999 behaalde ze haar middelbare school diploma aan het “Erasmus Gymnasium” in Rostock. In datzelfde jaar begon ze haar scheikunde studie aan de Universiteit van Rostock. Het afstudeerproject werd gedaan op de afdeling Technische, Analytische en Milieuchemie onder leiding van Prof. Dr. U. Kragl. De titel van het project was “Enzymatische racemaatsplitsing van Corollosporin *N*-analoga”. In augustus 2004 werd het diploma behaald. In september 2004 werd begonnen met het promotieonderzoek in de vakgroep Homogene Katalyse en Coördinatie Chemie onder leiding van Prof. Dr. D. Vogt. Het onderzoek was gericht op de immobilisatie van overgangsmetaal complexen via electrostatische interacties en hun toepassing in katalyse. De belangrijkste resultaten hiervan staan beschreven in dit proefschrift.

Dankwoord, Acknowledgement, Danksagung

I would like to express my sincere gratitude to those who have contributed to this thesis and without whom the thesis would never have been completed.

First of all, I would like to thank my promotor Prof. Dr. Dieter Vogt for giving me the opportunity to work in his group. Dieter, thanks for your support, the great discussions, advices, suggestions and your interest in my work. During these four years I learnt a lot, about chemistry and myself. A special thank goes also to my co-promotor Dr. Christian Müller. Christian, I thank you for all your help and support in these four years. Furthermore, I am grateful to Dr. Erik Abbenhuis for his suggestions and comments during my PhD.

I would like to thank the members of the commission, Prof. Dr. Stefan Mecking, Prof. Dr. Bert Klein Gebbink and Prof. Dr. André de Haan for reviewing the manuscript and for their valuable suggestions. Furthermore, I would like to thank Dr. Joachim Loos and Dr. John van de Schaaf for the interest in participating in the commission and for the great discussions.

For the correction of my thesis I would like to thank especially Christian, Michèle, Laura Marie-Claire and Dieter. You all helped me a lot.

I would like to thank also the Homogeneous Catalysis group. I had the honor to meet very special colleagues from whom I learnt a lot about chemistry and handling other people. Thanks to Bart, Leandra, Michèle, Jos, Grijsbert, Laura, Jarno, Barry, Dennis, Hendawy, Jarl Ivar, Patrick, Gilbert and Mathijs.

Ton, thank you very much to be always taking the time to help me during these 4 ½ years (GC, HPLC and autoclaves etc.)

Michèle you are a really special person and you will succeed without problems. Good luck, anyhow!

I am grateful to Maria with whom I shared the office in the beginning of the PhD.

Especially, I would like to thank my officemate and “paranimph” Laura. Laura, you are a really special person for me. Mi mancheranno molto le nostre belle chiacchierate sui tedeschi e sugli italiani e le nostre piccole liti: sono stata molto fortunata ad avere una persona come te come compagna di ufficio e ti ringrazio per tutti i consigli, i suggerimenti e il sostegno che mi hai sempre dato. Ti ringrazio perché sei stata sempre sincera con me e ti auguro buona fortuna per la tua futura carriera.

Eric you were a really close colleague and you are a good friend of mine, I thank you for helping me to see some things in another perspective. Ruben, Blondie thank you for the nice time, take care. Muchas grazias, Mabel I'm happy that you are back. Good luck. Thank you, Daniel for the nice time together with you and I hope we will meet for a lot of parties in the future.

Ariadna, I am really happy to have you as a friend. Good luck with your thesis. Tiina, “sugar girl” good luck with your thesis.

Furthermore, I would like to thank **all** the members of **the SKA group** for the good moments and the nice atmosphere during the coffee breaks, borrels, social and scientific activities. It was a nice time. Especially, I would like to thank our Secretaries, without you a lot of things would go wrong, thank you for helping us as much as you can with the organizational and administrative tasks.

Thank you, Evgeny, Bouke, Christian, Chretien, for the many nice lunch times. Christina and Joost ich hoffe ihr bleibt immer so glücklich und ihr werdet die Hürden des Familienlebens meistern. Viel viel Glück!!!!!!!!!!!!!!

I am grateful to the people who helped me with the different analytical methods and technical problems, A. Elemans-Mehring, Dr. P. Magusin, Dr. J. Laven, Dr. J. Loos, T. Verhoeven, Wout van Herpen, Paul Aedenroomer and Ton Staring.

Dennis, thank you for the ligand and I wish you good luck with your thesis.

A special thank should also go to the Emulsion group. Prof. Dr. Alex van Herk, thank you for the nice discussions and suggestions about the latexes. I would like to thank Hector for helping me with analyzing the latexes and nice discussions.

MC, you are a really nice person. It was so great of you to help me with the corrections of the thesis, to discuss with you the results and to spend time. Thank you!!!

Thank you, Rob for your help with the polymerization reaction.

Desweiteren danke ich der "L" Gruppe Claudia, Nicole, Tina, Christina und Christoph (Versorgungsmeister) ihr seit was Besonderes erhaltet Euch das und viel Glueck bei der Promotion. Auch Andreas, meinem „persönlichen Chaffeur“ möchte ich danken das wir immer heil ans Ziel kamen. Christina, ich danke Dir das du waehrend der Zeit hier in Eindhoven immer fuer mich da warst, ich konnte immer zu Dir kommen und habe wunderbare Parties und Samstage verbracht. Danke das du mein „paranimph“ bist.

Thank you, Lettie for being a friend and helping me in a really difficult situation.

I would also like also to thank Yvonne, Hanna, Nolliag, and Nicolas, for making me feel at home in Eindhoven.

Ein liebes Dankeschön soll auch an alle meine Freunde gehen, Antje & Torsten (Lisa, Mia), Pamela (Justin, Kiano), Anett, Jette, Adina, Anne-Katrin, Jens & Mirijam (Samantha, Jason), die mich immer unterstützt, aufgebaut und viel Verständnis für mich (uns) hatten in dieser Zeit. Torsten danke für dein immer offenes Ohr. Die heutige Technik machte es einfach immer möglich.

Aber auch Bernd & Simone möchte ich danken für die vielen schönen Abende die wir bisher verbracht haben. Desweiteren gebührt lieber Dank auch meinen „ zukünftigen“ Schwiegereltern. Ihr seid ein ein wichtiger Teil in meinem Leben.

Ganz besonderen Dank möchte ich meiner Familie zu kommen lassen. Mein Vater, der immer die Ruhe, die Kraft und Ausstrahlung eines starken Menschen hatte, gebührt besonderen Dank. Er hat mir beigebracht das Ehrgeiz, Kampfgeist und Streben meistens zum Erfolg führt und sich immer lohnt. Du bist und wirst immer im meinem Herzen sein und bleiben. Das Gleiche soll auch meiner Mutter zu teil werden, ihre Kraft, ihre Stärke und ihre unermüdliche Geduld mit mir hat mich soweit gebracht. Du bist ein ganz besonderer Mensch. **Liebe Mutti und Papa danke für alles, ohne Euch hätte ich nie dieses Ziel erreichen können!!!!!!!!!!!!!!!!!!!!!!**

Desweiteren möchte ich auch meiner Schwester Anja (Johannes, Phillip) von Herzen danken, für ihre Unterstützung und ihr Liebe.

Auch meiner Schwester Christiane und meinem Bruder Christoph danke ich, dass wir auch nach dem tragischen Einschnitt in unserem Leben eine Familie sind und zusammenhalten. Es gab mir Kraft meinen Weg weiter zu gehen.

Als Letztes aber ganz besonders möchte ich mich bedanken bei dem mit am wichtigstem Menschen in meinem Leben. Heiko, du hast mich immer wieder aufgebaut, unterstützt und mich angehalten mein Ziel zu verfolgen in dieser Zeit. „Ich liebe dich vom ganzen Herzen“. Danke das du ein grosser Teil meines Lebens bist.

Bedankt allemaal !!!

Katharina Kunna